Stony Brook University

DNA Damage Response Activates Interferon Signaling

A Dissertation Presented

by

Sabrina Ewa Racine Brzostek

to

The Graduate School

in Partial Fulfillment of the

Requirements

for the Degree of

Doctor in Philosophy

in

Molecular and Cellular Biology

(Immunology and Pathology)

Stony Brook University

August 2010

Stony Brook University

The Graduate School

Sabrina Ewa Racine Brzostek

We, the dissertation committee for the above candidate for the

Doctor of Philosophy degree, hereby recommend

acceptance of this dissertation

Nancy C. Marshall, Ph.D.,
Dissertation Advisor
Professor, Department of Molecular Genetics and Microbiology

Howard B. Fleit, Ph.D.
Associate Professor,
Department of Pathology

Michael A. Frohman, Ph.D.,
Chairperson of Defense
Professor and Chairperson,
Department of Pharmacological Sciences

Wei-Xing Zong, Ph.D.
Assistant Professor, Department of Molecular Genetics and Microbiology

Patrick Hearing, Ph.D.
Professor, Department of Molecular Genetics and Microbiology

Janet C. Hearing, Ph.D.
Associate Professor, Department of Molecular Genetics and Microbiology

This dissertation is accepted by the Graduate School

Lawrence Martin
Dean of the Graduate School

Abstract of the Dissertation

DNA Damage Response Activates Interferon Signaling

by

Sabrina Ewa Racine Brzostek

Doctor in Philosophy

in

Molecular and Cellular Biology

(Immunology and Pathology)

Stony Brook University

2010

The DNA damage response occurs in response to breaks in DNA and can elicit cell signaling pathways that result in cell cycle arrest, DNA repair, or apoptosis in order to maintain the integrity of the genome. The replication of viruses activates the host DNA damage response and many of these viruses have evolved mechanisms to inhibit apoptosis. To understand better the link between DNA damage and cellular defense, the effects of agents that create double-stranded DNA breaks were evaluated on cellular gene expression.

Etoposide, a chemotherapeutic drug used to treat various cancers, causes cell cycle arrest and death by apoptosis. Its mechanism of action involves the targeting of topoisomerase II, wherein it alters the ability of topoisomerase II to religate cleaved DNA strands, resulting in an increase the number of double stranded breaks in the DNA. This damage triggers cell death pathways, ultimately leading to apoptosis. The gene expression profile of etoposide-treated cells was compared to that of virally infected cells.

These studies indicate that etoposide treatment leads to expression of interferon (IFN) stimulated genes (ISGs). Further analysis indicated that a subset of IFNα and IFNλ genes, but not IFNβ, are induced by the DNA damage incurred with etoposide

treatment and the ISGs are expressed due to IFN signaling. The IFN Regulatory Factors (IRFs), IRF3 and IRF5 do not appear to be activated and thus are not responsible for this IFN gene induction. However, two other IRF family members, IRF1 and IRF7 are induced in response to etoposide treatment and have a role in IFNα and IFNλ induction. Furthermore, NFκB appears to be the master transcription factor that activates IFN signaling in response to etoposide. In addition to activating directly IFNλ gene expression, NFκB also induces the IRF1 and IRF7 genes and therefore plays an indirect role in IFNα induction.

Additionally, inhibition of PI-3-kinase ataxia-telangiectasia mutated (ATM) activation diminishes the IFNα and IFNλ response in etoposide-treated cells, indicating that the IFN induction appears to occur downstream of the (ATM) signaling pathway. These studies indicate a significant link between two host survival mechanisms - the DNA damage response and the response to viral infection.

DEDICATION

To my family,

especially to my husband Christian and my daughter Isla.

TABLE OF CONTENTS

LIST OF FIGURES

LIST OF TABLES

ABBREVIATIONS

aa	Amino Acid
Ab	Antibody
Bcl-2	B-Cell Lymphoma protein 2
Bcl-XL	Bcl-2 related large
BSA	Bovine Serum Albumin
CARD	Caspase Recruitment Domain
Cardif	CARD adapter inducing IFN-β
CBP	CREB Binding Protein
cDNA	Complementary Deoxyribonucleic Acid
Ci	Curie
DAPI	4’,6-diamidino-2-phenylindole
DBD	DNA Binding Domain
DMEM	Dulbecco’s Modified Eagles Medium
DN	Dominant Negative
DNA	Deoxyribonucleic Acid
DRAF	double-stranded RNA Activated Factor
ds	Double Stranded
DTT	Dithiothreitol
EDTA	Ethylene Diaminetetraacetic Acid
EGTA	Ethylene Glycol-Tetraacetic Acid
EMSA	Electrophoretic Mobility Shift Assay
FADD	Fas-Associated Death Domain
Fas	TNF Receptor Superfamily, Member 6
FBS	Fetal Bovine Serum
GAS	Interferon-γ Activated Site
GFP	Green Fluorescent Protein
HEPES	4-(2-Hydroxyethyl)-1-Piperazineethanesulfonic Acid
IFN	Interferon

IFNAR	Interferon-α receptor
IκB	Inhibitor of kappa B
IKK	IκB Kinase
IL	Interleukin
IRAK	Interleukin-1 Receptor-Associated Kinase
IRF	Interferon Regulatory Factor
ISG	Interferon-Stimulated Gene
ISGF3	Interferon-Stimulated Gene Factor-3
ISRE	Interferon-Stimulated Response Element
JAK	Janus Kinase
KCl	Potassium chloride
kDa	Kilodalton
μg	Microgram
μL	Microliter
mAb	Monoclonal antibody
MAVS	Mitochondrial Antiviral Signaling Protein
Mda5	Melanoma Differentiation Associated Protein-5
MEF	Mouse Embryo Fibroblasts
μg	Microgram
μM	Micromolar
mg	Milligram
ml	Milliliter
mm	Millimeter
mM	Millimolar
MyD88	Myeloid Differentiation Primary Response Protein 88
NaCl	Sodium Chloride
NaF	Sodium Fluoride
Na_2HPO_4	Disodium Hydrogen Phosphate
NaH_2PO_4	Sodium Dihydrogen Phosphate
Na_3VO_4	Sodium Ortho-Vanadate
NAK	NFκB Activating Kinase

NDV	Newcastle Disease Virus
NFκB	Nuclear Factor of Activated Immunoglobulin Light-Chain
NK	Natural Killer
NP-40	Nonidet-P40
PAGE	Polyacrylamide Gel Electrophoresis
PARP	Poly (ADP-Ribose) Polymerase
PBS	Phosphate Buffered Saline
PCR	Polymerase Chain Reaction
pDC	Plasmacytoid Dendritic Cell
Pin1	Peptidyl-Prolyl Isomerase 1
PKR	RNA-Dependent Protein Kinase
PMSF	Phenylmethylsulphonyl Fluoride
Pol-III	RNA polymerase III
PRD	Positive Regulatory Domain
pS	Phosphoserine
pY	Phosphotyrosine
RIG-I	Retinoic Acid-Inducible Gene I
RIP	Receptor Interacting Protein
RLR	RIG-I Like Receptor
RNA	Ribonecleic Acid
RNAi	RNA Interference
RSK1	Ribosomal S6 Kinase 1
RT	Room Temperature
RT-PCR	Reverse Transcription-Polymerase Chain Reaction
SDS	Sodium Dodecylsulfate
SH2	Src Homology 2
ss	Single Stranded
STAT	Signal Transducer and Activator of Transcription
SV40	Simian Virus 40
TBS	Tris Buffered Saline
TAD	Transactivation Domain

TBK1	Tank Binding Kinase 1
TBS	Tris Buffered Saline
TIR	Toll/IL-1 Region
TLR	Toll-like Receptor
TNF	Tumor Necrosis Factor
TPR	Tetratricopeptide Repeats
TRAF	TNF Receptor Associated Factor
TRIF	TIR Domain-Containing Adaptor Inducing IFNβ
Tris	tris (hydroxymethyl) aminomethane
Tween 20	20 Polyoxyethylene-sorbitan-monolaurate
U	Unit
VRE	Virus Response Element
WB	Western Blotting
WT	Wild Type

ACKNOWLEDGEMENTS

I would like to thank my advisor, Dr. Nancy C. Reich Marshall, for her guidance, patience and support. This project has had its ups and downs and she has always had faith in it.

I am thankful to all the past and present members of the Reich lab for producing a supportive and stimulating environment, which is crucial in our pursuits in science. I would especially like to thank Sarah VanScoy, not only for beginning this project with her microarray assay, but also for her excellent advice and friendship. Also, I am grateful for the help Chris Gordan gave me and for his contribution to all the microscopy studies in this dissertation. Thank you Janaki Iyer, for your friendship and constant reassurance, even from across the country in Tulsa, OK!

I would like to thank my committee members who have made many valuable suggestions that have improved this thesis project over the many years.

I thank my family. My parents Zygmunt and Jadwiga Brzostek, whose love and support has always encouraged me during my years as a "professional student." Also, my sisters – Lisa, Susie and Barbara, whose sense of humor has always managed to pull me out any slump.

Last, but most certainly not least, I would like to thank my husband and daughter. My husband Christian, for his unconditional love and understanding of the life of a graduate student. My daughter Isla for her smile. It has motivated me to finish this dissertation as quickly as possible so that I may spend more time with her.

.

INTRODUCTION

Survival of an organism is dependent on its ability to respond quickly and effectively to dangers in its environment. In response to environmental stresses, organisms must evolve means to protect themselves from permanent injury. On the cellular level, this is achieved through changes in gene expression, which lead to the production of proteins that often exert a positive or protective effect on the cell and ultimately the whole organism. For example, many stresses, whether through UV radiation, exogenous DNA damaging agents, or naturally occurring free radicals, often result in DNA damage that could promote dysregulation of cell growth and tumorigencity. To combat the disruption of normal physiological processes, cells will employ such tactics as triggering cell cycle arrest to allow time for DNA repair and rescue the normal functions of the cell. However, if irreparable damage ensues, the cell will initiate pathways that result in apoptosis to protect the whole organism.

Cells possess a number of distinct signal transduction pathways that couple environmental stimuli to specific changes of gene expression. Cellular responses to these environmental insults rely on the induction of many stress-inducible genes. In the case of exposure to viral pathogens, the cell induces the expression of the antiviral cytokine, interferon (IFN). IFN, in turn, stimulates the transcriptional induction of a set of genes that protect the cell and adjacent cells from viral infection. Cells already established with viral infection may not be protected effectively by the IFN they secrete. Therefore, as in cells with irreparable DNA damage, the cell sacrifices itself for the survival of the host.

In this dissertation, I determined that DNA damage induces IFN production in cells, indicating a link between the DNA damage response and IFN signaling, a response traditionally associated with viral infection. Furthermore, I discern differential regulation of IFN expression in cells responding to DNA damage and viral infection.

Part I: Recognition of Pathogens by Cells

A successful defense against pathogenic infection relies on a rapid response by the immune system following the detection of the microorganism. Pattern-recognition receptors (PRRs) are the host's cellular sensor molecules that specifically recognize a microbe's pathogen-associated molecular patterns (PAMPs). PAMPs include foreign material such as lipopolysaccharide (LPS) of Gram-negative bacteria and nucleic acids generated by viruses. Once a pathogen is detected by a PRR, specific signaling cascades occur, activating transcription factors that induce the expression of target genes which encode products that help control and eradicate the infectious agent. These gene products include cytokines such as the IFNs (184, 243).

Several PRR types exist in animal and plant cells, many of which can recognize foreign nucleic acids. PRR families that have been identified as nucleic acid sensors include: Toll-Like receptors (TLR), retinoic acid-inducible gene (RIG-I)-like receptors (RLRs), Nucleotide oligomerization domain (NOD)-like receptors (NLRs), Absent in melanoma 2 (AIM2) and DNA-dependent activator of Interferon Regulatory Factors (DAI). Both AIM2 and the NLRs primarily induce proinflammatory cytokines, such as interleukin (IL)-1β and not IFN. In addition to proinflammatory cytokines, the TLRs, RLRs and DAI can also specifically induce the production of IFN and are further described below (243).

Membrane-Bound Toll-Like Receptors

Toll involvement in host immunity was first reported in 1996 with the observation that *Drosophila* which were Toll-deficient were vulnerable to infection by fungi (95). In the following year, a protein homologous to the *Drosophila* Toll, the Toll-like Receptor (TLR) was identified in humans (124). To date, 13 TLRs have been identified – TLR1-9 are found in both humans and mice, while TLR10 is unique to humans and TLR11-13 are only found in mice (184). TLR1, TLR2, TLR4, TLR5 and TLR6 are localized to the plasma membrane and can be recruited to the phagosome. TLR3, TLR7, TLR8 and TLR9 are found in the endosomal compartment. Each TLR recognizes a specific type of PAMP, as listed in Table 1.

Table 1: Toll Like Receptor Ligands.

Toll Like Receptor	Ligand
TLR1/2	diacyl lipoprotein
TLR3	dsRNA
TLR4	LPS
TLR5	flagellin
TLR6/2	triacyl lipoprotein
TLR7/8	ssRNA
TLR9	CpG DNA

TLRs are single transmembrane proteins whose extracellular domain contains a variable leucine-rich repeat that is involved in ligand recognition. The intracellular domain, Toll/IL-1 resistance (TIR), is common to all TLR and Interleukin-1 (IL-1) receptor family members and is essential for downstream signal transduction. Upon ligand binding, each TLR triggers a signaling cascade by recruiting specific TIR domain-containing adaptor molecules to its own TIR domain. Adaptors utilized by TLR include myeloid differentiation factor 88 (MyD88), TIR-domain-containing Adapter Inducing IFNβ (TRIF), TRIF-Related Adapter Molecule (TRAM), and TIR domain-containing adaptor protein (TIRAP) (184, 243). The recruitment of these adapters to the TIR domain of the receptor leads to the activation of transcription factors, such as Nuclear Factor κB (NFκB) and the Interferon Regulatory Factors (IRFs). These transcription factors subsequently induce IFN and the antiviral IFN response in the cell.

TLR signaling can be divided into two main pathways – the MyD88-dependent and MyD88-independent pathways (Figure 1). MyD88 is considered a central adaptor molecule interacting with all TLR but TLR3. Upon ligand binding, TLR5, TLR7, TLR8, and TLR9 interact directly with MyD88 while TLR2 and TLR4 first recruit TIRAP in order to recruit MyD88 to the receptors. MyD88 then interacts with the IL-1R-associated kinases (IRAK) 1 and 4. The IRAKs activate TNF receptor-associated factor 6 (TRAF6), an ubiquitin E3 ligase that works with a ubiquitin enzyme complex to polyubiquitinate targets proteins, as well as itself. Activated TRAF6 may activate the NFκB signaling pathway by activating the IκB kinase complex. Active NFκB signaling results in the induction of inflammatory cytokines and aids the induction of IFNβ. IRF activation is also associated with MyD88-dependent TLR7**,** TLR8 and TLR9 signaling. IRAK and TRAF6 signaling activate IRF7, which is responsible for IFNα induction (71, 184).

MyD88-independent signaling is utilized by the TLR3 and TLR4 pathways and involves the adaptor protein TRIF. TRIF mediates the activation of the serine/threonine kinase TANK binding kinase (TBK1), the activator of IRF3. IRF3, as discussed below, is a major transcription factor involved in IFNβ induction. In the case of TLR4/TRIF signaling, TLR4 needs to utilize the adaptor TRAM to recruit and activate TRIF. NFκB signaling also occurs in MyD88 independent pathways since TRIF is able to activate TRAF6, resulting in NFκB activation (71, 184).

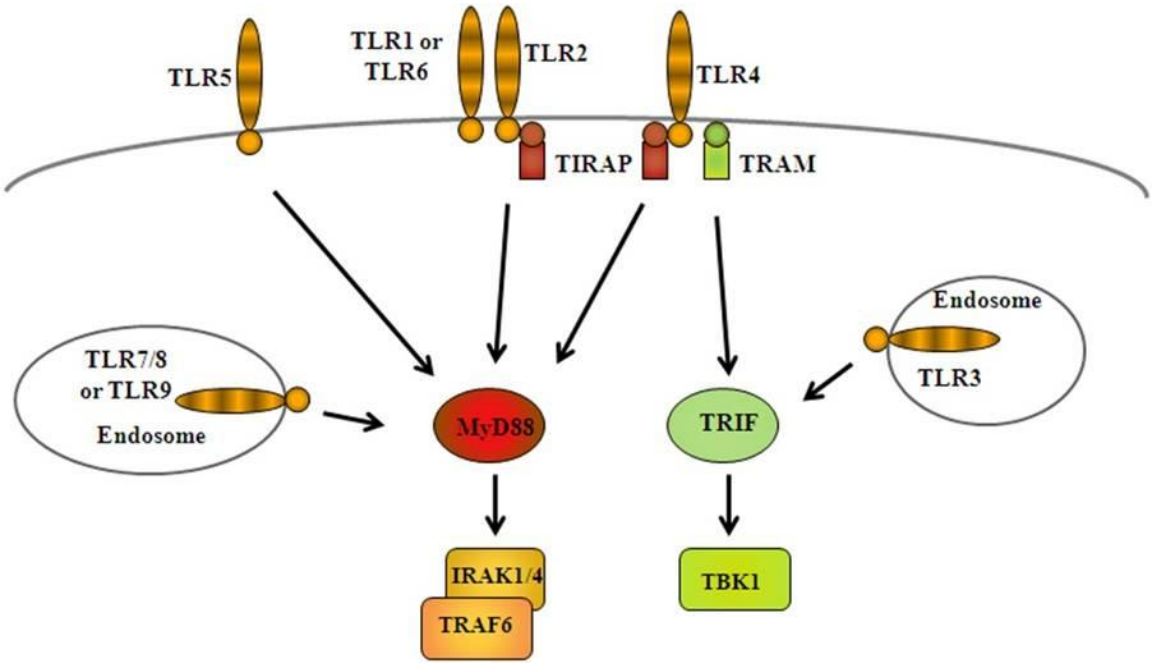

Figure 1: MyD88-dependent and MyD88-independent TLR signaling.

The MyD88 pathway is utilized by all TLR signaling pathways except TLR3. TLR5, TLR7, TLR8, TLR9 all interact with MyD88 directly, while TLR4 and TLR2 bind to the adaptor TIRAP in order to recruit MyD88. MyD88 binds the IRAK complex, which activates TRAF6. The MyD88 pathway is utilized by TLR3 and TLR4. Instead of MyD88, these TLRs interact with TRIF, which activates TBK1 signaling.

Figure adapted from Jenkins, K. A., and A. Mansell. Cytokine 49:237-44.

Cytoplasmic RIG-I Like Receptors

RLRs are RNA helicases that act as sensor molecules in the IFN signaling pathway, detecting viral RNA in the cytoplasm of infected cells. These receptors are expressed in most cell types and are themselves IFN-inducible genes, providing positive feedback regulation. Three members of the RLR family have been identified – RIG-I, melanoma differentiation associated gene 5 (MDA5), and laboratory of genetics and physiology 2 (LGP2) (244).

All three members contain a RNA helicase with RNA-dependent ATPase activity, which recognizes and binds dsRNA generated by viral infection. The N-terminal portions of RIG-I and MDA5 have two caspase recruiting domains (CARD), while LGP2 has no such domain. CARDs interact with other CARD-containing adaptor molecules, which initiate downstream signaling pathways that lead to the induction of IFN and proinflammatory cytokines. Such adaptor molecules include IFNβ promoter stimulator 1(IPS-1) (also called mitochondrial antiviral signaling, MAVS), virus-induced signaling adaptor (VISA), and CARD adaptor inducing IFNβ (CARDIF) (78, 131, 183, 238). The RLR family members also have a repressor domain (RD) in the C-terminal region of the protein, which allow repression of activity in the absence of viral RNA (70, 245, 246).

RIG-I detects short dsRNA and 5' triphosphates and initiates IFN signaling in response to RNA viruses such as vesicular stomatitis virus (VSV) and Sendai virus (SeV) (77, 141). On the other hand, MDA5 detects longer dsRNA and the synthetic dsRNA molecule poly I:C and is responsible for IFN production in response to picornaviruses, such as encephalomyocarditis virus (EMCV) (77, 177).

The functional role of LGP2 in the antiviral response is still under investigation. Several groups have suggested that LGP2 plays an inhibitory role in RIG-I and/or MDA5 signaling (85, 169, 173, 222). LGP2 may sequester RNA from RIG-I, modulating the level of antiviral signaling initiated by RIG-I or MDA5. Additionally, the LGP2 RD could interact with RIG-I, further inhibiting it activation (99, 169, 245).

One LGP2 knockout study (222) found that LGP2 functions as a negative regulator of RIG-I signaling but a positive regulator of MDA5 signaling, since LGP2 -/- mice were resistant to VSV but appeared sensitive to EMCV infection. Recently, another LGP2 knockout study verified LGP2's role as a positive regulator of MDA5 signaling

since cells from their LGP2 -/- mice demonstrated diminished IFN induction in response to EMCV (177). However, this same study questioned LGP2's role in negative regulation of RIG-I signaling since cells from LGP2 -/- mice were susceptible to VSV infection due to impaired IFN production.

Cytoplasmic DNA Sensors

The IFN response to single stranded DNA consisting of unmethylated CpG motifs, commonly found in the genome of bacteria and virus, is initiated by the membrane associated receptor, TLR9. However, IFN is also induced in response to viral, bacterial, mammalian and synthetic double stranded DNA that is transfected into the cytoplasm of cells. This IFN response does not require TRIF or MyD88 and was independent of TLR9 signaling, strongly suggesting the existence of a cytoplasmic DNA sensor (64, 191, 200, 241) in the IFN signaling pathway (Figure 2).

DAI

DNA-dependent Activator of IFN Regulatory Factors (DAI) was identified as a cytosolic sensor of AT-rich B-form DNA that induces IFN in a TLR/RIG-I independent manner (209). DAI contains two N-terminal DNA binding domains, that preferentially bind Z-DNA and B-DNA. The C-terminal region has no homology to any known structure and its functional role in IFN signaling has yet to be elucidated (228).

Upon binding DNA, DAI interacts with TBK1 and IRF3, two key players in IFNβ induction and does not appear to associate with the adaptor molecules involved in TLR signaling (64, 209). In addition to activating IRF3, DAI also activates NFκB, another transcription factor needed for the induction of IFNβ. Knockdown of DAI expression results in the inhibition of NFκB mediated induction of the cytokine IL-6, suggesting that DAI also plays a role in proinflammatory signaling as well. However, the exact mechanism by which NFκB is activated in the DAI signaling pathway needs further study (64, 200, 209).

Although DAI knockdown by siRNA diminished IFNβ induction in response to B-DNA, it did not completely abolish gene induction (209). Furthermore, DNA-

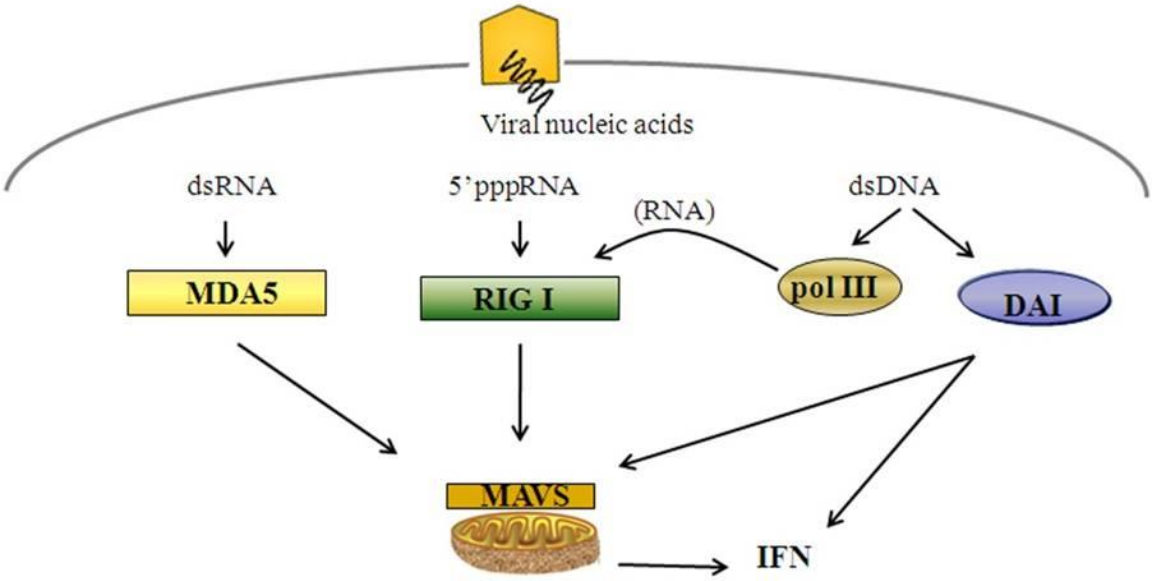

Figure 2: Cytoplasmic viral nucleic acid sensors.

RIG-I and MDA5 recognize viral 5'-ppp RNA with panhandle structure and long dsRNA, respectively. RIG-I and MDA5 interact with MAVS, which recruits downstream signalling to induce IFN. On the other hand, DNA sensors are thought to recognize cytoplasmic viral dsDNA, which induce IFN in a MAVS-dependent and -independent manner. Some cytoplasmic dsDNAs, such as poly(dA:dT), are transcribed by Pol-III, and the resultant dsRNA is recognised by RIG-I. Cytoplasmic DNA is also recognized by AIM2-containing inflammasome (not shown); however, this signaling pathway activates proinflammatory cytokines, such as IL-1 and IL-18, but not type I IFNs.

Figure adapted from Yoneyama, M., and T. Fujita. Rev Med Virol 20:4-22.

mediated activation of IFN and the innate immune response was found to be normal in DAI knockout mice (208). This data suggests that DAI is not the sole DNA sensor that activates IFN gene expression and there may exist a redundant cytosolic DNA sensor.

RNA Polymerase III as a Cytosolic DNA Sensor

RNA polymerase III (pol-III) synthesizes short untranslated transcripts that are essential for normal cell function, such as 5S rRNA and tRNA. Recently, RNA pol-III was found to play a novel role in detecting cytoplasmic dsDNA and triggering the IFN response (1, 29). A-T rich dsDNA is transcribed in the cytoplasm by RNA pol-III and the resulting dsRNA activates the RIG-I dependent IFN pathway. In human cells, knockdown of RNA pol-III expression, or the use of a specific chemical inhibitor of RNA pol-III, diminished the IFN response to transfected dsDNA as well as to infection by DNA viruses. However, in mouse cells, RNA pol-III knockdown did not fully abolish the IFN response to A-T rich dsDNA. This corroborates other mouse studies, which indicated that the lack of RIG-I signaling had little effect on the production IFN in response to dsDNA (90, 204). Although RNA pol-III plays a major role in the IFN response to dsDNA, it appears that there still exists another sensor for direct recognition of foreign DNA.

STING – A Central Adaptor for Cytoplasmic Sensors

Stimulator of Interferon Genes (STING) (also called Endoplasmic Reticulum IFN stimulator (ERIS) and Mediator of IRF3 Activation (MITA)) was recently identified as a new player in the cytosolic dsDNA- and RNA -mediated IFN signaling pathway (65, 66, 205, 247). STING is a ubiquitously expressed endoplasmic reticulum (ER) transmembrane protein, although its localization to the mitochondria has also been reported. Transfection of cells with STING rendered them resistant to infection by the negative-stranded RNA virus VSV and the inhibition of STING expression in cells markedly increased their susceptibility to VSV. While STING overexpression activates IFNβ gene expression, the transcription factors activated by the STING-mediated IFN pathway are still under scrutiny. IRF3 is activated in the STING-mediated IFN signaling pathway, but the involvement of NFκB is controversial (65, 247). Furthermore, the

STING-mediated response to cytoplasmic RNA depends on RIG-I, MAVS and TBK1 (247).

In addition to its role in the RNA activated RIG-I mediated IFN pathway, STING also plays a critical role in cytosolic dsDNA-mediated IFN signaling(66). STING-deficient MEFs have a deficiency in IFN production in response to poly dA-dT dsDNA, as well as to the DNA of Herpes Simplex Virus 1 (HSV-1) and the bacteria *Listeria monocytogenes*. Furthermore, STING knockout mice were susceptible to lethal infection by HSV-1, underlining the importance of the protein in the IFN signaling pathway. However, STING-deficient cells show an intact IFN response to exogenous CpG DNA, thus indicating that the TLR9 response is STING-independent. As in the STING/RIG-I pathway, the STING-mediated dsDNA IFN response depends on TBK1 and IRF3 activation. Based on these observations, it is believed that STING facilitates the detection of both viral RNA and dsDNA, converging the IFN pathways mediated by RIG-I, DAI and are yet unidentified cytosolic DNA sensor (Figure 3).

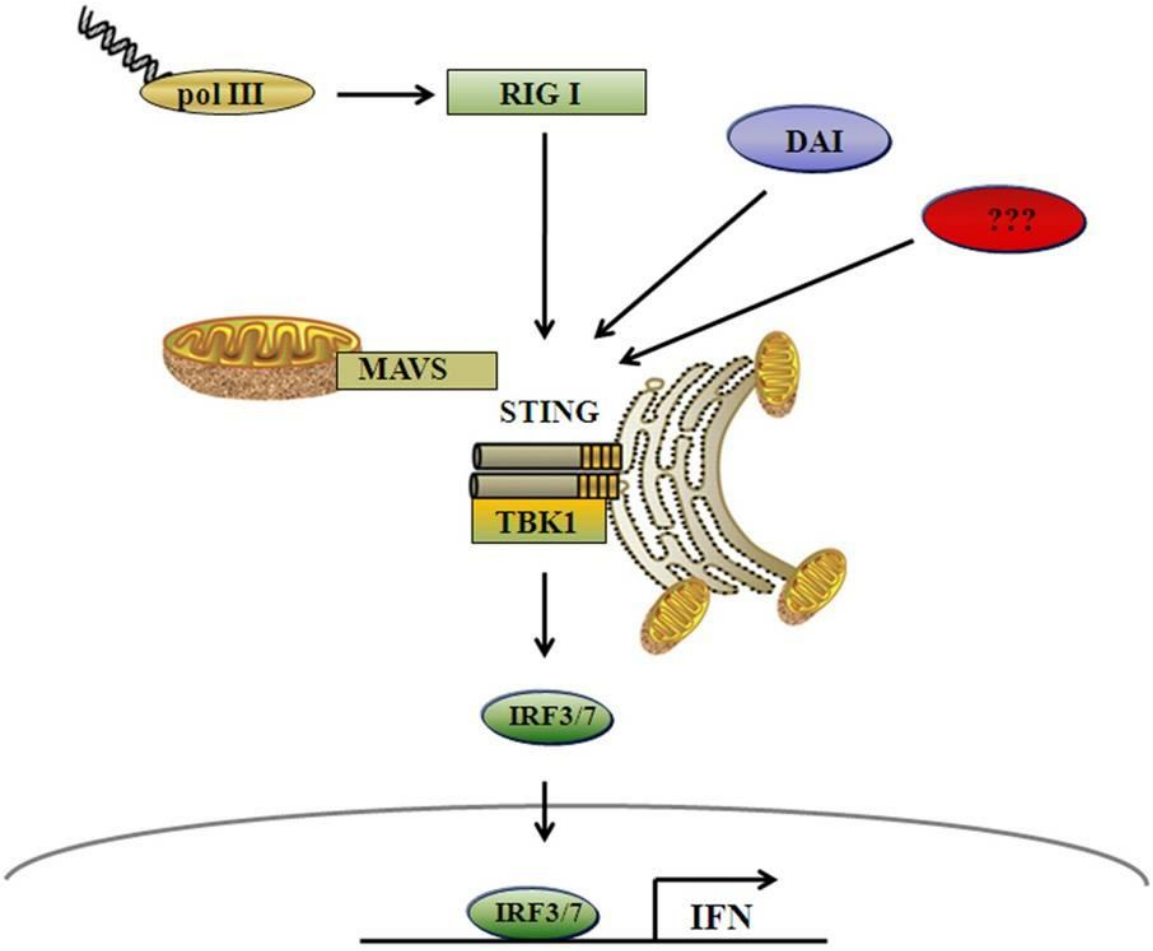

Figure 3: STING is an adaptor mediating the IFN responses to both intracellular DNA and RNA.

The efficient induction of a type I IFN response to viral RNA and DNA requires the central adaptor molecule STING, located at the ER. Cystolic RNA induces the IFN response via RIGI and its downstream mitochondrial associated adaptor molecule MAVS. RNA polymerase III (pol-III) detects cystolic microbial DNA that is transcribed and presented to the RIG-I sensor in the form of 5'-triphosphates dsRNA, triggering RIG-I activation. DAI and possibly a yet unknown DNA sensor also induce the production of IFN in response to foreign DNA. All four pathways induce IFN in a TBK1/IRF3 dependent manner.

Figure adapted from Nakhaei, P., J. Hiscott, and R. Lin. 2009. J Mol Cell Biol.

Part II: Interferons and Interferon Signaling

History of Interferons

IFN was the first discovered and described cytokine, a family of biological regulatory proteins secreted by cells (182). IFN's action was first noted for its induction of an antiviral state in cells infected by virus and those cells surrounding them. In 1957, Alick Iasaccs and Jean Lindenmann had shown that a supernatant derived from chick chorioallantoic membranes incubated with inactivated influenza virus was capable of protecting other membranes from infection by live influenza (62, 63). They dubbed the factors *interferon* because of the soluble protein's ability to *interfere* with virus replication.

Previously, in 1954, two Japanese virologists, Yasuichi Nagano and Yasuhiko Kojima, observed antiviral activity in rabbit skin or testis after injection with inactivated vaccinia virus (220). They published a report in a French journal (142) hypothesizing that a viral inhibitory factor in the infected tissue was responsible for the antiviral effects. They proceeded to show that the factor was not part of the virus and was in the supernatant of UV irradiated and fractionated infected tissue homogenate.

Today, it is known that the actions of IFN involve more than just the inhibition of virus replication. Through IFN signaling and the induction of the Interferon-Stimulated Genes (ISGs), they have both antiproliferative and proliferative effects as well as immunomodulatory and developmental roles in cell physiology (16).

The Interferon Family

The IFN family is divided into three types that bind to three distinct types of cell surface receptors. Type I consists primarily of one IFNβ gene and 13 IFNα gene subtypes; however other minor species also exist – IFNδ, IFNε, IFNκ, IFNω, IFNτ and IFNζ (16, 26). Type II, consists only of one IFNγ gene (50). The members of the third IFN family type, Type III, are the most recently described IFN and include IFNλ_1, IFNλ_2 and IFNλ_3 (6, 87).

Type I Interferons and Its Receptor Complex

IFNβ and α may be induced in most cell types, but IFNβ is highly produced by fibroblasts, while cells of lymphoid origin produce the most IFNα (182). The IFNβ gene and all the IFNα genes are encoded within a single exon on the short arm of human chromosome 9. IFNαs are more than 70% homologous to one another by amino acid sequence, whereas the IFNβ gene is only about 30% homologous to IFNα.

Crystallography studies (16, 76, 82, 164) show that the Type I IFNs contain 4-5 helixes connected by loops. The most conserved feature of the Type I IFNs is the disulfide bond – IFNαs contain two while IFNβ contains one (16). It is believed that the regions containing these disulfide bonds play a role in receptor binding. Mutations of the cysteine residues that form the disulfide bonds within the IFN protein result in loss of biological activity (16, 86, 182).

All members of the Type I IFNs bind to the same Type I IFN receptor complex, which is present on the surface of all vertebrate cells. The complex is made up of two subunits, IFNα receptors 1 and 2 (IFNAR-1 and IFNAR-2), which are encoded on human chromosome 21. The two subunits contribute to IFN binding to different extents, but both are necessary to form a functional binding site. While the IFNAR2 has good affinity for all the Type I IFNs, IFNAR1 alone has low intrinsic binding of Type I IFN. However, IFNAR1 has a strong affect on the affinity for ligand binding for the IFNAR complex as a whole. When IFNAR1 and IFNAR2 are expressed together, the affinity of IFN of the complex as a whole is ten times stronger than that of IFNAR2 alone (16, 103).

Although there is one Type I IFN receptor complex there are multiple Type I IFNs, creating redundancy in the Type I IFN system. The interaction between the different Type I IFNs and the receptor complex, as well as the mechanism of the biological response to the different IFN species, is still largely unclear. It has been speculated that the IFN species interact in slightly different ways or there may be more than one binding site for the IFNs within the IFNAR complex (55).

Type I Interferon Signaling and the Interferon-Stimulated Genes.

The IFNAR1 and IFNAR2 subunits do not have intrinsic activity but rely on their cytoplamic domains to associate with two tyrosine kinases, Tyrosine Kinase 2 (TYK2)

and Janus Kinase 1 (JAK1). The IFNAR1 associates with TYK2, while IFNAR2 associates with JAK1 (148). When IFN binds the extracellular domain of the IFNAR complex, the IFNAR subunits dimerize and the associated tyrosine kinases, TYK2 and JAK1, are phosphorylated. Knock out studies show that, of the two kinases, JAK1 is essential for Type I IFN signaling whereas TYK2 plays a more prominent role in interleukin (IL)-12 signaling (239).

Two transcription factors, Signal Transducers and Activators of Transcription (STAT) 1 and 2, are recruited to the receptor complex, where they are phosphorylated by the tyrosine kinases. The tyrosine phosphorylated STAT1 binds the tyrosine phosphorylated STAT2, which is associated with Interferon Regulatory Factor (IRF) 9. These three proteins form a complex called IFN-Stimulated Gene Factor 3 (ISGF3) and it translocates to the nucleus where it binds to the IFN-Stimulated Response Element (ISRE) within the promoter of ISGs and facilitates transcription (Figure 4) (196).

The expression of ISGs mediates the biological antiviral response within the cell. The biological functions of most IFN-induced proteins have yet to be uncovered, but several antiviral interferon-inducible gene products and their role in the antiviral and anti-proliferative state of the cell have been studied.

The RNA-dependent Protein Kinase (PKR) is a serine/threonine kinase that plays a role in transcription and translation. PKR is normally inactive, but after binding viral dsRNA it phosphorylates itself. Upon activation, PKR inhibits translation and prevents viral replication by phosphorylating the elongation initiation factor 2α (eIF-2α). Once phosphorylated, eIF-2α inhibits eIF-2β, the nucleotide exchange factor necessary for the recycling of eIF2 during protein synthesis (130, 199). Furthermore, PKR also modulates the activity of the transcription factor NFκB. It does so by phosphorylating and activating the Inhibitor of κB (IκB) Kinase complex (IKK), ultimately activating NFκB (see section on NFkB) (199).

Another interferon-inducible gene is 2'-5' oligoadenylate synthetase (OAS), which is also activated upon binding viral dsRNA. Its activation leads to the production of a series of short, 2',5'-oligoadenylates (2-5A) that activate the 2-5A–dependent ribonuclease, RNase L. RNase L activation leads to extensive cleavage of single-stranded RNA, effectively inhibiting protein synthesis (24, 199, 236).

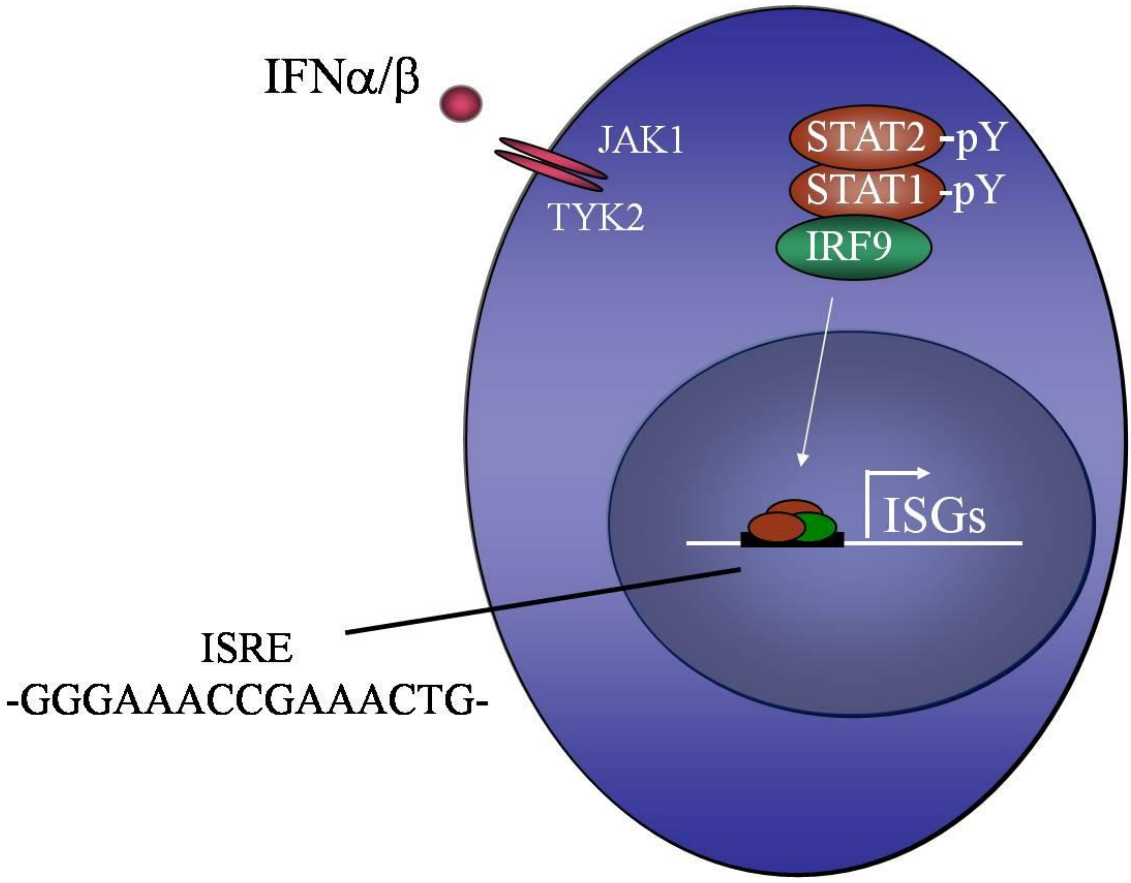

Figure 4: Model of Type I IFN Signaling.

IFN binding to the IFN cell surface receptor activates the associated Janus Kinases, JAK1 and TYK2. The JAKs, in turn, tyrosine phosphorylate STAT1 and STAT2, leading to their dimerization and translocation into the nucleus, along with the pre-associated IRF9. This complex, binds to the ISRE and leads to the transcription of target genes, such as the ISGs.

The MxA protein, another IFN-inducible protein, is a GTPase similar in homology to the dynamin family. The human MxA is induced in peripheral blood monocytes, plasmacytoid and myeloid dendritic cells (44, 223) and forms tight oligomeric complexes that interfere with viral replication and impair the growth of a virus by sequestering viral capsid proteins from nuclear import (84, 199). MxA displays its anti-viral effects on a variety of viruses, including orthomyxoviruses, rhabdoviruses, paramyxoviruses, and bunyaviruses (74, 83, 158, 159, 179).

Transcriptional Induction of Type I Interferons

The transcriptional induction of the type I IFNs is tightly regulated and involves various transcription factors and regulatory DNA sequences. Following virus infection, the IFNβ and IFNα genes are differentially induced in two waves - in an immediate response and a delayed response. In mice, the IFNβ gene and IFNα4 gene are induced after virus infection and do not require new protein synthesis. IFNs α2, 5, 6, and 8 display a delayed induction and are dependent on new protein synthesis. It is believed that the early expressing IFNs and the ensuing autocrine IFN signaling is required for the transcription of the second wave IFNs (118) (Figure 5).

Of the type I IFNs, IFNβ promoter activation has been studied to a greater extent. The virus responsive element (VRE) of the IFNβ gene functions as an enhancer, dependent on multiple transcription factors. The element resides in the promoter and contains Interferon Regulatory Factor (IRF) binding sites designated as Positive Regulatory Domain (PRD) I and III, to which activated IRF3 or IRF7 bind, although IRF5 has also been shown to also activate the IFNβ promoter in response to specific viruses and in certain cell types (180). This regulatory element is recognized by multiple factors, including High Mobility Group protein (HMG) I, to form an enhanceosome that can recruit the coactivator CBP/p300 and the polymerase II transcriptional machinery to initiate gene expression (Figure 6) (229). Further studies have found that activated NF-κB binds to PRDII and ATF-2/c-Jun binds PRDIV, respectively, in the IFNβ promoter. All of the DNA binding factors are required, as none alone can induce IFNβ gene expression(43).

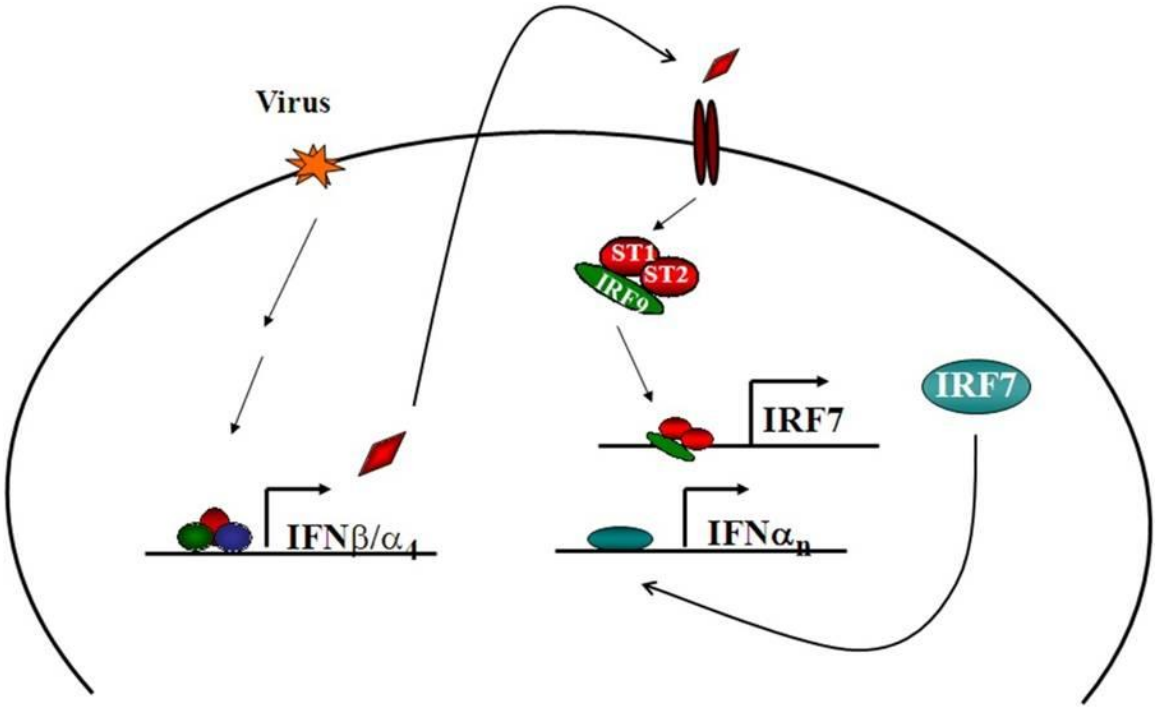

Figure 5: Multistage Induction of Interferon Genes.

In the early stage of interferon induction, IFNβ and IFNα4 are induced by activated transcription factors. Once secreted, the early stage interferons stimulate JAK/STAT signaling, which transcriptionally induces the IRF7 gene. The newly synthesized IRF7 is phosphorylated in response to the virus infection and is able to bind the promoter elements of the second wave IFNα genes.

Figure is adapted from Marie, I., J. E. Durbin, and D. E. Levy. 1998. EMBO J 17:6660-9.

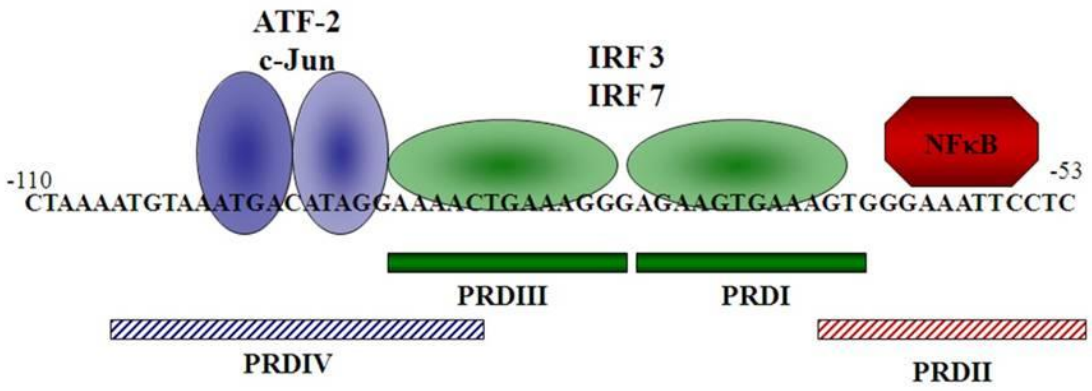

Figure 6: Interaction of Transcription Factors with the IFNβ Gene Promoter.

After virus infection, activated NFκB binds PRDII, while IRF3 binds PRDI and PRDIII; ATF-2/c-Jun bind PRDIV. IRF7 can participate in the secondary wave of IFNβ production.

Figure is adapted from Doly, J., A. Civas, S. Navarro, and G. Uze. 1998. Cell Mol Life Sci 54:1109-21.

As mentioned previously, following virus infection, members of the IFNα family are induced in two sequential phases. It is hypothesized that the second phase of IFN induction is reliant on the induction of IRF7 expression by IFNβ signaling (Figure 5). The transcriptional stimulation of the IRF7 gene results from the JAK/STAT signaling initiated by the first wave of IFN secretion (118). IRF7 may then induce the transcription of other IFNα subtypes, which IRF3 alone could not induce. It has also been found that IRF5 can substitute for IRF7; however, the activation of IRF5 is virus specific and results in the expression of a different group of IFNα subtypes (14).

Less is known of the regulation of the IFNα promoters. The early and delayed expression of the IFNα genes may be explained by naturally occurring nucleotide variations within the regulatory elements of the IFNα promoters (109) (Figure 7). The VRE of the IFNα promoters can possess up to four PRDI/III like elements (labeled A-D) to which transcription factors, like the IRFs, bind and participate in the genes' transcriptional induction (129). For example, the VRE within the promoter of the IFNα4 gene, which is expressed in the early stage of IFN induction, possesses four PRDI/III like elements and activated IRF7 preferentially binds to the first two overlapping elements, labeled A and B in Figure 7. The PRDI/III like elements A and B consist of the nucleotide sequences GTAAAGAAGT and GAAAGTGAAAAG, respectively. The third element, labeled C, is bound by activated IRF3 and consists of the sequence GAATTGGAAAGC. As with IFNα4, the VRE of the IFNα2 promoter contains the first two PRDI/III like elements. However, IFNα2's VRE does not possess the third PRDI/III like element due to two naturally occurring nucleotide variations at positions –80 and –78. The consequent GAATTAGGAAGC sequence is no longer able to recruit activated IRF3 to the IFNα2 promoter, perhaps explaining its delayed induction (136, 137).

Type II Interferon Signaling

IFNγ is the only member of the Type II IFN class. The gene encoding the IFNγ protein is found on human chromosome 12 (251) and is not related on a genetic nor protein level to the Type I IFNs. Two IFNγ polypeptides associate with each other in an

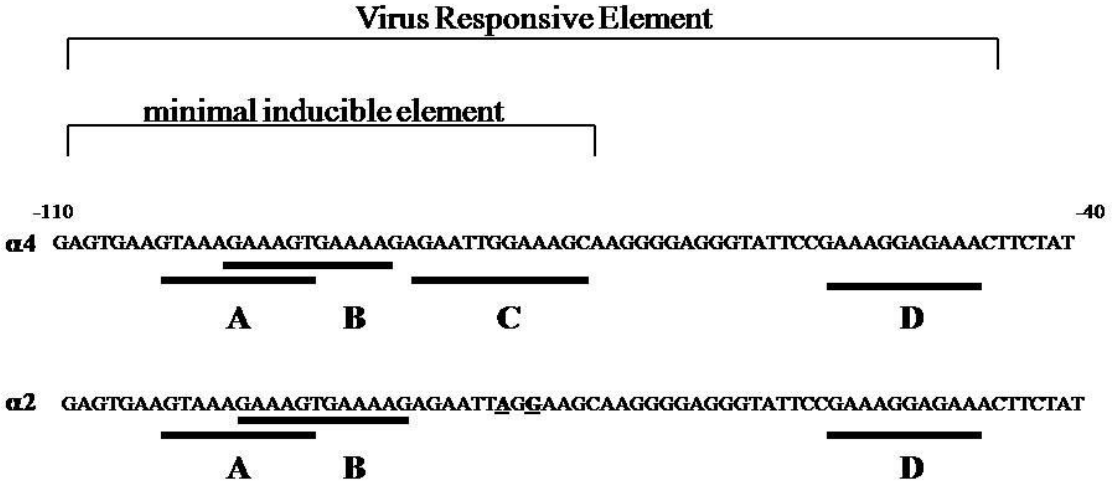

Figure 7: Comparison of the IFNα4 and IFNα2 Gene Promoters.

The -100 to -40 promoter region of IFNα4 and IFNα2 genes are aligned for comparison. Within the VRE of the IFNα promoters are PRDI/III like elements, labeled A-D, to which IRFs may bind. Activated IRF7 preferentially binds the first and second elements (A and B), while activated IRF3 prefers the third (C). The naturally occurring nucleotide variations at position -80 and -78 (underlined) in the IFNα2 promoter does not allow the binding of IRF3 to that region, perhaps explaining the delay in gene expression after virus infection.

Figure is adapted from Civas, A., M. L. Island, P. Genin, P. Morin, and S. Navarro. 2002. Biochimie 84:643-54 and Morin, P., J. Braganca, M. T. Bandu, R. Lin, J. Hiscott, J. Doly, and A. Civas. 2002. J Mol Biol 316:1009-22.

anti-parallel fashion to for the active IFNγ molecule (39, 226). The IFNγ molecule binds to a distinct IFNγ receptor (IFNGR) complex consisting of two IFNGR1 and two IFNGR2 chains, which are encoded on chromosomes 6 and 21, respectively. While nearly all cells express the IFNGR, only specialized cells of the immune system secrete IFNγ, including T cells, B cells, Natural Killer (NK) cells, dendridic cells (DC), monocytes and macrophages (181, 199).

IFNγ production is not only induced in response to infection, but also by cytokines secreted by antigen presenting cells (APCs), such as interleukin (IL)-12 and IL-18. While IFNγ can induce antiviral activity within the cell, IFNγ plays a more immunomodulatory role. For instance, the recognition of pathogens by macrophages induces secretion of chemokines and IL-12, which attracts NK cells to the site. IFNγ is induced by IL-12 in the NK cells, as well as the macrophages and any T cells in the vicinity. Furthermore, IFNγ also plays a role in the expression of the major histocompatibility complex (MHC) classes I and II, which are important for antigen presentation by these cells (181, 199).

Type II IFN signals through the Jak-Stat pathway, in a similar fashion to that of Type I, but with different players. IFNγ binds the two IFNGR1 chains, generating binding sites for the two IFNGR2 chains and the IFNGR1 and IFNGR2 chains come together. Each IFNGR chain associates with a Janus tyrosine kinase, IFNGR1 with JAK1 and IFNGR2 with JAK2 and the binding of IFNγ to the receptor initiates autophosphorylation of the JAKs and the phosphorylation of the IFNGR1 chain. STAT1 molecules are recruited to the phosphorylated receptor and are themselves tyrosine phosphorylated by the JAKs. Phosphorylated STAT1 molecules homodimerize and translocate into the nucleus and bind to the target gene promoters (181).

Type III Interferons

Type III IFNs are the most recently identified members of the IFN family and consist of IFNλ$_1$, IFNλ$_2$ and IFNλ$_3$ (also referred to as IL29, IL28A and IL28B, respectively). Human IFNλs and their receptor, the IFNλ receptor complex (IFNλR) (also referred to as IL28R), were uncovered by computational techniques focusing on

identifying new proteins based on sequence homology to members of the class II cytokine family, of which IFNs and IL-10 belong (87, 186). The IFNλs are expressed by most cell types but the expression of the IFNλR is limited to epithelial cells, pDCs (197) and, at low levels, cells of hemopoietic origin (4).

The genes encoding the IFNλs are found on chromosome 19 and, unlike the Type I IFNs, contain multiple exons. IFNλ_2 and IFNλ_3 are highly homologous on the amino acid level with 96% identity, whereas IFNλ_1 has only about 81% homology to its IFNλ_2 and IFNλ_3 counterparts. Although part of the IFN family, the Type III IFN have only about a 15% amino acid identity to IFNαs. Curiously, the mouse has only two intact IFNλ genes – IFNλ_2 and IFNλ_3 orthologs.

The IFNλR consists of IFNλR1 (also referred to as IL28Rα) and the accessory receptor chain IL10R2 (also referred to as IL10Rβ), which is also part of the receptors for the cytokines IL10, IL22 and IL26. Although the IFNλR subunits are not homologous to IFNAR, the IFNλs still signal through the JAK/STAT pathway. In fact, IFNλ JAK/STAT signaling occurs in an identical manner to that of Type I IFNs. STAT1 and STAT2 are phosphorylated by TYK2 and JAK1 upon IFNλ stimulation. Consequently, the IFNλs trigger a gene expression profile similar to that of the Type I IFN pathway and exhibit similar antiviral activity (4, 36, 37, 87, 250).

Although IFNλs differ genetically from the Type I IFNs, their regulation in response to virus appears to exhibit some similarities. Like IFNβ, IFNλ_1 is induced via RIG-I signaling, the TLR3 mediated signaling through TRIF, as well as the TLR7 mediated MyD88-dependent pathways (154). Furthermore, IFNλ_1 is regulated by the transcription factors IRF3 and NFκB (153). However, wherein both IRF3 and NFκB are required for IFNβ expression, NFκB plays the more dominant role in IFNλ_1 induction, perhaps due to a distal cluster of NFκB binding sites that act independently of the more proximal IRF binding site (67, 154, 216). To a lesser extent, it was found that IRF7 and IRF1 may also bind the IFNλ_1 promoter (154).

Whereas the IFNλ_1 gene promoter is regulated primarily by NFκB, the IFNλ_2 and IFNλ_3 gene promoters are regulated in a fashion more similar to that of the IFNα gene promoters. These promoters are activated by the MyD88-dependent signaling pathway

via IRF7, and to some extent, IRF1 (153, 154). Although it is believed that IRF7 plays the more dominant role in their induction, the IFNλ_2 and IFNλ_3 gene promoters do have NFκB binding sites within their promoters.

Part III: Transcription Factors Involved in IFN Signaling

STATs

Several transcription factor families play an integral role in response to viral infection. One family is signal transducers and activators of transcriptions (STATs) and is comprised of seven members – STAT1, 2, 3, 4, 5A, 5B and 6. These proteins are involved in immune function, development, cellular proliferation and survival. They are homologous in amino acid sequence and share several domain structures (Figure 8): an amino terminal coiled-coil domain, a DNA-binding domain (DBD), a Src Homology (SH2) domain, a linker region that contains a conserved tyrosine residue, which is phosphorylated, and a carboxy-terminal transcriptional activation domain (59).

IRFs

Another transcription factor family, the Interferon Regulatory Factors (IRFs), consists of nine members, IRF1-9, that help regulate the expression of genes involved in the response to pathogens, cellular survival and hematopoietic development (143). Some IRFs are expressed ubiquitously, while others are expressed in certain tissue types and still others are expressed only upon gene induction. IRFs share a homologous amino-terminal DBD that contains a helix-turn-helix motif and recognizes the core DNA sequence GAAA, which is found in the regulatory elements of target gene promoters. The less homologous carboxy-terminal region of the IRFs has a protein-protein interaction domain that allows the IRF to interact with distinct transcription factors (Figure 9). The diversity in this region results in the IRFs' ability to regulate both unique and common genes (166, 211).

NFκB

Having NFκB binding sites in their promoters, IFNβ and the IFNλs are directly regulated by NFκB. However, NFκB is a pleiotropic mediator of many cellular stresses. In addition to IFN induction, NFκB plays a role in cell growth, differentiation, inflammation and apoptosis (126).

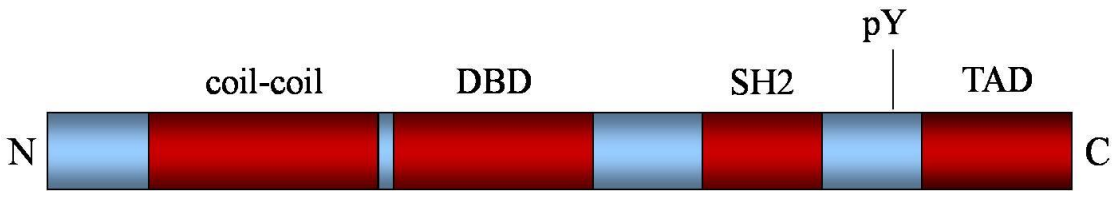

Figure 8: Domain Structures of the STAT Family.

Each STAT family member contains the following domains: the amino terminal coiled-coil domain, a DNA-binding domain, Src Homology 2 (SH2) domain, a carboxyl tyrosine that is phosphorylated and a carboxy-terminal transactivation domain (TAD).

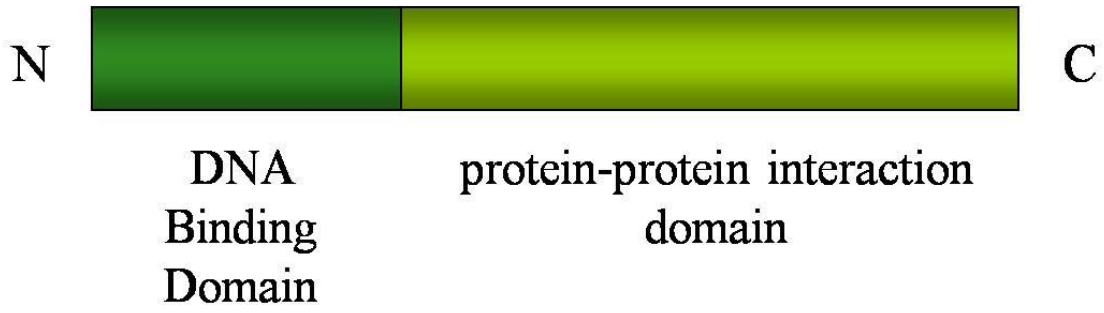

Figure 9: Domain Structures of the IRF Family.

The IRF family members share homology in their amino terminal DNA binding domain, which contains a helix-turn-helix motif and recognizes the DNA sequence GAAA. At their carboxy terminal end, IRFs contain a protein-protein interaction domain, which varies among the 9 different IRF family members.

Five proteins belong to the NFκB family – RelA (p65), RelB, C-Rel, p50, and p52. NFκB family members form homodimer or heterodimer complexes that vary in transcriptional activity. These complexes exist in the cytoplasm in an inactive form and require a stimulus for activation. The most common NFκB-activating pathway is the classical pathway, which involve RelA/p50 dimers and the pathway is triggered by tumor necrosis factor α (TNFα). When TNFα binds the TNF receptor (TNFR1), adaptor proteins such as TNF receptor-associated death domain protein (TRADD), receptor interating protein (RIP), and TNF receptor-associated factor 2 (TRAF2) are recruited to the cytoplasmic membrane, followed by the recruitment and activation of the IκB kinase (IKK) complex. The IKK complex consists of the scaffold protein IKKγ, and the serine kinases IKKα and IKKβ. The activated IKK complex phosphorylates the inhibitor of NFκB (IκB), which is then ubiquitinated and degraded through the proteasomal pathway. Once released from its inhibitor, NFκB is free to translocate into the nucleus and bind target gene promoters (126, 223) (Figure 10).

NFκB is also activated through an alternative pathway, which is independent of IKKγ and involves the subunits p52 and RelB. This alternative pathway is triggered by cytokines such as lymphotoxin B, B cell-activating factor (BAFF) or CD40 ligand (223). Adaptor proteins TRAF3, TRAF2, and TRAF6 are recruited to the cytoplasmic membrane and activate NFκB-inducing kinase (NIK). In turn, NIK activates a complex consisting of two IKKα proteins. IKKα phosphorylates p100, which is then ubiquitinated and processed and cleaved into p52. The p52/RelB dimer then is able to translocate into the nucleus (223) (Figure 11).

Postranslational modification of the NFκB complex before or after IkB degradation may enhance activation of the transcription factor. Phosphorylation of RelA has been studied the most extensively. RelA phosphorylation may occur in the cytoplasm or in the nucleus and is specific to certain stimuli. Stimulation of cells with LPS or TNFα activates a cytoplasmic protein kinase A (PKAc), which phosphorylates RelA on serine 276. This phosphorylation enhances RelA's ability to recruit histone acetyltransferase to the promoters of its target genes (248, 249).

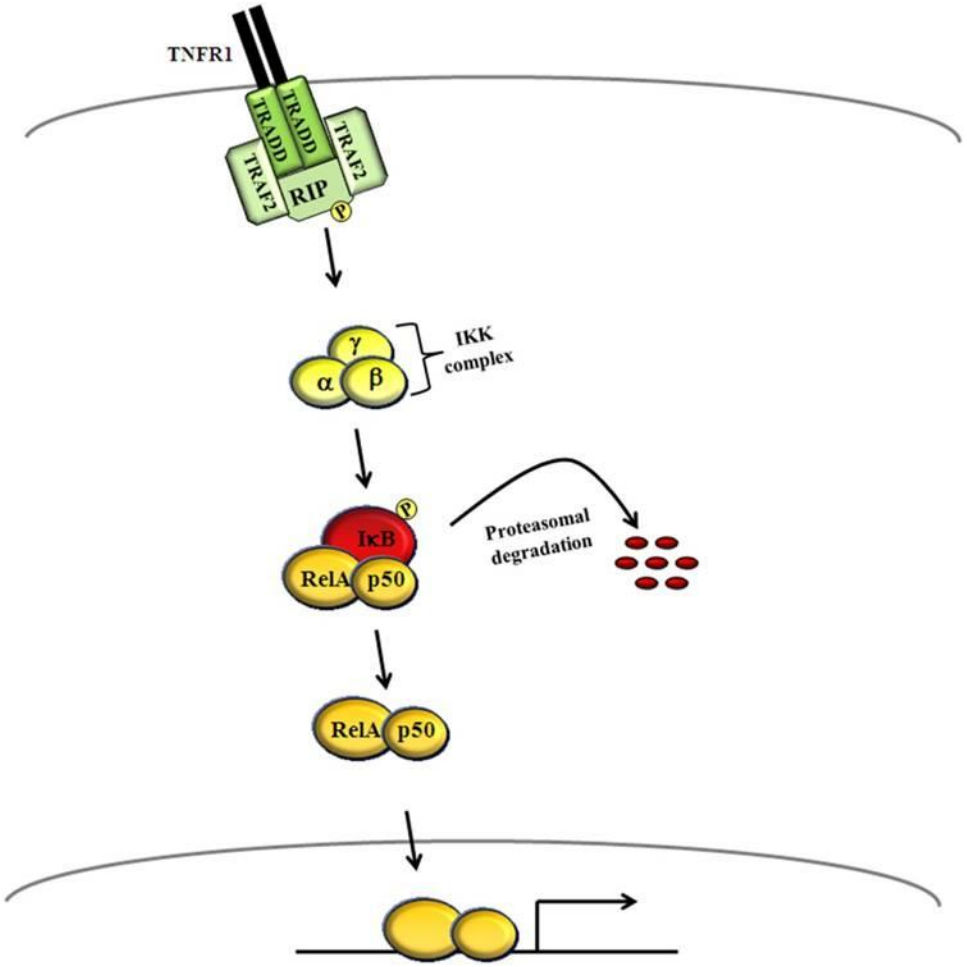

Figure 10: Classical Pathway of NFκB Activation.

RelA/p50 dimers are sequestered in the cytoplasm by the inhibitor IκB. The binding of TNFα to the TNF receptor recruits adaptor proteins TRADD, TRAF2 and RIP to the cytoplasmic domain of the receptor. These adaptors recruit and activate the IKK complex, which phosphorylates IκB. The phosphorylation of IκB leads to its ubiquitination and degradation by the proteasome. The NFκB complex is free to translocate into the nucleus and activate its target genes.

Figure adapted from Gilmore, T. D. 2006. Oncogene 25:6680-4.

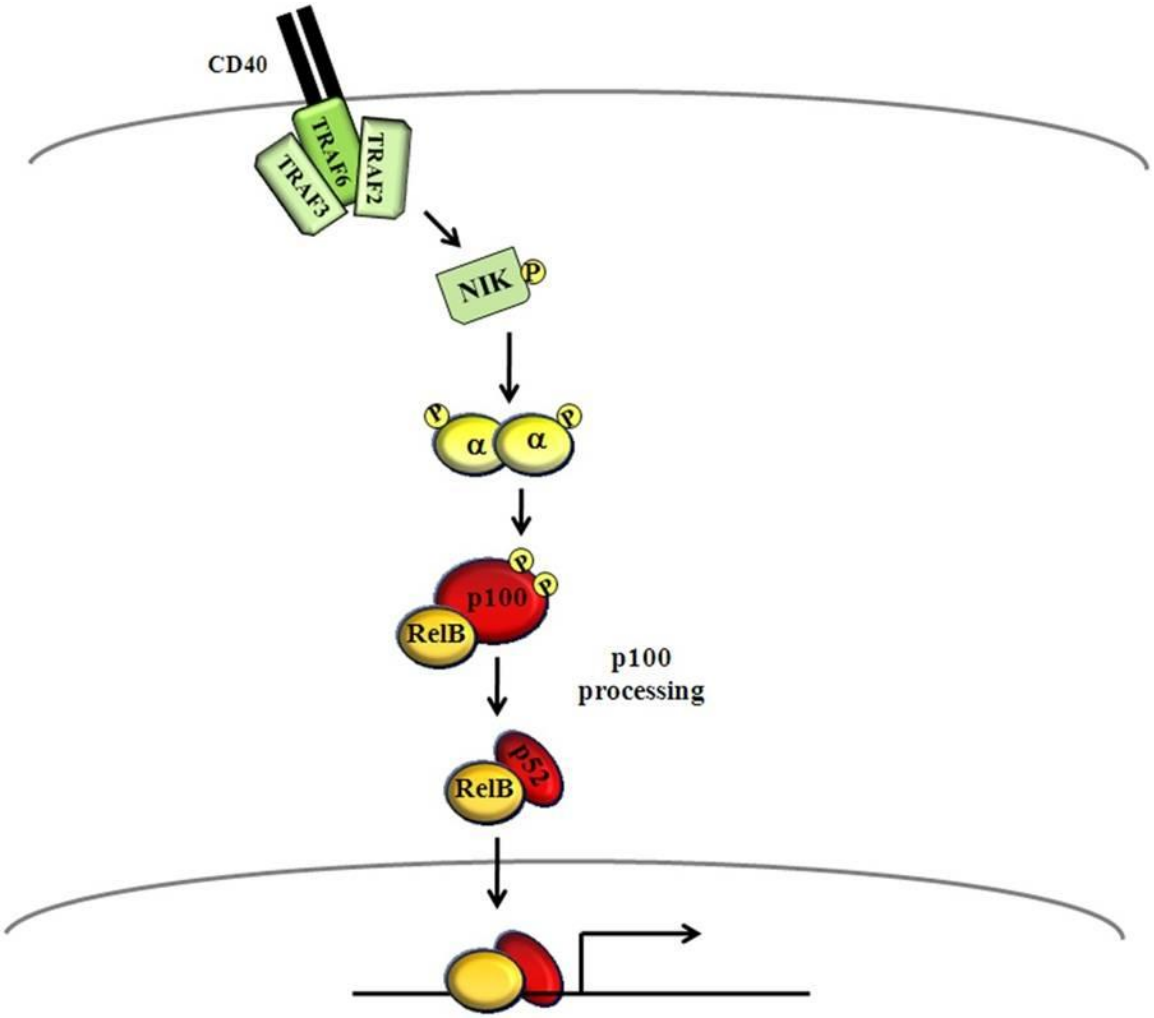

Figure 11: Alternative Pathway of NFκB Activation.

RelB is sequestered in the cytoplasm by the p52 precursor p100. The binding of CD40 ligand to CD40 recruits adaptor proteins TRAF6, TRAF3 and TRAF2 to the cytoplasmic domain of the receptor. These adaptors recruit and activate the NIK, which phosphorylates the IKKα complex. Activated IKKα phosphorylates p100, which leads to its partial proteolysis. The NFκB complex, consisting now of p52 and RelB, is free to translocate into the nucleus and activate its target genes.

Figure adapted from Gilmore, T. D. 2006. Oncogene 25:6680-4.

A number of kinases phosphorylate RelA on serine 536, including TBK1, IKKε, IKKα, IKKβ and Akt (20, 44, 114). Ribosomal S6 kinase 1 (RSK1) is one of the most recent kinases found to phosphorylates RelA on serine 536 in a p53-dependent manner (17). In response to DNA damage, p53 induces RSK1, which phosphorylates RelA. The phosphorylation of RelA decreases the affinity of RelA for IkB, releasing itself from the inhibitor in an IKK-independent manner (Figure 12).

Although many phosphorylation sites of the NFκB subunits and the kinases that are responsible for the phosphorylation have been identified (Table 2), it is still uncertain as to how these modifications regulate NFκB activity.

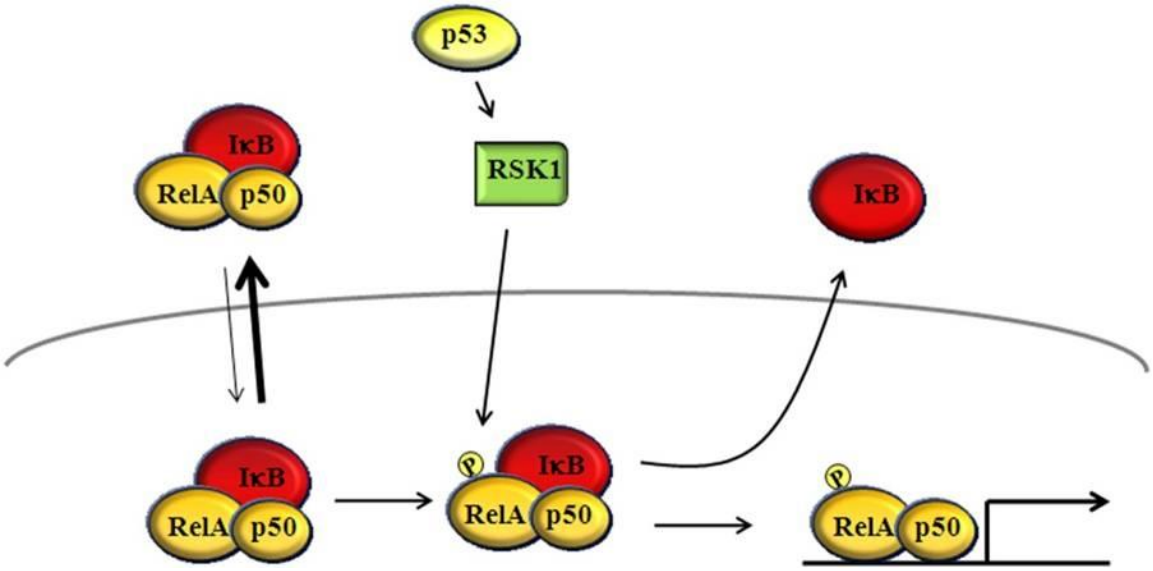

Figure 12: NFκB Activation by RSK1.

RelA/p50 dimers are kept inactive by the inhibitor IκB. In unstimulated cells, the NFκB/IκB complex shuttles between the cytoplasm and nucleus, but IκB mediates a stronger nuclear export and the complex remains predominately in the cytoplasm. p53 induces RSK1 activation, which promotes the phosphorylation of serine 536 of RelA in the nucleus. The phosphorylation of RelA decreases its affinity for IκB. Once IκB disassociates from the NFκB complex, it continues to shuttle in and out of the nucleus, while NFκB is free to activate its target genes.

Figure adapted from Bohuslav, J., L. F. Chen, H. Kwon, Y. Mu, and W. C. Greene. 2004. J Biol Chem 279:26115-25.

Table 2: Kinases known to phosphorylate RelA.

Kinase	Residue Phos.	Stimulus
PKAc	Ser276	LPS
MSK1/2	Ser276	TNFα
CK2	Ser529	TNFα IL-1β
IKKα	Ser536	virus Lymphtoxin β
IKKβ	Ser536	TNFα T cell stimulation
Akt	Ser536	IL-1β
RSK1	Ser536	DNA damage
TBK1	Ser536	IL-1β
IKKε	Ser536	IL-1β

Adapted from Viatour, P.,Merville, MP, Bours, B and Chariot, A. 2005.Trends Biochem Sci 30:43-52.

Part IV: DNA Damage Response

The DNA damage-response pathway is a complex system of interacting proteins that sense and repair DNA damage. In the absence of the DNA damage response, cells do not effectively process insults to the genome, which leads to chromosomal changes, gene mutations, and malignant transformations. Therefore, the proteins involved in the DNA damage-response are critical for maintaining genomic stability.

DNA Damage-Repair Mechanisms

Since there are a variety of DNA lesion types, the cell has developed several DNA repair mechanisms, which are characterized as either *direct-damage reversal* or *removal and replacement* (Figure 13). Direct-damage reversal of certain DNA lesions is the simplest of repair mechanisms since it only requires single enzyme-chemical reactions that can repair the DNA without incision of the sugar-phosphate backbone or removal of bases. Simply put, a chemical modification of the DNA is reverted and returned to its original state. Although this repair mechanism results in essentially error-free repair, only a few types of lesions are repaired in this manner. The two main types of direct DNA damage-reversal systems are the repair of alkylating damage and the repair of UV light-induced photolesions (40).

The remaining forms of DNA repair consist of complicated series of catalytic events mediated by multiple proteins and enzymes. These DNA repair mechanisms include single-stranded break (SSB) DNA repair, base-excision repair (BER), nucleotide-excision repair (NER), mismatch repair (MMR) and double-stranded break (DSB) DNA repair.

There is some overlap between the enzymes used to remove and repair DNA breaks. SSB, the most common type of DNA damage, are discontinuities in one strand of DNA and are associated with the loss of a single nucleotide and a damaged 5′- or 3′-terminal end. This may occur with exposure to intracellular metabolites, from spontaneous DNA decay or as normal intermediates of BER. Therefore, BER and NER may be considered sub-pathways of SSB repair. SSBs are repaired by a rapid process

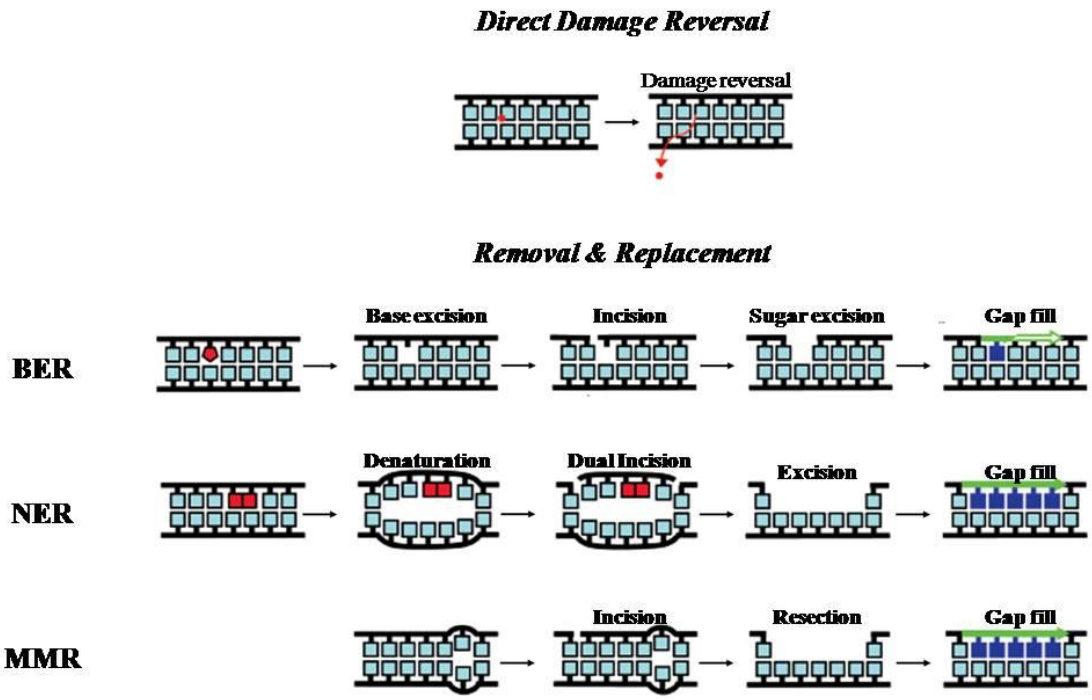

Figure 13: ***Direct-damage reversal*** **and** ***Removal and replacement*** **DNA repair strategies.**

Direc- damage reversal repair reverts chemical modifications of DNA and returns the DNA to its original state without incision of the backbone or removal of bases. *Removal and replacement* repair strategies include base-excision repair (BER), nucleotide-excision repair (NER), mismatch repair (MMR), Single-stranded break (SSB) repair and Double-stranded break (DSB) repair (see Figure 14 for SSB and DSB repair.) *Removal and replacement* repair strategies involves identifying the lesion, incising and excising the DNA, followed by DNA gap filling and ligation by DNA polymerases and ligases.

Figure adapted from Nouspikel, T. 2009. Cell Mol. Lif Sci. 66(6):965-967.

that can be divided into four basic steps - SSB detection, DNA end processing, DNA gap filling and DNA ligation (23).

BER consists of a multiple-step process that corrects damage to bases resulting from oxidation, methylation, deamination or the spontaneous loss of the base (125). Specific enzymes called glycosylases recognize these lesions on the DNA bases and remove the damaged base from its deoxyribose. The subsequent repair reactions are continued as in SSB repair wherein a common set of enzymes nick the DNA backbone, remove the deoxyribose, and fill the remaining gap (147).

NER is undertaken by a large complex called the nucleotide-excision repairosome. This set of enzymes senses the helical distortion and chemical modification of the DNA caused by the presence of a lesion. DNA is incised upstream and downstream of the lesion and a short piece of ssDNA, which contains the lesion, is removed and the resulting gap is repaired by DNA polymerases and ligases (146, 147).

MMR corrects replication errors, such as mismatches of bases and base insertions or deletions that result from polymerase misincorporation or template slippage. The actual MMR process is similar to BER and NER. The lesion is recognized, a segment of DNA is excised and the strand is corrected by DNA repair enzymes (92, 160).

DSB are the most severe and toxic DNA lesions. This type of damage is caused by a large variety of insults, including ionizing radiation, endogenously generated reactive oxygen species, replication of single stranded DNA breaks, viral replication and exogenouse genotoxic agents (115, 147, 193, 224). Two distinct repair systems are associated with DSB - non-homologous end joining (NHEJ) and homologous recombination (HR) (69). Through the creation of a synapsis between the damaged DNA and an undamaged homologous DNA region, the HR process allows the retrieval of genetic information from the homologous undamaged DNA molecule. This process occurs during late S phase or G2 phase of the cell cycle, when undamaged chromatids are available for use as DNA templates for the repair. On the other hand, NHEJ rejoins two DNA DSBs and does not require a homologous template during the repair process. As a result, the NHEJ repair process is prone to errors (Figure 14).

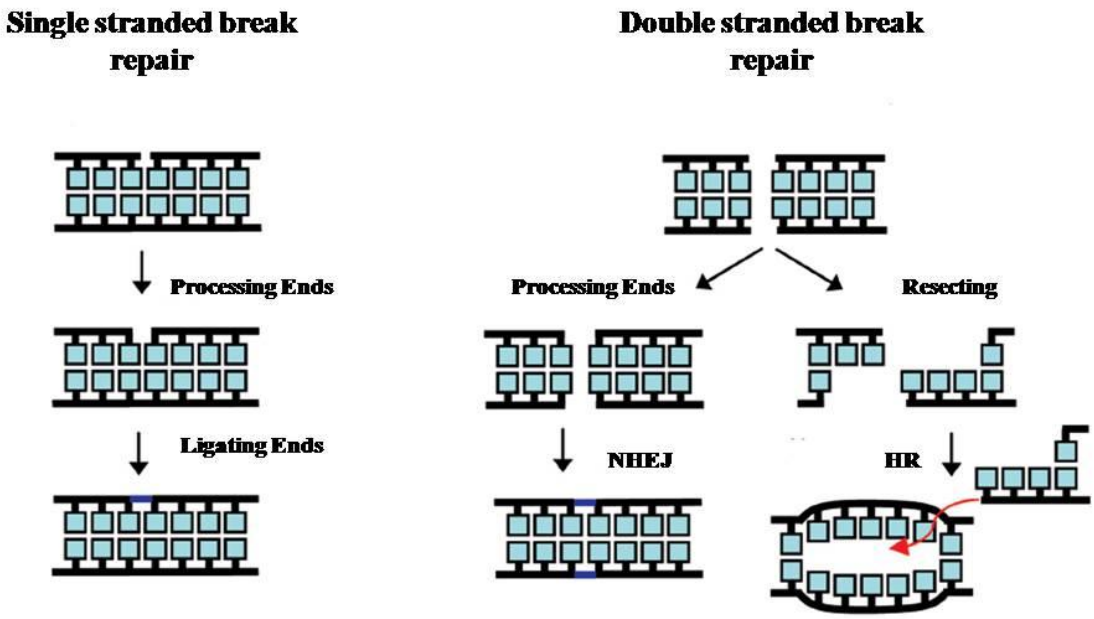

Figure 14: Single-stranded break repair and Double-stranded break repair strategies.

Single-stranded break (SSB) are repaired are detected and the DNA ends are processed to allow ligation of the two ends. BER and NER may be considered part of the SSB repair strategy since there is overlap in the mechanism and enzymes utilized during the repair process (see Figure 13). Double-stranded break (DSB) repair consists of two repair systems – Homologous recombination (HR) and Non-homologous end joining (NHEJ). HR allows the retrieval of genetic information from the homologous undamaged DNA strand. NHEJ rejoins the two DNA ends without a homologous template.

Figure adapted from Nouspikel, T. 2009. Cell Mol. Lif Sci. 66(6):965-967.

Signal Transduction Pathways Responding to DNA Damage

In addition to DNA-damage repair, the cellular response to DNA damage also entails signaling pathways that can result in cell cycle arrest, apoptosis or cellular senescence. Sensors interact directly with the damaged DNA and trigger the activation of a protein kinase cascade through a transducer, which amplifies the signal by targeting a number of effectors that carry out the response to the damage (69).

The DNA-damage signal transduction pathways are primarily regulated by phosphoinositide three-kinase-related protein kinases (PIKKs). Three PIKK family members, ataxia-telangiectasia mutated (ATM), ATM- and Rad3-related (ATR) and DNA-dependent protein kinase catalytic subunit (DNA-PKcs), are the key proteins that signal the presence of DNA damage by phosphorylating hundreds of proteins that are involved in the regulation of cell cycle progression, DNA repair and apoptosis (2, 111) (Table 3).

ATM

ATM is a serine/threonine protein kinase that is activated in response to DSB, such as those caused by ionizing radiation. Although the PIKKs mentioned above have the ability to bind DNA directly, they depend on other proteins to recognize DNA lesions (187, 189). The Mre11-Rad50-Nbs1 (MRN) complex binds to the ends of DSB and recruits ATM to the lesion (32). ATM molecules, in their latent state, are found as dimers. When cells are irradiated, however, the ATM molecules phosphorylate one another and separate to bind the damaged DNA (10). Upon activation, ATM functions as a regulator of a wide variety of downstream proteins, including tumor-suppressor protein p53, checkpoint kinase Chk2, structural maintenance of chromosome 1 (Smc1), which together cause cell cycle arrest at G1-S (69).

ATM signaling can also induce apoptosis. For example, ATM phosphorylates the transcription factor E2F1, preventing its degradation. The increase in E2F1 during the S-phase of the cell cycle, activation of Chk2 and the induction of p73 all lead to apoptosis (188, 203, 240).

A mutation in the ATM gene is the cause of a rare autosomal-recessive disorder called ataxia-telangiectasia. ATM deficiency predisposes patients to cancer and

Table 3: Components of the DNA damage response to SSB and DDB.

DNA damage	DNA response pathway	Adaptor to sense damage	Transducers	Effectors	Cellular outcomes
SSB	ATR	ATRIP RPA	ATR Chk1 BRCA1	H2AX p53 p21 Smc1	Cell cycle arrest DNA repair
DSB	ATM	MRN complex	ATM Chk1 Chk2	H2AX p53 p21 Smc1 53BP1 Mdm2 E2F1	Cell cycle arrest DNA repair Apoptosis
	DNA-PK	Ku70/Ku80	ATM DNA-PK	H2AX p53 p21 Mdm2 MRN XRCC4	Cell cycle arrest DNA repair Apoptosis

Adapted from Sinclair, A., Yarranton, S., Schelcher, C. 2006.Expert Rev Mol Med.8(5): 1-11.

immunodeficiency, increases sensitivity to ionizing radiation, and leads to progressive neurological degeneration (93, 170).

ATR

While searching and analyzing the human genome, ATR was initially described as a gene with sequence homology to ATM and Rad3. While ATM responds to DSB, ATR responds to SSB, such as those caused by UV light. ATR does not recognize DNA SSB directly and therefore requires ATR Interacting Protein (ATRIP) and Replication Protein A (RPA) to associate with the DNA lesion. ATR phosphorylates similar substrates to those phosphorylated by ATM. These include breast cancer type 1 susceptibility protein (BRCA1) and checkpoint kinase, Chk1, which recruit effectors such as histone H2AX, Smc1, p53, and p21 (193). These proteins initiate DNA repair and promote cell cycle arrest at the G2-M checkpoint. Since ATR and ATM can phosphorylate similar sets of proteins, there appears to be some redundancy in the DNA damage response. It has been observed that ATR overexpression can rescue some, but not all, of the ATM deficiency phenotypes (31, 38).

Knockout of ATR in mice causes embryonic lethality (19) and the only mammalian disease associated with ATR deficiency is a form of Seckel syndrome, wherein a splicing mutation causes partial loss of ATR activity (3). Although, patients with the ATR mutation have some overlapping symptoms as those of ataxia-telangiectasia, Seckel syndrome is predominately characterized by proportionate dwarfism, developmental delay, and microcephaly (150, 151).

DNA-PKcs

DNA-PKcs is recruited to DSB by interacting with Ku70/Ku80 and forming the complex DNA-PK. Unlike ATM, DNA-PK does not appear to signal to checkpoint pathways, such as CHK1/CHK2. However, DNA-PK does interact with p53 and regulates the p53-dependent apoptotic pathway (240). Another role of DNA-PK seems to be in promoting the rejoining of DSB in the NHEJ DNA repair mechanism. However, DNA-PK cells deficient in DNA-PK are defective in DSB repair by NHEJ as well as in

V(D)J recombination (195), a process in which antibodies and T-cell receptor diversity is generated (38).

Part V: Viral Attempts to Block IFN and DNA Damage Signaling

Defense against viral infection requires the cell to initiate multiple signaling cascades. These signal transduction pathways can activate IFN signaling in response to viral molecular motifs or they can induce DNA damage signaling in response to the presence of viral genetic material (233) or the integration of viral DNA into the host genome (194). In turn, viruses have responded to the host cell's defense strategies by evolving mechanisms to counteract or circumvent the IFN-antiviral response and tailor DNA damage-signaling pathways to promote their survival (49, 102, 182).

Viral Evasion of the IFN System

Viruses use several strategies to block different aspects of the IFN signaling pathway. These include attempts to block IFN synthesis and signaling or inhibit the function of IFN-simulated genes (Table 4).

In an attempt to minimize the amount of IFN produced by the host cell, viruses have developed ways to intervene at various points in the IFN induction pathway. Bovine viral diarrhea virus (BVDV) secretes a glycoprotein with RNAse activity, E_{rns}, that binds and degrades extracellular dsRNA in an attempt to block TLR3 activation (61). Other viruses block TLR activation by targeting downstream TLR adaptors. For example, the NS3/4a protein of Hepatitis C Virus (HCV) cleaves TRIF, thus blocking TLR3 signaling (97). Transcription factors responsible for IFN induction are other viral targets. The E6 oncoprotein of Human Papilloma Virus 16 (HPV16) blocks IFNβ gene induction by binding to IRF3 and inhibiting is transcriptional activity (168). Another transcription factor involved in IFN induction, NFκB, is also inhibited by viruses. For example, African swine fever virus (ASFV) produces an orthologue of IκB, inhibiting NFκB transcriptional activity by sequestering it within the cytoplasm (163).

Disruption of IFN signaling is another strategy employed by viruses to ensure their survival within the host. The poxviruses Myxoma virus (MYXV), ectromelia virus (ECTV), cowpox virus (CPXV), and vaccinia virus (VACV) all generate and secrete viral IFN-binding proteins that bind and neutralize IFN (138, 206, 221). Another point of interference by viruses is the JAK/STAT signaling pathway. Human cytomegalovirus

Table 4: Examples of viruses that inhibit IFN signaling and action.

Mode of Action	Virus	Viral Protein
Degrades dsRNA stimulus	BVDV	RNase activity of E^{rns}
Cleave TRIF, blocking TLR3 signaling	HCV	NS3/4a
Bind and inhibit IRF3	HPV 16	E6
Inhibit NFκB by sequestration in cytoplasm	ASFV	A238L
IFN sequestration/neutralization	poxviruses	Soluble IFN receptor orthologs
JAK1 proteasomal degradation	HCMV	IL-1β
STAT1/STAT2 sequestration	HCMV	IE1
Block IFN induced gene PKR action	VACV	K3L
Block IFN induced gene PKR action	HIV	Tat
Inhibit dimerization PKR	HCV	NS5A

Adapted from Randall, R and Goodbourn, S. 2008. J Gen Viro. 89(1):1-47. and Grandvaux, N. et al.2002 15(3):259-267.

(HCMV) disrupts signaling through JAKs and STATs several ways. For example, it decreases the levels of JAK1 by targeting it for proteasomal degradation (132, 133) and the IE1 protein sequesters STAT1 and STAT2, preventing their nuclear translocation (157).

Finally, viruses have evolved mechanisms to inhibit the function of IFN-inducible genes that interfere with viral replication. Protein kinase PKR activity is blocked by the K3L protein encoded by vaccinia virus and the Tat protein encoded by HIV (21, 210). These proteins function as decoys of the PKR substrate eIF-2. The HCV NS5A protein, on the other hand, is able to bind directly to PKR and block its dimerization (46).

Viral Interactions with the Host DNA Damage Response

Exposure of viral genomic material to the host's cellular machinery may occur during viral infection and replication and can become stimuli for the DNA damage response (233). Viruses attempt to inhibit the host's DNA damage response since processing of the viral genome could interfere with its life cycle. The most common tactic viruses undertake to inactivate the DNA damage response is either degradation or mislocalizaion of DNA repair proteins (102) (Table 5). For example, adenovirus (Ad) encodes the E4Orf3 protein that sequesters the MRN complex away from viral DNA and the E4Orf6 and E1b55K proteins target the MRN complex for proteasomal degradation (41, 201).

HSV1 also has mechanisms to inhibit DNA damage signaling. ATM activation is observed in HSV- infected cells (190), yet ATR signaling remains silent. HSV1 encodes the ICP0 protein which mislocalizes ATRIP, the ATR interacting protein required for ATR recognition of SSB (235). Furthermore, ICP0 also binds DNA-PKcs and targets it for proteasomal degradation (156).

While some viruses inhibit the DNA damage response in host cells, others attempt to take control of the DNA damage machinery to aid them in their own replication (233). The stability of concatemers during HSV-1 infection may require the MRN complex and cellular DNA damage response machinery. When HSV-1 infects cells expressing mutant Mre11 or ATM, significant defects in viral replication are observed (100).

Table 5: Examples of viruses that interact with DNA damage signaling.

Target	Mode of Action	Virus	Viral protein
MRN complex	Mislocalizes complex	Ad	E4Orf3
MRN complex	Proteasomal degradation	Ad	E4Orf6 E1b55K
ATRIP	Mislocalizes protein	HSV1	ICP0
DNA-PKcs	Proteasomal degradation	HSV1	ICP0

Adapted from Lilley, C., Schwartz, RA, Weitzman, MD 2007 Trends in Micro. 15(3):119-126.

Part VI: Etoposide

The chemotherapeutic drug etoposide has been used in modern clinical medicine for over thirty years in treating a wide variety of cancers, most commonly small cell lung cancer, testicular cancer and lymphomas. It is a preferred cancer drug in single and combination therapies, not only because of its significant anti-tumor activity, but also because of its low toxicity and side effects (11).

Etoposide is a derivative of a naturally occurring compound, podophyllotoxin, found in the roots of the mandrake or May apple plant. The dried roots of the plants have been used by native Americans as an emetic, cathartic, antihelmintic and cholagogue for hundreds of years (60, 79). The plant extract was used by American physicians as early as 1820 and became popular for curing genital warts in the 1940s (128).

Etoposide belongs to a class of anti-neoplastic drugs whose mechanism of action involves the targeting of topoisomerase II (52). Topoisomerase II carries out transient double stranded breakage and reunion reactions of DNA in order to relax negative and positive supercoils. This type of topological manipulation is essential for normal cellular functions, such as replication, transcription and genetic recombination (96).

Although etoposide is classified as a topoisomerase II inhibitor, it does not block total catalytic function of this enzyme, per se. Once topoisomerase II binds and cleaves DNA, etoposide stabilizes the intermediate topoisomerase II-DNA complex and alters the ability of topoisomerase II to religate the cleaved DNA stands. This enhancement of double stranded breaks in the DNA, results in a shift in the DNA cleavage/religation equilibrium towards the cleavage reaction (128). With a critical number of DNA breaks, cell death pathways may be triggered, leading to apoptosis (80).

Etoposide is a cell phase-specific cytotoxic drug. It prevents cells from entering mitosis, slowing down cell cycle progression in the late S and early G2 phases, resulting in G2 arrest. Neoplastic cells are much more sensitive to etoposide than normal host cells due to their more proliferative nature and the subsequent higher number of active topoisomerase II molecules. Furthermore, the general nature of most tumor cells lends them susceptible to the inability of regulating cell cycle progression in order to allow the proper repair of the DNA lesions (128).

RESEARCH RATIONAL

The IFN signaling pathway is a well-characterized response to viral infections, playing a vital role in both innate and adaptive immunity. However, there also have been studies suggesting that IFN signaling occurs in response to DNA damage. For example, one study found an increase in ISG15 expression with camptothecin treatment, while another study reported that STAT1 associates with cell cycle checkpoint proteins after γ-irradiation (105, 218). Yet, other studies reported interferon related gene expression profiles in cells resistant to chemotherapy and radiation (219, 232).

DNA viruses generate single stranded and double stranded DNA breaks during lytic replication. During viral infection, DNA damage response signaling pathways of the host can be activated. Viral genomic material can mimic single or double stranded DNA breaks, acting as a stimulus for the DNA damage response. Although viruses such as human immunodeficiency virus have RNA genomes, they integrate viral DNA into the host genome, also creating DNA strand breaks.

In this dissertation, I hypothesize that that there may be a link between the cellular response to virus infection and DNA damage. An IFN arm of the DNA damage response may have evolved as an antiviral response to the DNA damage induced by viruses. I examine whether IFN signaling occurs during DNA damage, by studying ISG and IFN gene expression after treatment by the DNA damaging agent etoposide. Furthermore, I begin to characterize the convergence of the DNA damage signaling and IFN signaling pathways, studying the role that ATM, NFκB and the IRF family members in the IFN response to DNA damage.

MATERIALS AND METHODS

Cell cultures.

Hec-1B, HeLa S3, HT1080 and THP-1 cells were obtained from American Type Culture Collection. With the exception of the THP-1 cells, all cells were grown in DMEM with 8% FBS. THP-1 cells were maintained in RPMI with 8% FBS. HCT116 cells were obtained from Dr. Bert Vogelstein (Johns Hopkins Medical Institutions, Baltimore, MD) and cultured in McCoy's 5A medium supplemented with 10% FBS.

New Castle Disease Virus (NDV) (NJ-LaSota-1946) was a gift from Dr. P.M. Pitha-Rowe (Johns Hopkins University, Baltimore, MD) and was propagated as described previously (231). Infections were performed at 200 hemagglutination units/mL for the times indicated.

A tetracycline-regulated expression system (T-Rex system; Invitrogen, Carlsbad, CA) was used as directed to generate an IRF7-inducible HT1080 cell line. In short, the coding sequence of IRF7 was obtained from Dr. Joseph S. Pagano (University of North Carolina, School of Medicine, Chapel Hill, NC) and subcloned into the pcDNA4/TO/Myc-His vector. The IRF7-myc plasmid was cotransfected with the pcDNA6/TR plasmid that encodes the tet repressor at a 1:6 (w/w) ratio. Stable transfectants were obtained by drug selection using Zeocin (1mg/ml) and blasticidin (5ug/mL). Cells were maintained in DMEM with 8% FBS and myc-IRF7 was induced using 2ug/mL doxycycline.

Primary monocytes were isolated from leukopaks that were obtained from three different healthy donors (Long Island Blood Services, NY). Leukocytes were purified from the leukopak using a hyperosmotic medium (AccuPrep; Accurate Chemical Co., Westbury, N.Y.) and monocytes were isolated from the leukocyte population using the MACS Monocyte Isolation Kit II (Miltenyi Biotec Inc., Auburn, CA) and maintained in RPMI with 10% FBS. The leukopak was diluted 1:1 with sterile PBS without Ca^{2+} or Mg^{2+} and mixed gently by inversion. 15mL of AccuPrep was overlayed with 30mL of diluted leukopak in 50mL conicals and centrifuged at room temperature for 20 minutes at 800xg, without brake. The top plasma layer was carefully aspirated to the 25mL mark on the conical and discarded. The lymphocytes are found at the interface between the

plasma and AccuPrep layers and were collected with a sterile Pasteur pipette and placed in a sterile 50mL conical and diluted 1:1 with MACS buffer (PBS without Ca^{2+} or Mg^{2+}, 2mM EDTA, 0.5% low endotoxin BSA; solution sterilized with 0.45um filtration unit). Once the diluted lymphocytes were mixed well by inversion, they were centrifuged at 800xg for 6 minutes. The pellets were washed in 10mL of MACS buffer until the ratio of residual platelets to lymphocytes is no greater than 1:1 (about 4-5 washes). After the last wash, the lymphocyte pellets were resuspended in 10mL MACS buffer and further processed using the MACS Monocyte Isolation Kit to isolate monocytes. 10^7 lymphocytes were resuspended in 30uL of MACS buffer for each MACS column used. 10uL of FcR Blocking Reagent (included in kit) was added to each lymphocyte sample, followed by 10uL of Biotin Antibody Cocktail. Samples were mixed well and incubated for 10 minutes at 4°C. 30uL of additional MACS buffer was added to each sample followed by 20uL of anti-Biotin MicroBeads. Samples again were mixed well and incubated for 15 minutes at 4°C, followed by centrifugation at 800xg for 10 minutes. Each pellet was resuspended in 500uL MACS buffer and immediately applied onto the MACS column, which was previously washed with 3mL MACS buffer. The effluent (containing monocytes) was collected in a sterile 15mL conical and centrifuged at 800xg for 5 minutes. Monocytes were resuspended and maintained in RPMI with 10% FBS.

Reagents.

Etoposide, camptothecin, adriamycin, mitomycin, were purchased from Sigma-Aldrich and used at the concentrations described in figure legends. NFκB inhibitor BAY 11-7085 was obtained from Alexis Biochemicals (San Diego, CA) and used at 5uM concentration and ML120 was obtained from Millennium Pharmaceuticals (Cambridge, MA) and used at 20uM concentration. The ATM inhibitor, AZ12622702/KU55933, was a gift from AstraZeneca (Cheshire, UK) and used at 10uM. Antibodies against STAT2 (C-20), c-myc epitope (sc-40), IRF1(C-20), CBP (A-22), p65 (C-20), and normal rabbit IgG were purchased from Santa Cruz Biotech, Inc. (Santa Cruz, Calif.). Anti-STAT2 (Tyr689) phosphotyrosine antibody was obtained from Upstate Biotechnology Inc. (Lake Placid, NY). Antibody against p65 phosphorylated on serine 536 and STAT1 phosphorylated on tyrosine 701 were obtained from Cell Signaling (Beverly, MA). Antibody against HA epitope (12CAS) was purchased from Roche (Indianapolis, IN).

Antibodies derived against IRF3 and STAT1 were described previously (122, 231). Antibody to IRF7 was raised in rabbits against the 246-432 amino acid region of IRF7. Anti-mouse or anti-rabbit secondary antibodies conjugated to IRDye800 or 700 were obtained from Rockland Immunochemicals (Gilbertsville, PA). TNFα was obtained from Invitrogen (Carlsbad, CA). DNA transfections were performed using FuGENE 6 (Roche Diagnostics Corp., Indianapolis, IN) or TransIt (Mirus, Madison,WI) according to the manufacturers' instructions. The Dual-Luciferase reporter assay system (Promega; Madison, WI) was used for luciferase assays. As an internal control for the Dual-Luciferase assay, the *Renilla* luciferase construct pRL-null (Promega; Madison, WI) was used.

Plasmid constructs.

IRF3, STAT1 and STAT2 constructs were described previously (12, 91, 122). The dominant negative IκB construct was obtained from Dr. Dean Ballard (Howard Hughes Medical Institute, Vanderbilt University School of Medicine, Nashville, TN) (18). The K63only UB HA plasmid was obtained from Dr. Dafna BarSagi (New York University, NY). The IFNλ_1 promoter luciferase reporter plasmid was obtained from Dr. Takashi Fujita (Kyoto University, Kyoto Japan) (153). The IFNα_{14} promoter was cloned by PCR from lymphocyte genetic DNA using the IFNα_{14} promoter primers (see below) and subcloned using BamH1 and HindIII restriction sites into the pZ-luc luciferase reporter vector (Addgene).

DNA Transfections.

The indicated cells were transfected using Fugene6 or Trans-It as indicated by manufacturer's instructions. In short, 60 or 100mm plates of cells were plated the night prior at 50% confluency. The next morning, the cell media was replaced with fresh media. For each sample, 0.5-1ug of plasmid DNA was diluted in 10uL sterile water. 1-3ul of Fugene6 or Trans-It was diluted in 100uL DMEM or OPTI-MEM and incubated at room temperature for 5-10 minutes. The diluted DNA was added to the diluted Fugene or Trans-It and further incubated for 15-20 minutes. The DNA-Fugene6 or DNA-TransIt mixture was added slowly to the tissue culture medium and the cells were returned to 37°C overnight. Cell media was removed the next morning and fed with fresh media.

Luciferase Assay.

The Dual-Luciferase reporter assay kit was used for luciferase assays, as instructed by manufacturer's instructions. The procedure is summarized as follows. The night prior, a well of a 12 well plate was seeded at 25% confluency for each sample with the desired cell line. The following morning, cells were transfected with DNA, as described above. For each well, 0.08ug of pRL-null plasmid, 0.25ug of the reporter plasmid, and (as desired) 0.25-0.5ug of transactivator encoding plasmid was used. The day after transfection, cell media was refreshed and the cells were treated as indicated in each figure.

The day of the luciferase assay, cell lysates were obtained using the passive lysis method. Cells were washed twice with room temperature PBS and 250uL Passive Lysis Buffer (provided by manufacturer) was added to each well. The 12 well plates were rocked at room temperature for 15-20 minutes. 20uL of lysates was transferred to a luminometer tube. 100uL of prepared Luciferase Assay Reagent II was added to each sample a gently swirled. The tube was read by the luminometer for 10-20 seconds and the firefly luciferase activity was recorded. 100uL of prepared 1x Stop and Glo Reagent was added to the reaction and the tube again was gently swirled. The tube was once again read by the luminometer for 10-20 seconds and the Renilla luciferase activity was recorded.

Primers.

Primers used in this thesis corresponded to:

GAPDH	(+528)	5'-cacagtccatgccatcactg-3'
	(+1007)	5'-tactccttggaggccatgtg-3'
actin (123)	(+714)	5'-gagctacgagctgcctgacg-3'
	(+833)	5'-gtagtttcgtggatgccacag-3'
ISG54	(+1370)	5'-tggagtctggaag cctcatcc-3'
	(+1608)	5'-attctatcaccaagcccgtgg-3'
IFNβ	(+27)	5'-tgctctcctgttgtgcttctccac-3'
	(+243)	5'-atagatggtcaatgcggcgtcc-3'
pan IFNα		5'-cacacaggcttccaggcattc-3'
		5'-tcttcagcacaaaggactcatctg-3'
IFNα_6 (110)	(+239)	5'-tccatgaggtgattcagcagac-3'
	(+346)	5'-gctgctggtaaagttcagtatagagttt-3'
IFNα_7	(+106)	5'-agggccttgatactcctgg-3'
	(+194)	5'-tcctcctccgggaatctgaat-3'

IFN$\alpha_{1/13}$ (110)	(+261)	5'-cttcaacctctttaccacaaaag-3'
	(+344)	5'-tgctggtagagttcggtgca-3'
IFNα_{14}	(+65)	5'-tgggctgtaatctgtctcaaac-3'
	(+315)	5'-taggagggtctcatcccaagc-3'
IFNλ_1 (5)	(+165)	5'-cgccttggaagagtcactca-3'
	(+244)	5'-gaagcctcaggtcccaattc-3'
IRF-7	(+1343)	5'-tggtcctggtgaagctggaa-3'
	(+1476)	5'-gatgtcgtcatagaggct gttgg-3
IRF-1	(+190)	5'-cgatacaaagcaggggaaaagg-3'
	(+397)	5'-tcttagcatctcggctggacttc-3'
IFNα_{14} prom	(-457)	5'-ttttagcagagacggggtttcaccatg-3'
	(+71)	5'-attgggaatcccgaagatgctgctg-3'

RNA Isolation.

RNA was isolated from cells using SV Total RNA Isolation Kit (Promega, Madison, WI). In short, the cell pellet was lysed in 175uL of the provided lysis buffer and mixed by inversion. The lysate was mixed with 350uL of the provided dilution buffer and the mixture was mixed again by inversion. The lysate was cleared of debris by centrifugation at room temperature at 12,000 x g for 10 minutes and the cleared lysate was mixed with 200uL of 95% ethanol and mixed by pipetting. The ethanol-lysate mixture was transferred to the provided spin column basket assembly and centrifuged for 1 minute at 12,000 x g. The column, containing the genomic material, was washed by centrifugation for 1 minute at 12,000 x g with 600uL of the provided wash solution. DNA was removed from the column by applying 50uL of the provided DNase incubation mixture to the column and incubating for 15 minutes at room temperature. The DNase's action was halted using 200uL of the provided DNase Stop Solution. The column was washed with 250uL of the RNA wash solution and centrifuged at 12,000 x g for 1 minute. RNA was eluted off the column with 50-100uL of RNase free water and centrifugation for 1 minute at 12,000 x g. RNA was used immediately to generate cDNA or was mixed with 1/10th volume of 3M sodium acetate and 3x volume 100% ethanol and stored at -70°C.

Generation of cDNA.

A 25uL sample of cDNA was generated using Oligo(dT)$_{12-18}$ (Invitrogen) and SuperScriptII Reverse Transcriptase (Invitrogen, Carlsbad, CA)) according to the manufacturers' protocols. In short, 1-5ug of RNA was mixed with 0.5ug Oligo(dT) $_{12-18}$

and incubated at 65°C for 5 minutes and cooled on ice 5 minutes. A mixture consisting of (at a final concentration) 1x Reaction Buffer, 0.5mM dNTPs, 5mM $MgCl_2$, 10mM DTT, 1U RNase inhibitor, and 1U SuperScriptII Reverse Transcriptase was incubated at 42°C for 5 minutes. The pre-warmed mixture was added to the RNA-primer samples and incubated at 42°C for 1 hour. The reaction was halted by incubation at 70°C for 15 minutes. The reaction was cooled on ice, aliquoted and stored at either -20°C or -70°C.

Polymerase Chain Reaction (PCR).

PCR was performed using the indicated primers and Taq polymerase (Invitrogen, Carlsbad, CA). Each 25-50uL PCR reaction consisted of the following components: 50-100ng ds cDNA, 1x PCR Buffer (provided by manufacturer), 0.2mM dNTP, 1.5mM $MgCl_2$, 0.2uM each primer, and 1U Taq polymerase. Sterile water was added to the reaction mixture to bring the final volume up to 25 or 50uL. The PCR reaction was performed in an Eppendorf Mastercycler Thermal Cycler using the following program:

Initial denaturation 94°C for 2 minutes

25–35 cycles of PCR amplification as follows:

Denaturation at 94°C for 30 seconds

Annealing at 55°C for 30 seconds

Extention at 72°C for 1 minutes per kb

The reaction was kept at 4°C after cycling

Products were analyzed on a 1% agarose gel.

Quantitative real-time PCR.

Alternatively, quantitative real-time PCR was performed using the indicated primers at their optimal conditions as suggested by the manufacturer's instructions for the LightCycler-FastStart DNA Master SYBR Green I kit (Roche Molecular Biochemicals). In short, each 20uL PCR reaction was mixed in an eppendorf tube and consisted of the following components: 2uL of ds cDNA, 0.5mM $MgCl_2$, 0.5uM each primer, and 4uL of the 5x SYBR Green Master Mix. Sterile water was added to the mixture to bring the final volume up to 20uL. The mixture was mixed gently and centrifuged for 10 seconds at 12,000 x g. The samples were transferred to capillaries, which were placed in the cooled centrifuge capillary adapters. After capping the capillaries, the capillaries within the adapters, were centrifuged for 30 seconds at 700 x g. The capillaries were transferred

to the LightCycler Sample Carousel and then into the LightCycler instrument. The following program was used to amplify the PCR products:

Activation of enzyme at 95°C for 10 minutes

45-50 cycles of amplification as follows:

Denaturation at 95°C for 10 seconds

Annealing at 55°C for 7 seconds

Extention at 72°C for 9 seconds with a single acquisition mode

The amplification program was followed with a melting temperature analysis program:

Denaturation at 95°C for 0 seconds

Annealing at 65°C for 60 seconds

Melting at 95°C for 0 seconds with a continuous acquisition.

The reaction was cooled to 40°C and then kept at 4°C after cycling.

Following the reaction, amplification curves were analyzed using the LightCycler software and values were normalized to actin mRNA levels. For quantification analyses, serial dilutions of an actin external standard with predefined concentration were included in the experiment to create a standard curve. The LightCycler software uses the Second Derivative Maximum method to determine crossing points on the amplification curves of the standards and unknown samples and then determines the concentration of target DNA.

The specificity of the amplified PCR product was assessed by performing a Melting Curve analysis using data from the melting temperature program. The analysis displays Melting Peaks, which are plots of the first negative derivative of the sample fluorescence curves over temperature. A specific product within each sample is displayed as a peak at a the specific melting temperature, while nonspecific by-products are displayed a wide and weak peaks.

Immunoblotting and Immunoprecipitations:

Cells were lysed in 50mM Tris (pH 7.5), 400mM NaCl, 0.5% Nonidet P-40, 5mM EDTA, 10% glycerol, 50mM NaF, 0.1mM Na_3VO_4, and protease inhibitor mixture for 30 min on ice. The lysates were cleared by centrifugation at 12,000 *g* for 10 min, and the supernatants were boiled in SDS sample buffer. The cell lysates were separated on 8% SDS-PAGE and transferred to nitrocellulose membrane (Pierce Biotechnology, Rockford,

IL). The membrane was then reacted with indicated antibodies and images were detected using the Odyssey infrared imaging system (Li-COR Biosciences, Lincoln, NE, USA). Alternatively, secondary anti-rabbit or anti-mouse antibodies linked to HRP (Amersham/GE Healthcare, Piscataway, NJ) were used and the membrane was incubated in enhanced chemiluminescence reagents and exposed to film.

Immunoprecipitations were carried out by first lysing cells in a buffer containing 50mM Hepes (pH 7.2), 250mM NaCl, 0.5% Nonidet P-40, 5mM EDTA, 1mM dithiothreitol, 1mM NaF, 0.1 mM Na_3VO_4, and protease inhibitor mixture for 30 min on ice. Lysates were cleared by centrifugation for 5 min at 15,000g and were immunoprecipitated for 3 h with the indicated antibodies, and the immunoprecipitates were collected using rProtein G-conjugated agarose (Invitrogen, Carlsbad, CA). Immunoprecipitated proteins were separated by SDS-PAGE and visualized by immunoblotting with the indicated antibodies as described above.

Fluorescence imaging:

Cells seeded on coverslips were fixed in 4% paraformaldehyde and either visualized directly for GFP with a Zeiss Axiovert 200 M digital deconvolution microscope or processed for immunofluorescence prior to visualization. For immunofluorescence , cells were permeablized in 0.2% Triton X-100 in PBS, blocked in 3% BSA in PBS, and incubated in anti-myc antibody in blocking solution in 1:200 dilution at 4°C for 15 hours. Secondary antibodies conjugated to Rhodamine (Jackson ImmunoResearch Laboratories, Inc., West Grove, PA.) were applied at 1:200 dilution for 1 hour at room temperature. Coverslips were washed with PBS and mount in anti-fade solution (Vectashield, Vector Laboratories, Inc. Burlingame, CA.)

DNA binding assay.

RelA binding:

Nuclear extracts were generated by dounce homogenizing cells in a hypotonic lysis buffer (1.5 mM Hepes (pH 7.9), 0.02mM spermine, 0.05mM spermidine, 8mM KCl, 0.2mM EDTA, 0.1% glycerol, 0.1mM dithiothreitol (DTT), 0.1mM PMSF, 1mM Na_3VO_4, and protease inhibitor cocktail). Nuclei were collected by centrifugation at 500g and lysed in a high salt buffer (20 mM Hepes (pH 7.9), 0.2mM spermine, 0.5mM spermidine, 0.4M NaCl, 1mM DTT, 0.2mM EDTA, 0.2mM EGTA, 10% glycerol, 1mM

PMSF, 20mM NaFl, 1mM Na_3VO_4, protease inhibitor cocktail). Cleared lysates were dialyzed against Buffer D (20mM Hepes (pH 7.9), 20% glycerol, 100mM KCl, 1mM DTT, 1mM PMSF, 0.2mM EDTA, 0.2mM EGTA) and incubated with radiolabeled double-stranded DNA oligonucleotide representing the NFκB binding site (5'-tcaacagaggggactttccgagagg -3') in binding buffer (10mM Tris (pH 8.0), 150mM KCl, 0.5mM EDTA, 0.1% Triton X-100, 12.5% glycerol, 0.2mM DTT, 5ng/ul polydIdC) for 30 min. As noted, 1ug specific antibody or 100-fold excess nonradiolabeled dsDNA oligonucleotide was added to lysates before radiolabeled DNA. Probe DNA and probe-protein complexes were separated on nondenaturing gels and exposed to X-ray film for autoradiography.

IRF1 binding:

Nuclear extracts were generated by dounce homogenizing cells in a hypotonic lysis buffer (10 mM Hepes (pH 7.9), 10mM KCl, 1.5mM $MgCl_2$, 0.5mM dithiothreitol (DTT), 2mM PMSF, 1 mM Na_3VO_4, and protease inhibitor cocktail). Nuclei were collected by centrifugation at 500g and lysed in a high salt buffer (20 mM Hepes (pH 7.9), 1.5mM $MgCl_2$, 0.3M KCl, 0.5mM DTT, 0.2mM EDTA, 25% glycerol, 0.2mM PMSF, 1mM Na_3VO_4, protease inhibitor cocktail). Cleared lysates were dialyzed against Buffer D (20mM Hepes (pH 7.9), 20% glycerol, 100mM KCl, 1mM DTT, 1mM PMSF, 0.2mM EDTA, 0.2mM EGTA) and incubated with radiolabeled double-stranded DNA oligonucleotide representing the NFκB binding site (5'-tcaacagaggggactttccgagagg -3') in binding buffer (10mM Tris (pH 8.0), 150mM KCl, .5mM EDTA, 0.1% Triton X-100, 12.5% glycerol, 0.2mM DTT, 5ng/ul polydIdC) for 30 min. As noted, 1ug specific antibody or 100-fold excess nonradiolabeled dsDNA oligonucleotide was added to lysates before radiolabeled DNA. DNA and probe-protein complexes were separated on nondenaturing gels and exposed to X-ray film for autoradiography.

Ubiquitination assays (213):

Ubiquitination assays were carried out using the Tet-inducible IRF7myc/his HT1080 cell line described above. K63only UB-HA was transfected into cells and IRF7myc/his was induced 24 hours after transfection using doxycycline. Where indicated, cells were concurrently treated with etoposide. Cells were collected and disrupted by sonication in Buffer A (6 M guanidine HCl, 0.1 M Na_2HPO_4/NaH_2PO_4(pH

8.0) and 10 mM imidazole) and lysates were incubated with Ni-NTA agarose beads (Qiagen, Chatsworth, CA) for 3 hours at room temperature. The beads were collected, washed twice with buffer A, twice with buffer A2/TI (1 volume buffer A and 3 volumes buffer TI (25 mM Tris(pH 6.8), 20 mM imidazole)) and twice with Buffer TI. Beads were collected and ubiquitylated proteins eluted with 2x SDS loading buffer by boiling (213). Proteins were then resolved by SDS-PAGE and analyzed by Western blot, using anti-HA and anti-IRF7 antibodies.

Microarray Assay

A comparison of the genes expressed in etoposide treated Hec1B cells versus mock treated HEC1B cells were evaluated by Affymetrix DNA microarray. Hec1B cells were treated with 40ug/mL etoposide or mock treated with DMSO for 52 hours. RNA was isolated from both samples and sent to DNA Microarray Core Facility at SUNY Stony Brook. The RNA was compared y hybridization to Affymetrix DNA microarrays. Increase in gene expression in the etoposide treated sample was reported as a relative fold increase over the mock treated. Results are listed in Appendix A.

RESULTS

Part 1: DNA Damaging Agents Activate Interferon Signaling

Interferon-Stimulated Gene (ISG) induction in etoposide-treated cells.

The induction of new genes is crucial for the response to cellular stress. For instance, the cytokine interferon (IFN) is not expressed constitutively in healthy cells but is induced in response to viral or bacterial infection. However, microarray assays examining the transcriptional response to the cellular stress brought about by the DNA damage caused by etoposide indicated that within the etoposide response genes were IFN-inducible genes. The transcriptional response to the cellular stress brought about by etoposide was performed by Sarah VanScoy, a member of the lab, by isolating RNA from untreated or etoposide treated endometrial cancer Hec1B cells. The DNA Microarray Core Facility at SUNY Stony Brook compared them by hybridization to Affymetrix DNA microarrays (Appendix A).

The microarray data indicated that more than 1400 genes were induced in response to a 52-hour treatment with etoposide. Included in the etoposide response genes were IFN induced genes, such as ISG15 and 54. In addition, IRF genes, such as IRF7 and IRF1, which are normally found at low levels in unstimulated cells, were also induced in the etoposide treated cells. This data was rather peculiar since these genes are normally induced by IFN signaling.

To confirm that IFN stimulated genes are induced in etoposide-treated cells, RT-PCR was performed studying ISG54 mRNA, as a representative of the IFN-inducible genes. Hec1B cells were treated with etoposide for 0, 24, 36 and 48 hours. RNA was extracted from the cells, reverse transcribed into cDNA and ISG54 levels were detected by quantitative RT-PCR by using primers specific to ISG54. Actin primers were used to standardize the amount of cDNA used in each reaction. Data was analyzed using the LightCycler software and PCR products were visualized on an agarose gel (Figure 15). The mRNA levels of ISG54 increased 6-, 10- and 18- fold with 24, 36, and 48 hours of etoposide treatment, respectively, verifying the microarray data, which suggested ISG54 mRNA levels increased with etoposide treatment.

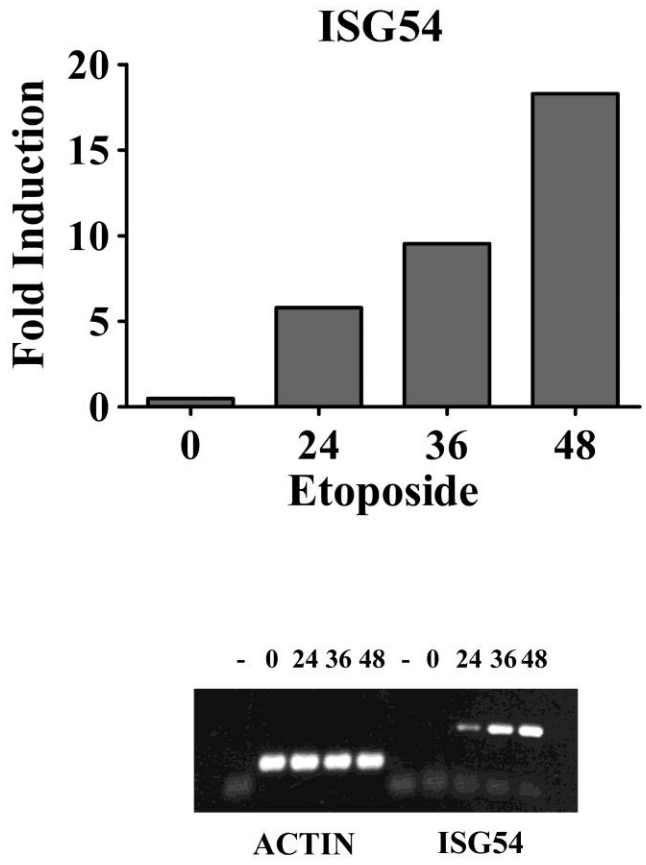

Figure 15: ISG54 induction in Hec1B cells after etoposide treatment.

(Top) ISG54 mRNA levels in Hec1B cells were measured by quantitative RT-PCR 0, 24, 36 or 48 hours after etoposide treatment. Data was analyzed and normalized to actin mRNA levels using the LightCycler software. (Bottom) PCR products were visualized on an agarose gel.

The ISG15 promoter is activated following etoposide treatment and requires STAT1.

Several IFN-inducible genes are induced in etoposide-treated cells (Appendix A). In order to identify an etoposide-responsive DNA regulatory element within the promoter of ISGs, the ISG15 gene promoter was selected as a representative gene promoter for study. The etoposide responsive DNA regulatory element within the ISG15 promoter was identified by generating a specific reporter gene plasmid and testing it for its response to etoposide. A -366 nucleotide region of the ISG15 promoter (165) was subcloned upstream of a luciferase reporter gene. This construct was transfected into the human cervix epithelial carcinoma HeLa cell line or the Signal Transducers and Activators of Transcription (STAT)1-deficient fibrosarcoma U3A cell line (73). Cells were treated for 36 hours with etoposide and cell lysates were prepared for evaluation of the ISG15 promoter activation by performing a luciferase assay, using the Dual Luciferase Assay System. Etoposide treatment activated the ISG15 promoter in the HeLa cells, but the gene promoter remained relatively silent in the U3A cells (Figure 16). STAT1 is necessary for the induction of IFN-stimulated genes via type I and type III IFN signaling. Disabling the cell's ability to respond to IFN by using STAT1-deficient U3A cells (73) may have hindered the cells ability to induce the ISG15 promoter activity in response to etoposide. This data suggest that IFN signaling may play a role in the cellular stress response to etoposide and that the etoposide-response element is within -366 nucleotides of the ISG15 promoter.

Interferon-stimulated genes, such as ISG15, contain an Interferon-Stimulated Regulatory Element (ISRE), that is sufficient for the transcriptional response to type I IFNs (33). IFNα and IFNβ activate the ISGF3 complex (STAT1/STAT2/IRF9), which binds to this DNA sequence and activates the transcription of the gene. If IFN signaling plays a role in the cellular response to etoposide, the resulting activated transcription factors should be able to bind and activate a promoter containing an ISRE.

In order to test the possibility that the ISRE of the ISG15 gene was the responsive DNA element to etoposide, the expression of a luciferase gene reporter, regulated by an ISRE, was tested. After transfecting this construct into HeLa or U3A cells, cells were treated with etoposide for 36 hours. Cells lysates were used in a luciferase assay to

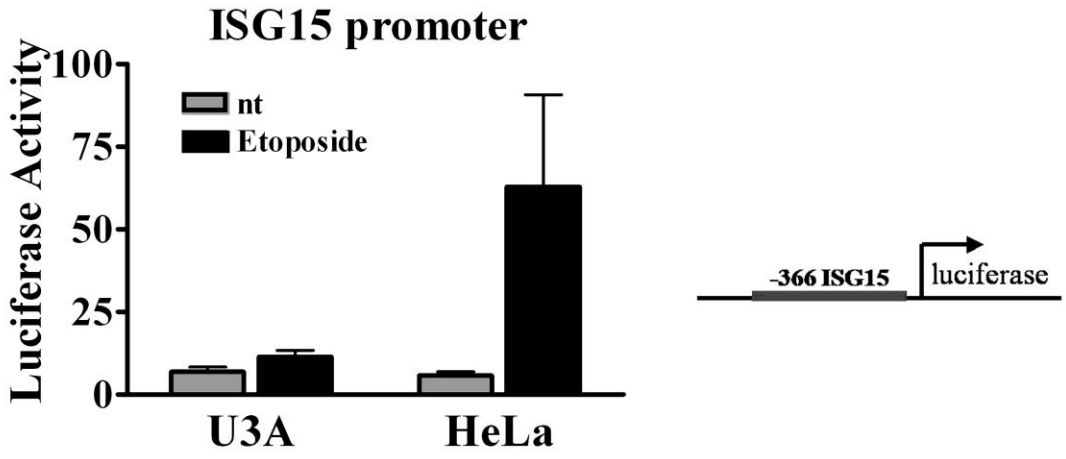

Figure 16: ISG15 promoter is activated in etoposide-treated HeLa cells, but not in etoposide-treated U3A cells.

A luciferase reporter gene driven by -366 promoter region of ISG15 (right) was transfected into HeLa or U3A STAT1 -/- cells. Cells were untreated (nt) or treated with 40ug/mL etoposide for 36 hours before a luciferase assaywas performed (left).

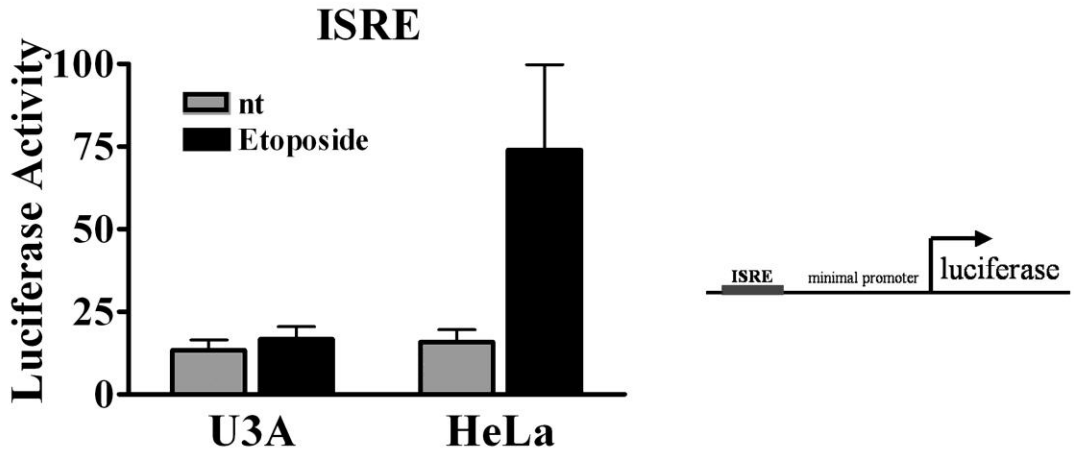

Figure 17: ISRE promoter is activated in etoposide-treated HeLa cells, but not in etoposide-treated U3A cells.

A luciferase reporter gene driven by the ISRE promoter (right) was transfected into HeLa or U3A STAT1 -/- cells. Cells were untreated or treated with 40ug/mL etoposide for 36 hours before a luciferase assaywas performed (left).

assess the promoter activity (Figure 17). In HeLa cells, etoposide stimulated the ISRE-containing promoter, while promoter activity in U3A cells remained unresponsive. The data suggests that the etoposide-response element of the ISG15 gene is the ISRE. Again, the lack of promoter response in the U3A cells is highly suggestive of IFN signaling playing a role in the cell's response to etoposide.

Activation of STAT1 and STAT2 following etoposide treatment.

Interferon-stimulated genes, such as ISG54 and ISG15, are expressed in an interferon-dependent or -independent manner. Evidence of IFN signaling in etoposide-treated cells may be studied by observing STAT activation. STAT1 and STAT2 are resident in the cytoplasm in a latent state and the binding of IFNα/β to the type I and type III IFN receptor leads to tyrosine phosphorylation and nuclear accumulation of STAT1 and STAT2 (34, 37, 121). For this reason, the cellular localization of STAT1 and STAT2 following etoposide treatment was evaluated. HeLa cells were transfected with a plasmid encoding GFP-tagged STAT1 or GFP-tagged STAT2 and then treated with etoposide for 24 hours before they were visualized using fluorescence microscopy (Figure 18). The GFP-tagged STAT1 and STAT2 appeared to be present in the nucleus upon etoposide treatment, suggesting its activation and involvement in transcriptional processes in the nucleus.

Following IFN stimulation, the STAT1 and STAT2 transcription factors are activated by tyrosine phosphorylation (34). To determine whether STAT1 and STAT2 are phosphorylated with etoposide treatment, specific STAT1 or STAT2 phospho-tyrosine antibodies were used in Western blot analyses. HeLa cells were treated with etoposide between zero and 24 hours and whole cells lysates were separated by SDS-PAGE. Western blotting, using the phospho-STAT1 and STAT2 antibodies, revealed that STAT1 and STAT2 are tyrosine phosphorylated with etoposide treatment (Figure 19). Equal levels of total STAT1 and STAT2 were verified by reprobing the membrane with a STAT1 or STAT2 antibody. Together with the STAT1 and STAT2 fluorescence microscopy results, these data strengthen the hypothesis that IFN signaling through STAT1 and STAT2 is responsible for the induction of the ISGs during the cellular

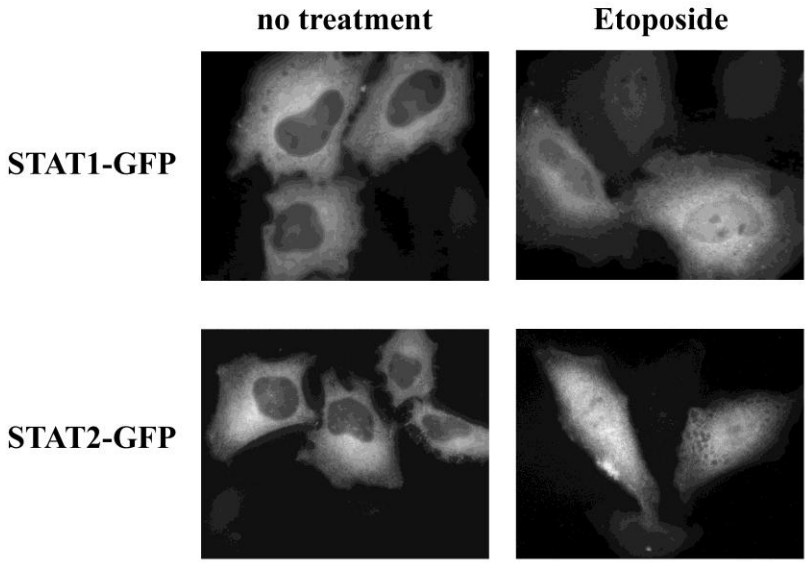

Figure 18: Nuclear localization of STAT1 and STAT2 in etoposide-treated cells.

A plasmid encoding a STAT1 or STAT2 protein tagged with GFP was transfected into HeLa cells. 24 hours after transfection, cells were treated with 40ug/mL etoposide for 24 hours before visualizing the transfected cells by fluorescence microscopy.

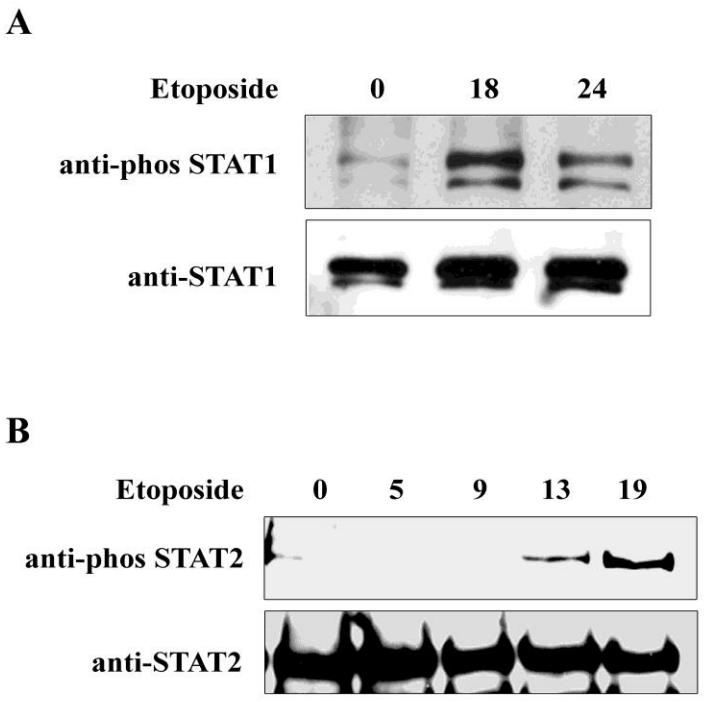

Figure 19: STAT1 and STAT2 are phosphorylated in etoposide-treated cells.

HeLa cells were treated with etoposide for the times indicated. Proteins from cell lysates were separated on an SDS PAGE and a Western blot was performed using STAT1, STAT2, phospho-STAT1 or phospho-STAT2 antibodies.

response to etoposide exposure.

IFNα species and IFNλ$_1$, but not IFNβ, are induced in response to etoposide.

The activation of an ISRE-containing promoter, as well as STAT1 and STAT2 activation, suggests the activation of type I/III IFN signaling in etoposide-treated cells. For this reason, the production of type I and type III IFN by cells exposed to etoposide was evaluated using quantitative real time PCR. RNA was isolated from untreated or etoposide-treated primary monocytic cells, reverse transcribed into cDNA and IFNβ levels were detected by quantitative RT-PCR by using primers specific to IFNβ. Cells were also infected with Newcastle Disease virus as a positive control. Data was analyzed using LightCycler software and actin primers were used to standardize the amount of cDNA used in each reaction. IFNβ mRNA levels did not increase in etoposide-treated cells while virus infected cells had an approximately 200- and 400- fold increase of IFNβ mRNA levels with 6 and 12 hours of viral infection, respectively (Figure 20).

Since IFNβ was not detected in etoposide-treated cells, other IFN family members were studied to determine whether they were induced with etoposide treatment and consequently induce the ISGs. Quantitative real-time PCR was performed using primers that amplified a 100bp consensus region found in most IFNα subtype genes (pan-IFNα primers) and actin primers were used to standardize the amount of cDNA used in each reaction. Data was analyzed using LightCycler software and it was found that the mRNA levels of consensus IFNα genes increased over 20 fold with a 20 hour etoposide treatment (Figure 21). Since there are 13 IFNα genes, it would appear that one or more IFNα genes may be induced with etoposide treatment and further studies were performed to determine which subtype(s) was induced.

To determine which IFNα subtypes are expressed in etoposide-treated cells, segments of the induced IFNα mRNAs were cloned and sequenced from etoposide-treated HeLa cells. RNA was isolated from etoposide-treated cells and cDNA was generated and, using primers that amplified a 392bp segment of most IFNα subtypes, an IFNα PCR fragment was generated and subsequently cloned into pST-Blue-1 Perfectly Blunt vector, which contained sp6 and T7 priming sites. These IFNα containing

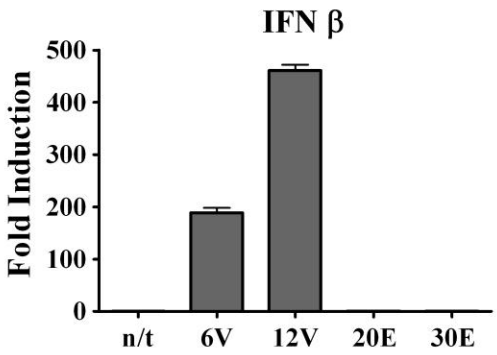

Figure 20: IFNβ is not induced in etoposide-treated primary monocytes.

Monocytic cells were isolated from blood donors and treated with 40ug/mL of etoposide for 20 (20E) or 30 (30E) hours. As a positive control, cells were also treated with Newcastle Disease Virus for 6 (6V) or 12 hours (12V). Total RNA was isolated and used to synthesize cDNA. Real Time PCR was performed using primers specific for IFNβ. Data was analyzed using the LightCycler software and values were normalized to actin mRNA levels.

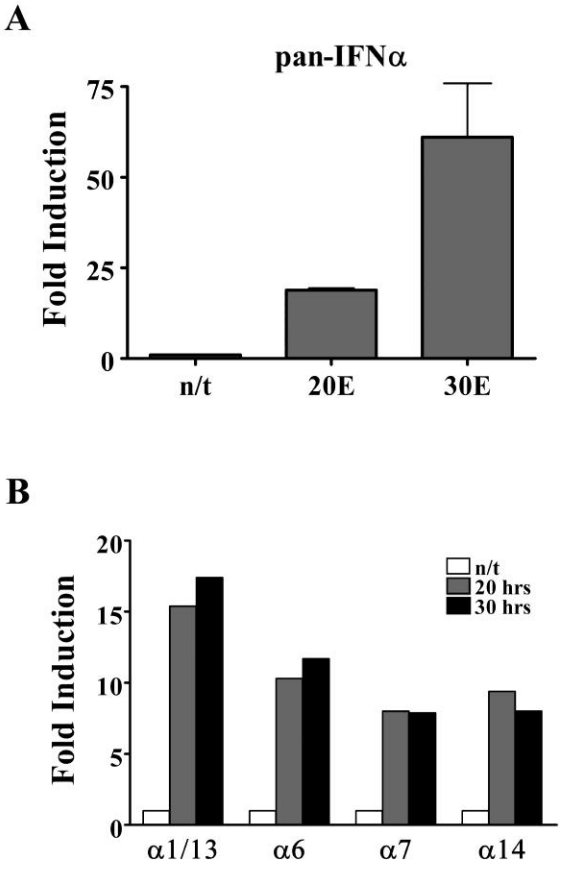

Figure 21: IFNα species are induced in etoposide-treated primary monocytes.

Monocytic cells were isolated from blood donors and treated with 40ug/mL of etoposide for 20 (20E) or 30 (30E) hours. Total RNA was isolated and used to synthesize cDNA**.** Quantitative real time PCR was performed using primers that are complementary to most IFNα species (pan-IFNα) (A). Additionally, quantitative real time PCR was performed using primers specific to $IFN\alpha_{1/13}$, $IFN\alpha_{6}$, $IFN\alpha_{7}$, and $IFN\alpha_{14}$ (B). Data was analyzed using the LightCycler software and values were normalized to actin mRNA levels.

plasmids were transformed into competent bacteria and over 20 colonies were isolated, followed by DNA extraction. Using either the T7 or sp6 priming sites, the DNA was sequenced with the Big Dye Terminator Cycle Sequencing system. The IFNα subtypes expressed in the cell after etoposide treatment were identified by comparing the cloned sequences to those in the GeneBank database (NCBI). Several subtypes were found to be present in HeLa cells after etoposide exposure (Table 6), the most abundant being IFNα1/13 and IFNα6.

PCR primers were designed by Loseke *et al* (110) for the identification of the IFNα subtypes by RT-PCR and the authors had analyzed and verified the specificity of these primers. Real time PCR was performed using these primers specific to the IFNα subtypes to verify and quantify the induction of the IFNα subtypes in etoposide-treatedcells. cDNA was generated from untreated and etoposide-treated primary monocytic cells isolated from blood donors and real-time PCR was performed (Figure 21). Data was analyzed using LightCycler software and actin primers were used to standardize the amount of cDNA used in each reaction. The real-time PCR results indicated that IFNα1/13, IFNα6, IFNα7, and IFNα14 were induced by ~7-15 fold with etoposide treatments.

In addition to Type I IFN, Type III IFNs have also been implicated in the induction of the ISGs (250). Therefore, the induction of IFNλ_1, a member of the Type III IFN family, in response to etoposide was investigated by real-time PCR (Figure 22). RNA was isolated from untreated or etoposide-treated primary monocytic cells, reverse transcribed into cDNA and IFNλ_1 levels were detected by quantitative RT-PCR by using primers specific to the IFNλ_1 gene (5). As in previous experiments, data was analyzed using LightCycler software and were standardized to actin mRNA levels in each sample. IFNλ_1 mRNA levels increased by ~10 fold in response to etoposide. Together, these quantitative real-time PCR experiments revealed that IFNβ is not induced in primary monocytes; instead both IFNα and IFNλ_1 mRNA levels increase in response to etoposide treatments.

Subtype	*Number clones detected*
IFN α1/13	10
IFN α6	4
IFN α10	3
IFN α14	2
IFN α8	2
IFN α7	1

Table 6: IFNα subtypes detected in etoposide-treated HeLa cells.

IFNα subtypes from etoposide-treated cells were cloned by RT-PCR using primers that amplified a 392bp region of most IFN s. The PCR products were cloned into the pST-Blue Perfectly Blunt vector. DNA was isolated from over 20 transformed bacterial clones and sequenced. The IFNα subtypes were identified by comparing the sequences to published data in GeneBank (NCBI). The frequency of detection are listed above.

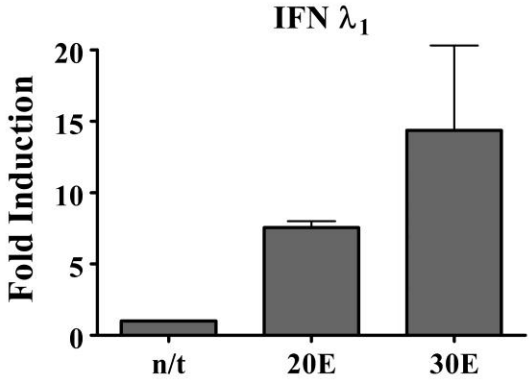

Figure 22: IFNλ_1 is induced in etoposide-treated primary monocytes.

Monocytic cells were isolated from blood donors and treated with 40ug/mL of etoposide for 20 (20E) or 30 (30E) hours. Total RNA was isolated and used to synthesize cDNA. Real Time PCR was performed using primers specific for IFNλ_1 Data was analyzed using the LightCycler software and values were normalized to actin mRNA levels.

Various DNA damaging agents induce ISG54 and IFN.

Etoposide enhances DSB in DNA by inhibiting topoisomerase II's ligating ability (127). To determine whether IFN and ISG production was a general response to DNA damage or one specific to etoposide, three other antineoplastic agents that trigger DNA damage by distinct mechanisms were tested – camptothecin, mitomycin, and adriamycin. Camptothecin induces single-stranded breaks through a ternary complex with DNA and topoisomerase I; adriamycin is a DNA intercalating agent that binds to topoisomerase II and causes DNA strand breaks; mitomycin C alkylates DNA (7). THP-1 monocytic cells were treated with these DNA damaging agents for 24 hours. Cell lysates were separated by SDS-PAGE and ISG54 protein expression in the cells was analyzed by Western Blot using antibodies specific to ISG54 (Figure 23). ISG54 protein levels increased in cells treated by all four DNA damaging agents.

Camptothecin, mitomycin and adriamycin induced ISG54, suggesting that these drugs, like etoposide, induce IFN. To verify that IFN is produced in these treated cells, THP-1 monocytic cells were incubated with these DNA damaging agents for 24 hours and quantitative RT-PCR was performed using pan-IFNα or IFNλ_1 primers as described previously. Both IFNα and IFNλ_1 mRNA levels increased in response to treatments with all four neoplastic drugs (Figure 24).

Despite the different DNA damage mechanisms employed by the four agents, they all induced ISG54, IFNα and IFNλ_1. This indicates that the production of IFN in etoposide-treated cells is a general DNA damage response and not one specific to a single drug or mechanism.

IFNα_{14} and IFNα_6 promoters are not induced by etoposide treatment.

In an attempt to identify etoposide-responsive regions within the IFNα promoter, 3.8 kb region of the IFNα_{14} promoter was subcloned from a Bacterial Artificial Chromosome plasmid (BAC RP11-380P16) containing genomic DNA from human male white blood cells. By utilizing PCR and primers specific to the IFNα_{14} promoter, the 3.8kb promoter fragment was subcloned upstream of a luciferase reporter gene and evaluated by luciferase assays to study the promoter's responsiveness to etoposide treatments (Figure 25). The IFNα_{14} promoter construct was transfected into HeLa cells

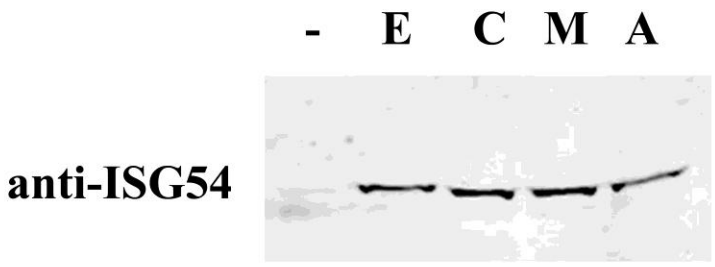

Figure 23: Various DNA damaging agents induce ISG54.

THP-1 cells were treated with 40ug/mL of etoposide (E), 5uM camptothecin (C), 20ug/mL mitomycin (M) or 20ug/mL adriamycin (A) for 24 hours. Cells lysates were used in Western Blot analysis for ISG54.

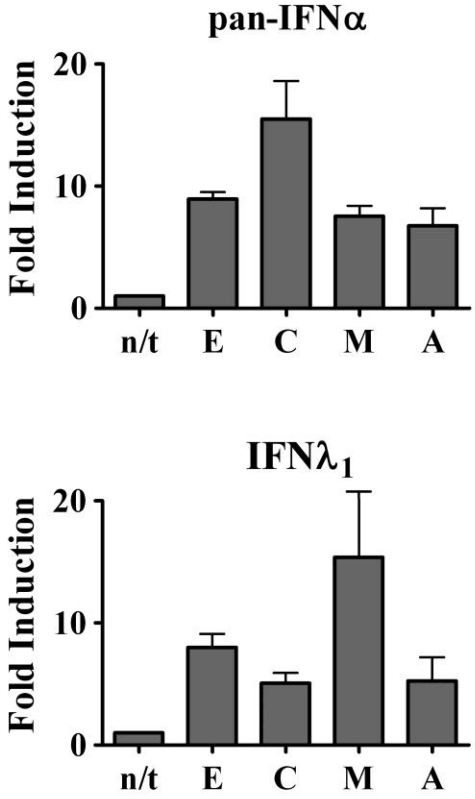

Figure 24: Various DNA damaging agents induce IFNα and IFNλ genes.

THP-1 cells were treated with 40ug/mL of etoposide (E), 5uM campthothecin (C), 20ug/mL mitomycin (M) or 20ug/mL adriamycin (A) for 24 hours. Total RNA was isolated and used to synthesize cDNA. Real Time PCR was performed using primers complementary to most IFNα subtypes (pan IFN) or $IFN\lambda_1$. Data was analyzed using the LightCycler software and values were normalized to actin mRNA levels.

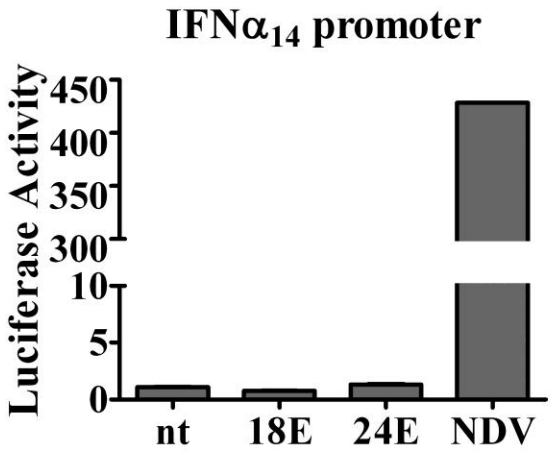

Figure 25: IFNα_{14} promoter is nonresponsive to etoposide treatment.

A -3.8 kB promoter region of IFNα_{14} driving a luciferase reporter plasmid was transfected into HeLa cells. Cells were treated with 40ug/mL etoposide for 18 or 24 hours before a luciferase assay was performed. As a positive control, cells were infected with Newcastle Disease Virus.

and treated with either etoposide or NDV before using the cell lysates in luciferase reporter assays. The IFNα_{14} promoter remained unresponsive to etoposide treatments, while viral infections effectively induced the promoter. Additionally, the IFNα_6 promoter was subcloned and tested in the same manner, resulting in similar results (data not shown). Both the IFNα_{14} and IFNα_6 promoters were not induced in response to etoposide treatments.

IFNλ_1 promoter is activated by etoposide treatment.

The IFNλ_1 promoter was also tested for activation by etoposide. A plasmid containing a -554 nucleotide promoter region of IFNλ_1 driving a luciferase reporter plasmid was obtained from Dr. Takashi Fujita (Kyoto University, Kyoto Japan) (153) and transfected into HeLa cells. After treating the cells with etoposide for 18 or 24 hours, cellular lysates were used in luciferase assays to evaluate IFNλ_1 promoter activity. With etoposide treatment, luciferase activity increased substantially, by 30 fold, indicating that the IFNλ_1 gene is actively transcribed in response to etoposide and the responsive element is within this -554 promoter region.

In a parallel experiment, as a negative control, a promoterless luciferase vector was transfected into HeLa cells and evaluated by luciferase assays to ensure that the vector itself is not responsive to etoposide treatments (Figure 26).

ISG54 and IFN genes are actively transcribed in response to etoposide treatment.

RT-PCR experiments indicated that there is an increase in IFN and ISG54 mRNA levels in response to etoposide. This was interpreted as an induction of IFN and ISG54 gene transcription. However, since prolonged etoposide treatment initiates cellular death pathways, the possibility exists that cellular processes no longer function properly and mRNA transcript stability in the cytoplasm increases. This became a concern since the IFNα promoters were not induced in response to etoposide treatment (Figure 25), although IFNα mRNA levels increased in etoposide-treated cells (Figure 21). To determine if the IFNα mRNA levels were actively transcribed, RNA was extracted from nuclei for further analysis by RT-PCR (Figure 27a).

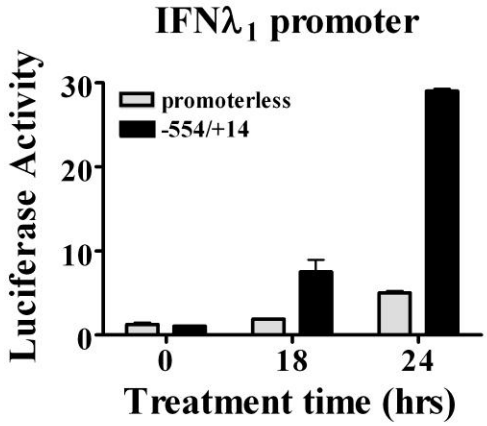

Figure 26: IFNλ_1 promoter is activated in etoposide-treated cells.

A -554 nucleotide promoter region of IFNλ_1 driving a luciferase reporter plasmid was transfected into HeLa cells. Cells were treated with 40ug/mL etoposide for 18 or 24 hours before a luciferase assay was performed. As a negative control, a promoterless luciferase vector was transfected in a parallel experiment.

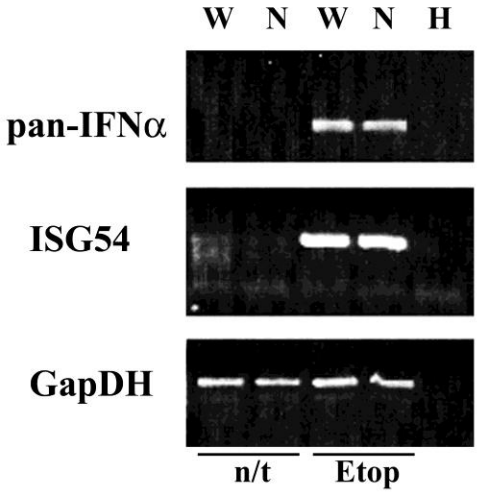

Figure 27a: ISG54 and IFNα are actively transcribed in etoposide-treated cells.

Total and nuclear RNA was extracted from whole cells (W) and nuclei (N) (see figure 27b) of untreated and etoposide-treated cells. ISG54 and IFNα gene induction was investigated by performing RT-PCR using primers specific to ISG54 and most IFNα species (pan-IFNα) and PCR products were visualized on an agarose gel. As a PCR negative control, cDNA was excluded from the reaction in lane H.

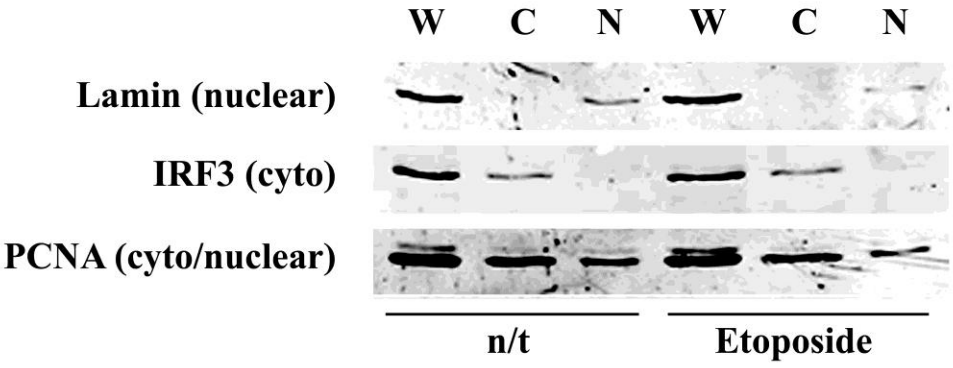

Figure 27b: Cellular fractionation to acquire pure nuclei.

Untreated or etoposide-treated cells were incubated in a hypotonic buffer and dounce homogenized to release nuclei. Whole cells and isolated nuclei were used for RNA isolation and RT-PCR (figure 27a). To determine purity of the nuclear fractions whole cell lysates (W), cytoplasmic lysates (C) or nuclear lysates (N) were used in Western blot analysis. Antibodies to lamin and IRF3 were used to determine the purity of the nuclear and cytoplasmic fractions, respectively. Western blotting using PCNA antibody was used for loading control.

In order to obtain nuclei, cellular fractionation was undertaken. Etoposide-treated and -untreated HeLa cells were swollen in hypotonic buffer and carefully dounce homogenized so that no intact cells remained. Nuclei were collected by centrifugation and used for RNA extraction and RT-PCR (Figure 27a). Purity of the extracted nuclei was first verified by Western blot (Figure 27b). 25ug of nuclear, cytoplasmic and total cellular protein of untreated and etoposide-treated cells were separated by SDS-PAGE and analyzed by Western Blot using antibodies to lamin, as a nuclear marker, and antibodies to IRF3, as a cytoplasmic marker. Antibodies to PCNA also were used as a general loading marker to ensure equivalent protein amounts were loaded into each lane. The nuclear marker, lamin, was found primarily in the nuclear fraction and there appeared to be no cytoplasmic contamination of the nuclei by whole cells since IRF3 was found only in the cytoplasmic fraction and not the nuclear fraction. These observations indicated successful fractionation and collection of nuclei.

RNA was extracted from the purified nuclei of untreated and etoposide-treated cells. As a comparision, total RNA was also extracted from another set of untreated and etoposide-treated cells. cDNA was generated and used in PCR experiments using pan-IFNα and ISG54 primers. To ensure equal amounts of cDNA were used in each reaction, PCR using GAPDH primers was also performed. Both ISG54 and IFNα RNA levels increased in the nuclei of etoposide-treated cells, suggesting that these genes are actively transcribed in response to etoposide treatment.

Etoposide-treated cells secrete functional IFN that is able to induce ISG54.

IFN induction, thus far, has been measured by studying IFN mRNA levels by RT-PCR. Protein levels of IFN within cells are difficult to measure and study since IFN is a cytokine that is secreted out of the cell. Therefore, a functional assay was designed to determine if functional IFN is secreted by etoposide-treated cells. In short, media from thoroughly washed THP-1 cells treated with etoposide was used to treat HeLa cells. IFN signaling was then evaluated by studying the induction of ISG54 by Western blot analysis (Figure 28). If the media of the etoposide-treated THP-1 cells contained functional IFN, ISG54 would be induced in HeLa cells that were incubated its media. As a negative control and to ensure that THP-1 cell media itself did not induce ISG54 in

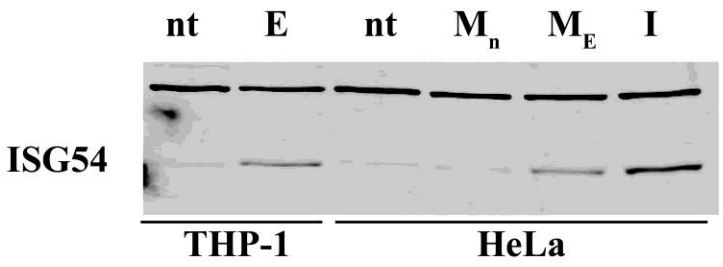

Figure 28: Etoposide-treated THP-1 cells secrete functional IFN that induces ISG54 in HeLa cells.

THP-1 cells were left untreated or treated with etoposide for 6 hours to induce DNA damage. Following 3 washes with DMEM to remove etoposide from the media the THP-1 cells were incubated without etoposide for another 18 hours. Media of the untreated (M_n) and treated (M_E) THP-1 cells was cleared of cells by centrifugation and layered onto HeLa cells. Cellular lysates of untreated and the THP-1 media treated HeLa cells, as well as the untreated and treated THP-1 cells, were used for Western blot anaylsis to analyze ISG54 induction using an antibody against ISG54. As a positive control, lysates from IFN treated HeLa cells (I) were also used in the Western Blot.

HeLa cells, media of untreated THP-1 cells was used to treat HeLa cells. Also, to ensure that the THP-1 cells were sufficiently exposed to etoposide, the lysates of the THP-1 cells were also evaluated for ISG54 expression in the Western blot analysis.

In order to address concerns of introducing residual etoposide from THP-1 cells into HeLa cell media, the experiment was repeated, including a brief 10 minute etoposide treatment. Media from thoroughly washed untreated, 10 minute or 6 hour etoposide-treated THP-1 cells was overlayed onto HeLa cells. IFN signaling was then evaluated by studying the induction of ISG54 by Western blot analysis (Figure 29). If residual etoposide remained within the THP-1 cell media, the induction of ISG54 in HeLa cells would be similar using the short 10 minute and longer 6 hour THP-1 media.

The induction of IFN by etoposide was found to be functionally significant. HeLa cells incubated in media collected from (etoposide pretreated) THP-1 cells had increased protein levels of ISG54, indicating functional interferon signaling due to the IFN secreted by THP-1 cells into the media. Furthermore, etoposide residue within the THP-1 media played a minor, if any, role in the induction of ISG54 in HeLa cells, since the shorter 10 minute treated THP-1 media induced minimal amounts of ISG54.

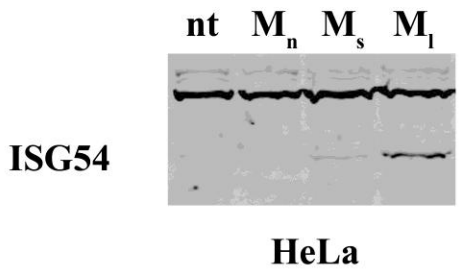

Figure 29: Effect of short and long etoposide-treated THP-1 cell's media on ISG54 induction in HeLa cells.

THP-1 cells were left untreated or treated with etoposide for 10 minutes or 6 hours. Following 3 washes with DMEM to remove etoposide from the media the THP-1 cells were incubated without etoposide for another 18 hours. Media of the untreated (M_n), 10 minute- (Ms) and 6 hour-treated (M_l) THP-1 cells was cleared of cells by centrifugation and layered onto HeLa cells. Cellular lysates of untreated and treated HeLa cells were used for Western blot anaylsis to analyze ISG54 induction using an antibody against ISG54.

Part II: IRF7 induces the IFNα_{14} gene.

The IFN Regulatory Factor (IRF) family has been shown to play an essential role in the regulated expression of both type I and type III IFN genes. Three members of the IRF family, IRF-3, IRF-5, and IRF-7, have been identified as direct transducers of virus-mediated IFN induction (13). The activation of these transcription factors was investigated in etoposide-treated cells in an attempt to identify transcription factors responsible for the induction of IFN in response to etoposide treatment.

IRF3 is not activated in etoposide-treated cells.

One IRF member, IRF3, is constitutively expressed in cells and exists in a latent state in the cytoplasm. Upon viral infection, IRF3 is post-translationally modified and activated by serine phosphorylation. With this activation, IRF3 dimers accumulate in the nucleus and associate with NFκB, ATF/cJun and the histone acetyl transferases CREB binding protein (CBP) and p300 (91, 230), where it may bind the promoter of target genes, such as the IFN genes.

Since IRF3 is known to relocalize from the cytoplasm to the nucleus upon activation, IRF3 cellular localization in etoposide-treated cells was examined by microscopy. Cells were transfected with a plasmid encoding a GFP IRF3 fusion protein, 24 hours later cells were treated with etoposide and visualized by fluorescence microscopy. IRF3 remained within the cytoplasm after treatment with etoposide for 24 hours (Figure 30). As a positive control, IRF3-GFP localization was also investigated in NDV infected cells, where it clearly accumulated in the nucleus. IRF3 localization after etoposide treatment was also investigated by microscopy at earlier and later time points and, in all cases, IRF3 remained within the cytoplasm (data not shown), suggesting that IRF3 is not activated in response to etoposide.

To further study whether IRF3 is activated upon etoposide treatment, another indicator of IRF3 activation was investigated. Since activated IRF3 associates with CBP/p300 in the nucleus, this association was investigated in etoposide-treated cells utilizing a coimmunoprecipitation assay. Endogenous CBP/p300 complexes were immunoprecipitated using CBP and p300 antibodies from untreated, NDV infected, or

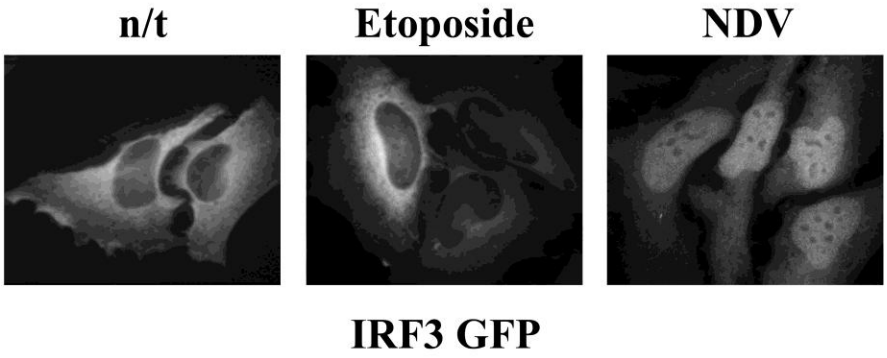

Figure 30: IRF3 does not accumulate in the nucleus with etoposide treatment.

HeLa cells were transfected with a GFP-IRF3 encoding plasmid. The cellular localization of GFP-IRF3 was evaluated after treatment with etoposide for 24 hours or Newcastle Disease Virus (NDV) for 6 hours.

etoposide-treated cells. The immunocomplexes were separated by SDS-PAGE and the association of IRF3 with the CBP/p300 complex was evaluated by Western blot analysis using an anti-IRF3 antibody (Figure 31). Although IRF3 is found within the CBP/p300 complex in virally-infected cells, it did not associate with CBP/p300 in etoposide-treated cells. This data, together with the previous cell localization strongly indicates that IRF3 is not a transcription factor involved in etoposide induced IFN production.

IRF5 is not activated in etoposide-treated cells.

Another IRF family member, IRF5 participates in the induction of interferon IFNβ and IFNα genes (14). Like IRF3, IRF5 exists in a latent state in the cytoplasm and is post-translationally modified and activated by serine phosphorylation. With this activation, IRF5 accumulates in the nucleus.

Since IRF5 is known to relocalize from the cytoplasm to the nucleus upon activation (28), IRF5 cellular localization in etoposide-treated cells was examined by microscopy. Cells were transfected with a plasmid encoding a GFP IRF5 fusion protein, 24 hours later cells were treated with etoposide and visualized by fluorescence microscopy. IRF5 remained within the cytoplasm after treatment with etoposide for 24 hours (Figure 32). IKKε is a serine/threonine kinase that phosphorylates and activates IRF5 (28). As a positive control, IRF5-GFP localization was also investigated in cells cotransfected with an IKKε encoding plasmid, where IRF5-GFP clearly accumulated in the nucleus. IRF5 localization after etoposide treatment was also investigated by microscopy at earlier and later time points and, in all cases, IRF5 remained within the cytoplasm (data not shown), suggesting that IRF5 is not activated in response to etoposide.

IRF5 is activated via phosphorylation by the serine/threonine kinases IKKε and TBK1 (28) and this modification results in a slower migration when an N-terminal region deleted form of IRF5 (ΔN-IRF5) is visualized by SDS-PAGE analysis (27). The migration of ΔN-IRF5 was studied in etoposide-treated cells in order to determine if IRF5 is activated in response to etoposide treatment (Figure 33). A plasmid encoding T7-tagged ΔN-IRF5 was transfected into HeLa cell. As a positive control, where indicated, cells also were transfected with a plasmid encoding the kinase IKKε. Cell lysates were

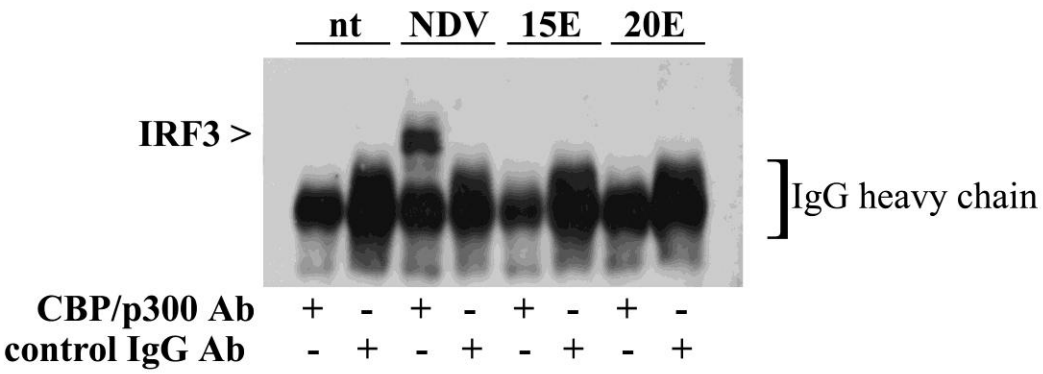

Figure 31: IRF3 does not bind CBP/p300 in etoposide-treated cells.

THP-1 cells were treated with etoposide for 15 or 20 hours or, as a positive control, New Castle Disease Virus (NDV) for 10 hours. Whole cell lysates were incubated with CBP/p300 antibodies or control IgG. Immunocomplexes were run on SDS-PAGE and Western Blot analysis was performed using IRF3 antibody.

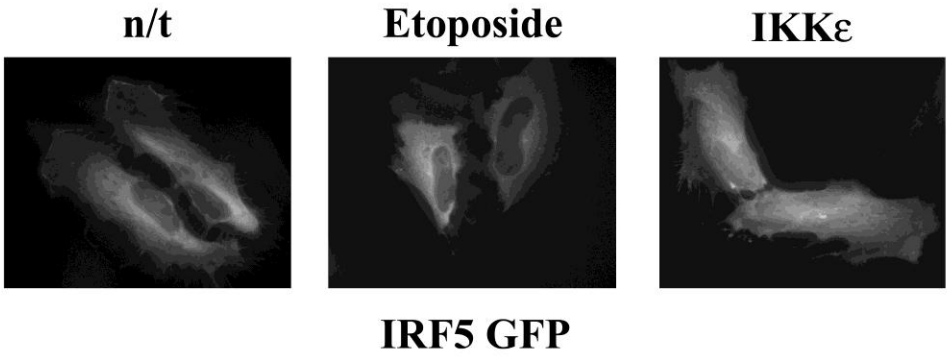

Figure 32: IRF5 does not accumulate in the nucleus with etoposide treatment.

HeLa cells were transfected with a GFP-IRF5 encoding plasmid. The cellular localization of GFP-IRF5 was evaluated after treatment with etoposide for 24 hours. Where indicated, as a positive control, an IKKε encoding plasmid was cotransfected with the GFP-IRF5 plasmid.

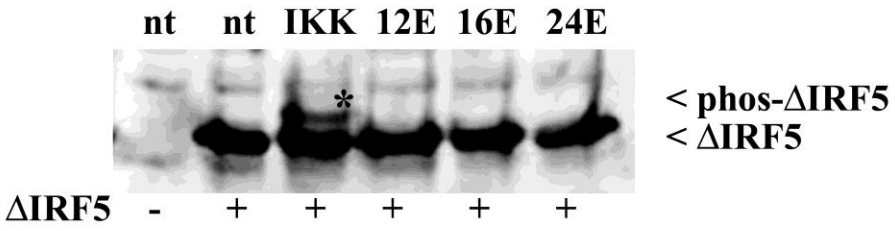

Figure 33: IRF5 is not phosphorylated in etoposide-treated cells.

HeLa cells were transfected with a plasmid encoding T7 tagged DIRF5 (IRF5 with a deleted N- terminal region), and then treated for 12, 16 or 24 hours with 40ug/mL etoposide or left untreated. Where indicated, as a positive control, a plasmid encoding the serine/threonine kinase IKKε was also transfected. IRF5 phosphorylation was investigated by Western blot analysis, using whole cell lysates and a T7 antibody. IRF5 phosphorylation is visualized as a slower migrating band, indicated by *.

separated by SDS-PAGE and IRF5 protein was visualized by Western Blotting using an antibody against the T7 epitope. When compared to the positive control sample, a slower migrating IRF5 species did not appear in the lanes containing the etoposide-treated cell lysates, indicating that IRF5 is not phosphorylated upon etoposide treatment. As in the cell localization study above, this suggests that IRF5 is not activated and involved in the induction of IFN in etoposide-treated cells.

IRF7 is activated in etoposide-treated cells.

IRF7 is an IRF family member that is a key regulator of the type I IFN response to viral and bacterial infection (54). It is expressed constitutively at low levels in lymphoid cells but can be induced to high levels in all cell types (8). Once induced, IRF7 primes infected cells for a second and more diverse wave of IFN production (116). Previous microarray data indicated that IRF7 was induced in response to etoposide treatment (Appendix A). This observation was confirmed using RT-PCR and primers specific for IRF7 (Figure 34). RNA was extracted from untreated or 24 hour etoposide-treated THP-1 cells, reverse transcribed into cDNA and IRF7 mRNA levels were evaluated using primers specific to IRF7 or actin. PCR products were visualized on an agarose gel. The mRNA levels of IRF7 increased with etoposide treatment, verifying the microarray data.

IRF7 resides latent in the cytoplasm and, upon activation, translocates into the nucleus. To evaluate whether IRF7 is activated with etoposide treatment, IRF7 cellular localization was studied using fluorescent microscopy. HT1080 tetracycline-inducible IRF7-myc stable cells were treated concurrently with etoposide and doxycycline for 24 hours and IRF7 was visualized using a myc antibody (Figure 35). With etoposide treatment, IRF7 accumulated in the nucleus, consistent with its activation.

IRF7 activation induces a conformational change in IRF7 that allows the transcription factor to homodimerize (104, 119). A dimerization assay that studied altered migration in non-denaturing gel electrophoresis (68) was performed to determine whether IRF7 homodimerized in response to etoposide (Figure 36). IRF7 was induced in HT1080 tetracycline-inducible IRF7-myc cells with doxycycline. As indicated, cells were also concurrently treated with etoposide. Cell lysates were prepared and proteins

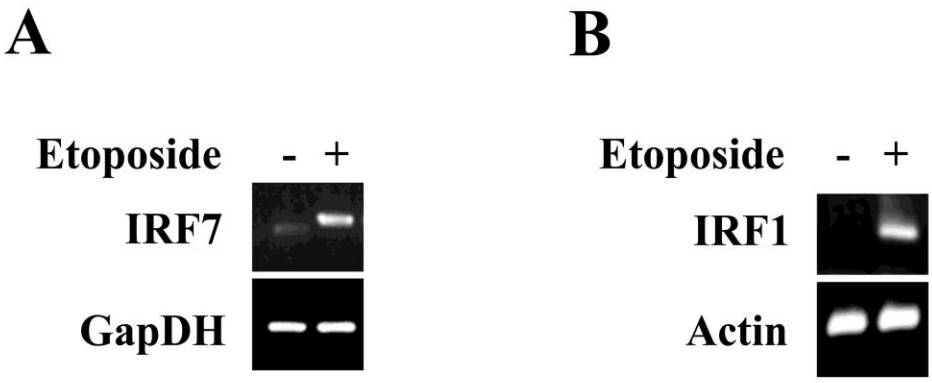

Figure 34: IRF7 and IRF1 are induced in etoposide-treated cells.

Induction of the IRF7 (A) or IRF1 (B) gene in untreated or 24 hour etoposide-treated THP-1 cells was investigated using RT-PCR and primers specific to IRF7 or IRF1. Primers specific to actin or GAPDH were also utilized to ensure equal amounts of cDNA were used in each reaction. PCR products were visualized on an agarose gel.

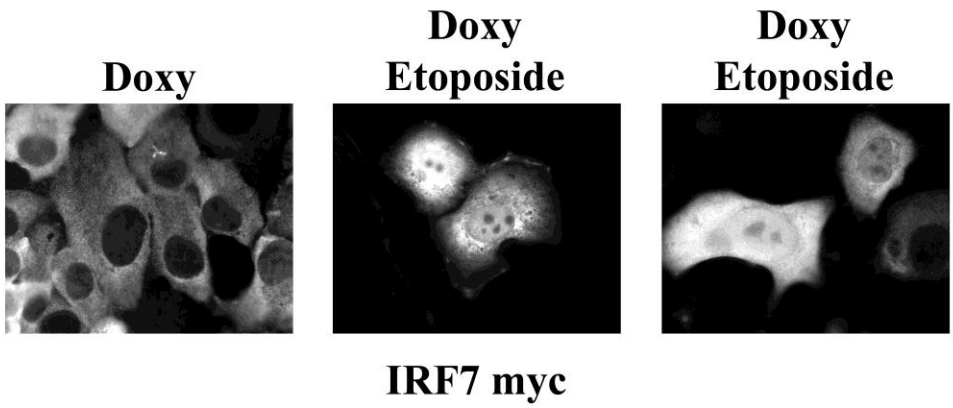

Figure 35: IRF7 accumulates in the nucleus with etoposide treatment.

Cellular localization of myc –tagged IRF7 was visualized in a HT1080 tetracycline inducible IRF7-myc stable cell line. Cells were treated with 2ug/mL doxycycline only or concurrently with 40ug/mL etoposide and for 24 hours. Using a myc antibody, immunofluorescence was performed and cells were visualized under a fluorescence microscope.

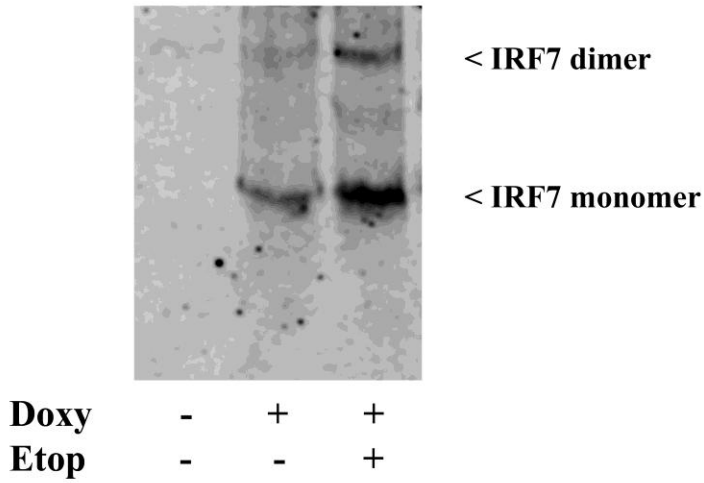

Figure 36: IRF7 dimerizes after etoposide treatment.

HT1080 tetracycline inducible IRF7-myc stable cells were treated with doxycycline only or concurrently with etoposide. Cell lysates were run on native PAGE and analyzed by Western blotting for IRF7 dimerization.

were separated by electrophoresis in a non-denaturing gel. Western blot anaylsis using IRF7 or myc antibodies was performed to identify IRF7 monomers and dimers. IRF7 dimers were visualized as a distinct slower migrating complex and the levels of this complex increased with etoposide treatment. The dimerization of IRF7 in etoposide-treated cells suggests that IRF7 is activated with etoposide treatment.

IRF7 is activated via phosphorylation by the serine/threonine kinase IKKε (185) and this modification results in a slower migration when visualized by SDS-PAGE analysis, which was studied in etoposide-treated cells. IRF7 was induced in HT1080 tetracycline-inducible IRF7-myc cells with doxycycline treatment. As indicated, cells were concurrently treated with etoposide or, as a positive control, transfected with a plasmid encoding the kinase IKKε. Cell lysates were separated by SDS-PAGE and IRF7 protein was visualized by Western Blotting using an antibody against the myc epitope. When compared to the positive control sample, a slower migrating IRF7 species did not appear in the lanes containing the etoposide-treated cell lysates, indicating that IRF7 is not phosphorylated upon etoposide treatment (Figure 37).

In addition to serine phosphorylation (9, 22), IRF7 is also activated by RIP-dependent K63-linked ubiquitination, which regulates its function (58). To evaluate whether IRF7 is ubiquitated in etoposide-treated cells by K63-linkage, in vivo ubiquitination assays were performed (144). HT1080 tetracycline-inducible IRF7-myc/His cells were transfected with a plasmid encoding an HA-tagged ubiquitin mutant, termed K63-only ubiquitin. This mutated ubiquitin protein has all lysines except K63 modified to alanines. The overexpression of this modified ubiquitin allows proteins to only be ubiquitinated by K-63 linkage. Twenty-four hours after transfecting the cells with the HA-tagged K63-only ubiquitin-encoding plasmid, cells were treated with doxycycline to induce IRF7-myc/His expression and, as indicated, were concurrently treated with etoposide for 24 hours. Lysates were incubated with Ni-NTA beads and the associated complexes were disrupted by boiling. Samples were subjected to SDS-PAGE and analyzed by Western blot using an anti-IRF7 antibody (Figure 38). In cells treated with etoposide, slower migrating bands, identified as IRF7 by Western blot, indicate IRF7 ubiquitination, thus supporting the hypothesis that IRF7 is activated via ubiquitination in etoposide-treated cells (58, 144).

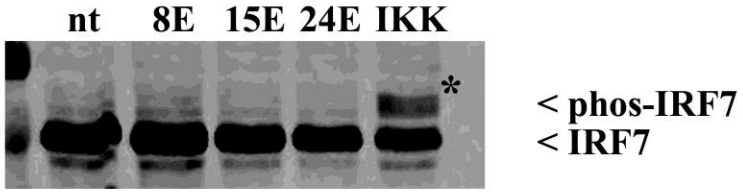

Figure 37: IRF7 is not phosphorylated in etoposide-treated cells.

HT1080 Tet inducible IRF7myc cells were treated with 2ug/mL doxycycline to induce myc-tagged IRF7 and then treated for 8, 15 or 24 hours with 40ug/mL etoposide or left untreated. Where indicated, as a positive control, a plasmid encoding the serine/threonine kinase IKKε was also transfected. IRF7 phosphorylation was investigated by Western blot analysis, using whole cell lysates and an anti-myc antibody. IRF7 phosphorylation is visualized as a slower migrating band, indicated by *.

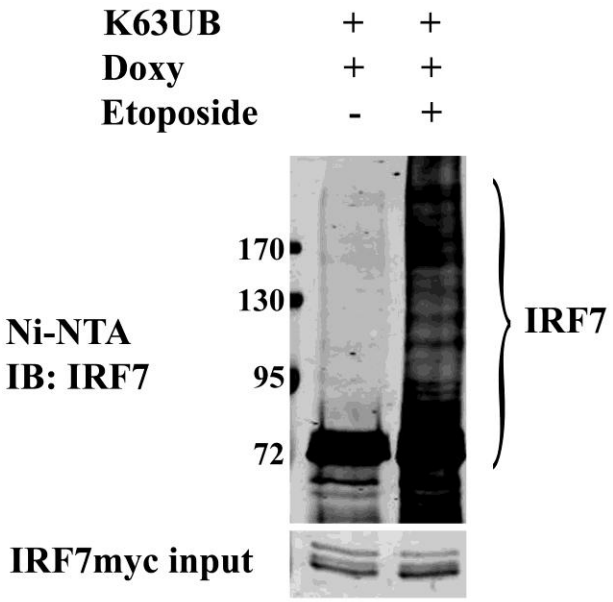

Figure 38: IRF7 is ubiquitinated by K63 linkage following etoposide treatment.

Tetracycline-inducible IRF7-myc stable cell line were transfected with an HA tagged K-63 only ubiquitin construct. 24 hours after transfection, myc/his tagged IRF7 was induced with doxycycline. Cells were left untreated or were concurrently treated with etoposide for 24 hours. Lysates were incubated with Ni-NTA beads and the complexes were distrupted by boiling. Samples were subjected to SDS-PAGE and analyzed by Western blot using an anti-IRF7 antibody. Inputs of IRF7 are shown by Western blot using an anti-IRF7 antibody.

IRF7 activates the IFNα_{14} gene in etoposide-treated cells.

Since the above studies indicate that IRF7 is activated in etoposide-treated cells, the transcriptional activity of IRF7 was evaluated using a luciferase reporter assay. HT1080 tetracycline-inducible IRF7-myc stable cells were transfected with a plasmid containing a -500 nucleotide promoter region of IFNα_{14} driving a luciferase reporter. Cells were treated with etoposide and/or doxycycline for 24 hours before a luciferase assay was performed (Figure 39). Luciferase activity increased substantially with IRF7 overexpression and etoposide treatment, indicating IFNα_{14} promoter activation by IRF7.

IRF7's role in IFNα induction was also evaluated using primers specific to IFNα in quantitative RT-PCR assays (Figure 40). HT1080 tetracycline-inducible IRF7-myc stable cells were treated with etoposide and/or doxycycline for 24 hours before performing quantitative RT-PCR using primers specific to most IFNα. Data was analyzed using the LightCycler software and values were normalized to actin mRNA levels. IFNα mRNA levels significantly increased in etoposide-treated cells with IRF7 overexpression. All together, these data indicate that IRF7 plays a role in IFNα production in response to etoposide treatment.

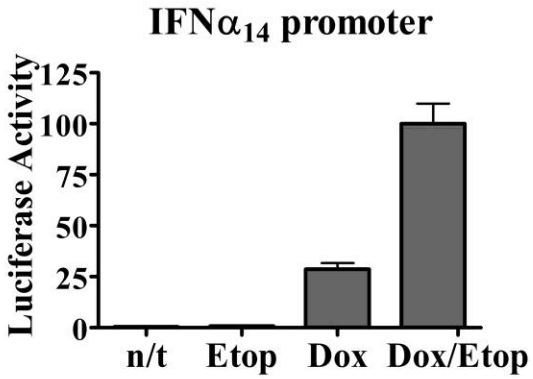

Figure 39: IRF7 activates the IFNα_{14} promoter with etoposide treatment.

HT1080 tetracycline-inducible IRF7-myc stable cell line was transfected with a luciferase reporter construct containing a -457 nucleotide region of IFNα_{14} gene promoter. Cells were treated with etoposide and/or doxycycline for 24 hours before a luciferase assay was performed.

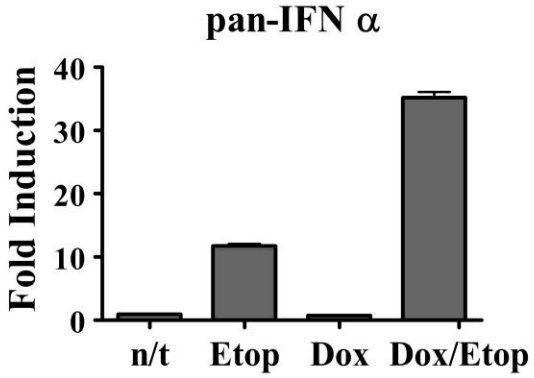

Figure 40: IRF7 induces IFNα with etoposide treatment.

HT1080 tetracycline-inducible IRF7-myc stable cells were treated with etoposide and/or doxycycline for 24 hours before performing quantitative RT-PCR using primers specific to most IFNα genes. Data was analyzed using the LightCycler software and values were normalized to actin mRNA levels.

Part III: IRF1 and NFκB Activate the IFNλ$_1$ Gene.

IRF1 is induced in etoposide-treated cells and activates the IFNλ1 gene.

IRF-1 is another member of the IRF family with diverse functional roles in the cellular response to pathogens, tumor prevention, and the development of the immune system (89). Like IRF7, IRF1 was identified as an etoposide-induced gene in previous microarray data (Appendix A). This observation was confirmed using RT-PCR and primers specific for IRF1 (Figure 34). RNA was extracted from untreated or 24 hour etoposide-treated THP-1 cells, reverse transcribed into cDNA and IRF1 mRNA levels were evaluated using primers specific to IRF7 or GAPDH. PCR products were visualized on an agarose gel. The mRNA levels of IRF1 increased with etoposide treatment, verifying the microarray data.

The IFNλ$_1$ promoter contains an IRF binding site (153) (Figure 41). To evaluate IRF1's role in IFNλ$_1$ promoter activation with etoposide treatment, luciferase reporter assays were performed using a luciferase reporter plasmid containing a -554 nucleotide promoter region of IFNλ$_1$ gene (Figure 42). A plasmid encoding IRF1was transfected into HeLa cells and, as indicated, treated with etoposide 24 hours after transfection. Cell lysates were used in a luciferase reporter assay to evaluate IFNλ$_1$ promoter activation. IFNλ$_1$ promoter activity increased with IRF1 overexpression, and increased further when cells were both treated with etoposide and transfected with IRF1.

Since luciferase reporter assays indicated that IRF1 is involved in activating the IFNλ$_1$ gene, IRF1's ability to bind the IFNλ$_1$ promoter was investigated using a DNA binding assay. An Electrophoretic Mobility Shift Assay (EMSA) was performed using radiolabeled oligonucleotide corresponding to the IRF binding site within the IFNλ$_1$ gene promoter and 24 hour etoposide-treated HCT116 cell lysates (Figure 43). IRF1 formed a DNA binding complex in etoposide-treated cells and this binding was specific, as indicated by the elimination of the IRF-DNA complex when cold oligonucleotide or IRF1 antibody was included in the reaction. Together with the luciferase reporter assay data, it has been demonstrated that IRF1 has a role in the induction of the IFNλ$_1$ gene in response to etoposide treatment.

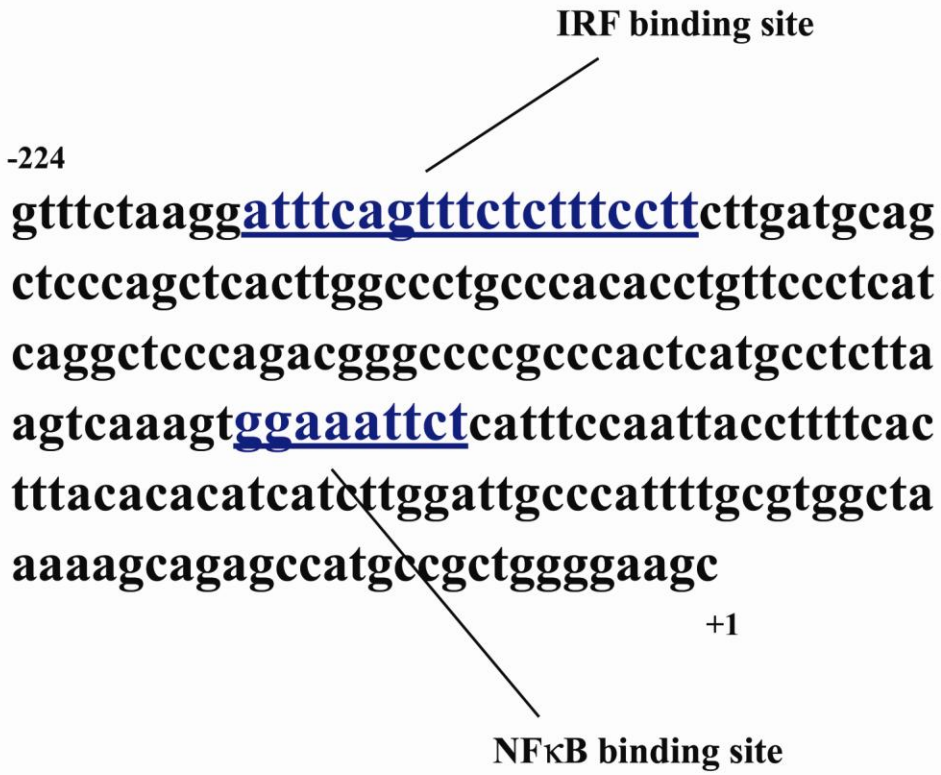

Figure 41: IFNλ_1 promoter contains IRF and NFκB binding sites.

-224 nucleotide region of IFNλ_1 promoter sequence is shown above, indicating an IRF binding site and NFκB binding site.

Figure adapted from Onoguci et al., J. Biol. Chem., Vol. 282, Issue 10, 7576-7581.

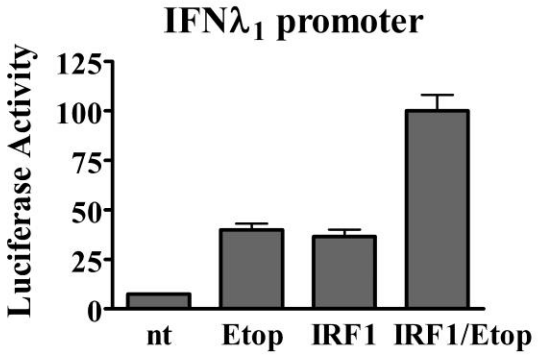

Figure 42. IRF1 activates the IFNλ_1 promoter.

A luciferase reporter plasmid containing a -554 nucleotide promoter region of IFNλ_1 gene was transfected into HeLa cells. Where indicated, an IRF1 encoding plasmid was also transfected. 24 hours after transfection, indicated cells were treated with etoposide for 24 hours before a luciferase assay was performed.

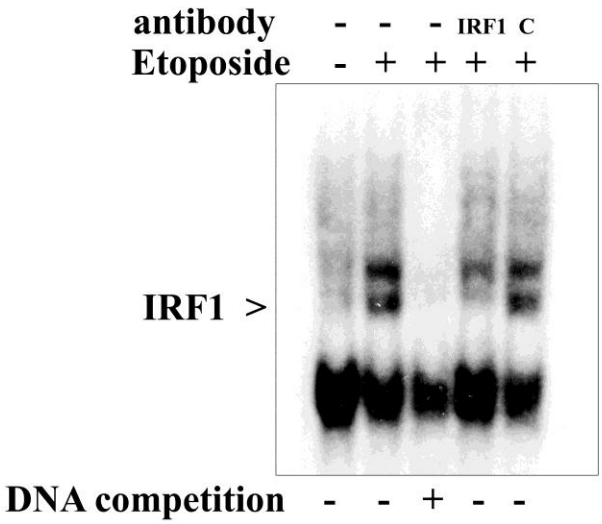

Figure 43: IRF1 binds the IRF binding site in the IFNλ_1 gene promoter.

EMSA using the IRF binding site within the IFNλ_1 promoter was evaluated with extracts from untreated or 24 hour etoposide treated HCT116 cells. Where indicated, IRF1 antibody (IRF1), normal rabbit antibody (C), or an unlabeled IRF binding site oligo nucleotide were included in the reaction.

NFκB is activated in etoposide-treated cells.

It has been reported in previous studies that NFκB is activated in response to etoposide treatment (17, 202) and these findings were further evaluated in this study. In unstimulated cells, the NFκB complex is sequestered in the cytoplasm by its inhibitor, IκB (18). In response to stimuli, such as virus infection or TNFα treatment, IκB is phosphorylated and degraded, allowing NFκB to translocate into the nucleus. Since NFκB shuttles between the cytoplasm and nucleus and accumulates in the nucleus upon activation, its activation was evaluated by studying it cellular localization. NFκB localization in untreated and etoposide-treated HeLa cells was evaluated by immunofluorescence microscopy using antibodies to the NFκB subunit RelA (Figure 44). While, NFκB in untreated cells remained in the cytoplasm, in etoposide-treated cells it accumulated in the nucleus. This nuclear accumulation suggests NFκB is activated upon etoposide treatment.

Upon its release from IκB and its translocation into the nucleus, the NFκB subunits bind to the NFκB DNA recognition site of target gene promoters, such as the IFNλ_1 promoter (Figure 41) (153). NFκB activation was further studied by performing a DNA binding assay. An Electrophoretic Mobility Shift Assay (EMSA) was performed using radiolabeled oligonucleotide corresponding to a consensus NFκB binding site and lysates from HeLa cells that were treated with etoposide for 12 or 24 hours or infected with NDV, as a positive control (Figure 45). NFκB bound the radiolabeled oligonucleotide in etoposide-treated cells and this binding was specific, as indicated by the disappearance of the complex with cold oligonucleotide competition.

NFκB activation also was evaluated by studying RelA phosphorylation on serine 536, an indicator of NFκB activation (72, 227). Cell lysates from etoposide or TNFα–treated cells were used in immunoprecipitations using an anti-RelA antibody and the immunocomplexes were subjected to Western blot analysis using anti-RelA or anti-phosphoSerine-536 RelA antibodies. Phosphorylation on Serine-536 was clearly demonstrated in etoposide-treated cells (Figure 46). Together with the DNA binding assay data, this indicates that NFκB is activated in cells exposed to etoposide.

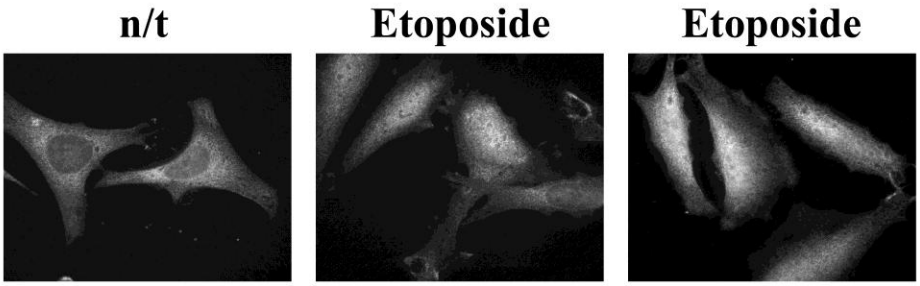

Figure 44: NFκB accumulates in the nucleus after 2 hours of etoposide treatment.

The cellular localization of the NFκB subunit RelA was evaluated in HeLa cells after treatment with 40ug/mL etoposide for 2 hours using immunofluorescence with a RelA antibody.

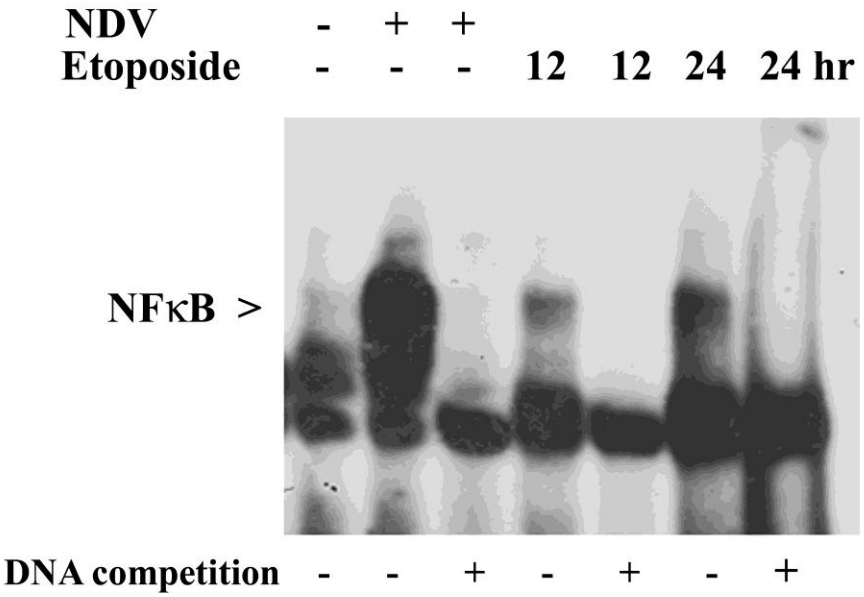

Figure 45: NFκB binds DNA in response to etoposide treatment.

Nuclear lysates were prepared from HeLa cells that were untreated, etoposide treated for 12 hours or 24 hours, or infected with NDV for 6 hours. Lysates were incubated with a ^{32}P radiolabeled DNA probe consisting of a NFκB binding site. Prior to the addition of the radioactively labeled probe, an unlabeled NFκB binding site oligo nucleotide was also included as competitor to demonstrate the specificity of NFκB binding. The position of the NFκB complex is noted by an arrow.

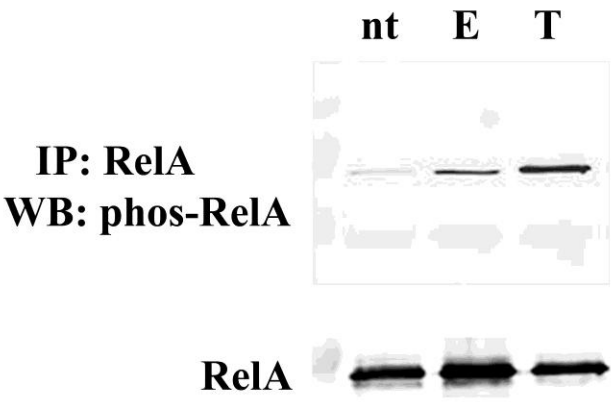

Figure 46: RelA is phosphorylated on Serine 536 in etoposide-treated cells.

HCT116 cells were treated with etoposide (E) for 15 hours or TNFα (T) for 1 hour. Whole cell lysates were incubated with an anti-RelA antibody and the immunocomplexes were subjected to SDS-PAGE and Western blot with either anti-phosphoSerine 536 RelA or anti-RelA antibodies.

IFNλ_1 promoter activity in etoposide-treated cells is dependent on NFκB.

NFκB has been identified as a transcription factor that takes part in the induction of several IFN genes, including IFNλ_1 and IFNβ (153, 229). The promoters of the IFNλ family contain NFκB binding sites (Figure 41) and NFκB binding to the promoter is essential for gene expression (153). In order to determine whether NFκB plays a transcriptional role in the activation of this promoter, a plasmid encoding a dominant-negative IκB was employed. The dominant-negative form of IκBα is not inactivated by phosphorylation and ubiquitination due to double serine to alanine mutations at the phosphorylation sites S32 and S36. This mutated IκBα functions as a negative interfering mutant and blocks NFκB activation by indefinitely sequestering NFκB in the cytoplasm and effectively inhibiting NFκB activity (18, 25).

HeLa cells were transfected with a plasmid containing a -317 nucleotide promoter region of the IFNλ_1 gene driving a luciferase reporter, together with either an empty vector or the plasmid encoding the IκB dominant-negative protein. After treating the transfected cells with etoposide, luciferase assays were used to evaluate IFNλ_1 promoter activity in the context of NFκB inhibition. In the samples where this dominant-negative IκB was employed to block NFκB activity, the promoter activity of IFNλ_1 was greatly diminished (Figure 47), strongly suggesting that NFκB plays a role in the activation of the IFNλ_1 promoter in response to etoposide treatment.

IFNλ_1 induction in etoposide-treated cells is NFκB dependent.

As indicated by data above, NFκB is activated in etoposide-treated cells (Figures 44-46) and is needed for the transcription of the IFNλ_1 gene (Figure 47). The role of NFκB in IFN signaling in etoposide-treated cells was further investigated by studying the induction of the interferon-inducible gene, ISG54. NFκB activity was inhibited by utilizing an inhibitor of IKKβ, the kinase that phosphorylates and inactivates IκB. HeLa cells were treated with etoposide for 24 hours or first pretreated with the IKKβ inhibitor ML120 before etoposide treatment. Cell lysates were separated by SDS-PAGE and Western blotting analysis was performed using an ISG54 antibody (Figure 48). ISG54 was induced in etoposide-treated cells, indicating the activation of IFN signaling. By

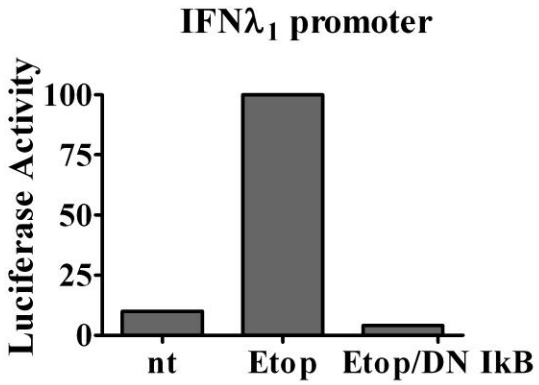

Figure 47: NFκB inhibition decreases IFNλ_1 promoter activity in etoposide-treated cells.

A luciferase construct containing a -317 nucleotide region of IFNλ_1 was cotransfected into HeLa cells with either empty vector or a plasmid expressing a dominant negative (DN) IκB. Cells were treated with 40ug/mL etoposide for 24 hours before a luciferase assay was performed.

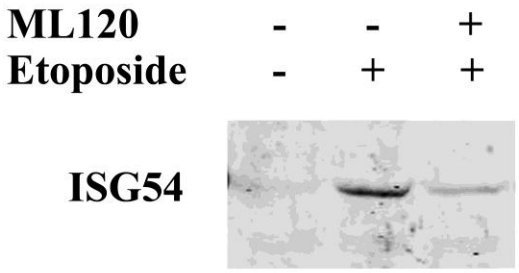

Figure 48: ISG54 induction in etoposide-treated cells is NFκB dependent.

HeLa cells were treated with 40ug/mL of etoposide for 24 hours or first pretreated with the IKKβ inhibitor ML120 before etoposide treatment. Whole cells lysates were prepared and used in Western blot analysis for ISG54.

inhibiting NFκB activation with ML120, ISG54 induction diminished, suggesting the NFκB activation plays a major role in the activation of IFN signaling.

To further verify that NFκB is a major transcription factor involved in the IFNλ$_1$ response to etoposide, NFκB was again inhibited using the ML120 IKKβ inhibitor in etoposide-treated cells and IFNλ$_1$ gene induction was evaluated. HeLa cells were treated with etoposide for 24 hours or first pretreated with the IKKβ inhibitor ML120 before etoposide treatment. Quantitative RT-PCR was performed using primers specific to IFNλ$_l$ (Figure 49). With NFκB inhibition, the mRNA levels of IFNλ$_l$ were diminished in etoposide-treated cells.

To summarize, in etoposide-treated cells, the transcription factor NFκB is activated by phosphorylation on Serine 536, binds DNA elements of gene promoters, and activates the transcription of the IFNλ$_1$ gene (Figures 45-47). Furthermore, NFκB is required for IFNλ$_1$ induction in response to etoposide treatment (Figure 49).

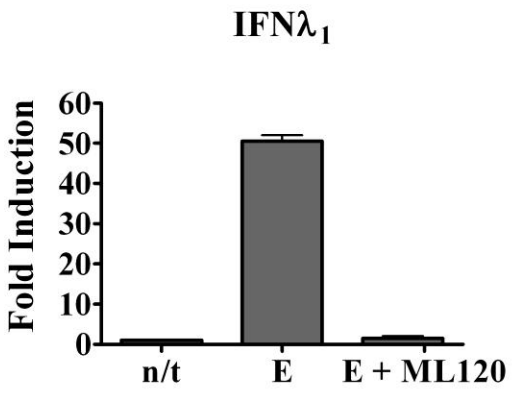

Figure 49: IFNλ_1 induction is NFκB dependent in etoposide-treated cells.

HeLa cells were treated with 40ug/mL of etoposide for 24 hours or first pretreated with the IKKβ inhibitor ML120 before etoposide treatment. Total RNA was isolated and used to synthesize cDNA. Real Time PCR was performed using primers specific to IFNλ_1. Data was analyzed using the LightCycler software and values were normalized to actin mRNA levels.

Part IV: NFκB is the master transcription factor of IFN induction in response to etoposide.

IFN and IRF induction over time in etoposide-treated cells.

IRF7 and IRF1 have been implicated in inducing the IFN genes, but these IRF family members are themselves induced by interferon in a positive feedback loops (37, 118, 134, 145, 176). To ensure that IRF7 and IRF1 are responsible for the primary induction of IFN and not simply part of a positive feedback loop, IRF7, IRF1, IFNα and IFNλ_1 gene expression was evaluated over time in etoposide-treated cells using quantitative RT-PCR. THP1 cells were treated with etoposide from 0 to 24 hours, and quantitative RT-PCR was performed using primers specific to IRF7 or IRF1 (Figure 50) and IFNα or IFNλ_1 (Figure 51). Clearly, IRF7 and IRF1 expression precedes that of the IFN species, suggesting that IRF7 and IRF1 are two primary transcription fators involved in transcriptionally regulating IFN gene expression.

Etoposide-induced IFNα expression is dependent on NFκB.

The transcriptional role of NFκB in IFNλ_1 promoter activation in etoposide-treated cells (Figure 47 and 49) was not unexpected due to the presence of an NFκB DNA binding site within the promoter (Figure 41). Although IFNα promoters do not contain NFκB DNA binding sites (153), NFκB may play a role in etoposide-induced IFNα expression further upstream. To determine whether NFκB plays a role in IFNα expression in etoposide-treated cells, NFκB was inhibited using the ML120 IKKβ inhibitor in etoposide-treated cells and IFNα gene induction was evaluated. HeLa cells were treated with etoposide for 24 hours or first pretreated with the IKKβ inhibitor ML120 before etoposide treatment. Quantitative RT-PCR was performed using primers specific to IFNα (Figure 52). With NFκB inhibition, the mRNA levels of IFNα were diminished in etoposide-treated cells.

NFκB is responsible for the induction of IRF7 and IRF1 in etoposide-treated cells.

Previous data (Figures 39 and 40) indicated that IFNα induction in etoposide-treated cells was dependent on IRF7. Despite a lack of a NFκB DNA binding site, the

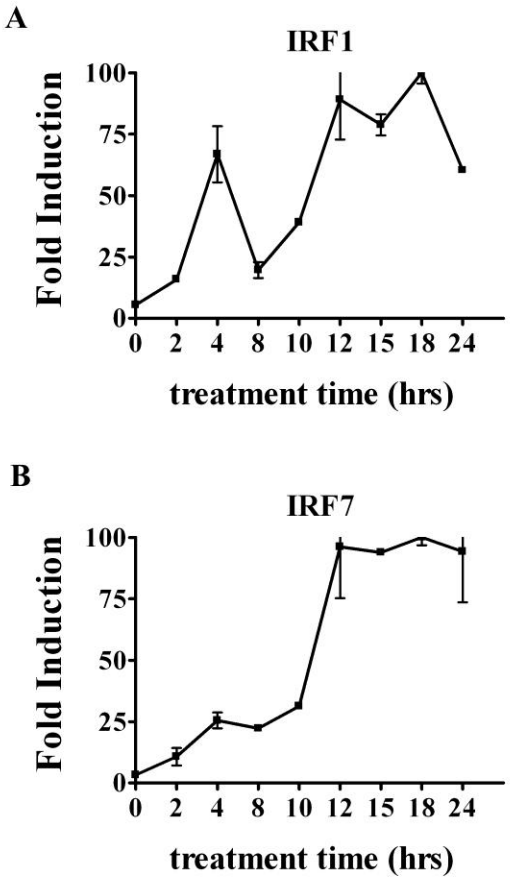

Figure 50: Evaluation of IRF1 and IRF1 expression over time in etoposide-treated cells.

THP1 cells were treated with etoposide for the times indicated. Quantitative RT-PCR was performed using primers specific to IRF1 (A) or IRF7 (B). Data was analyzed using the LightCycler software and values were normalized to actin mRNA levels

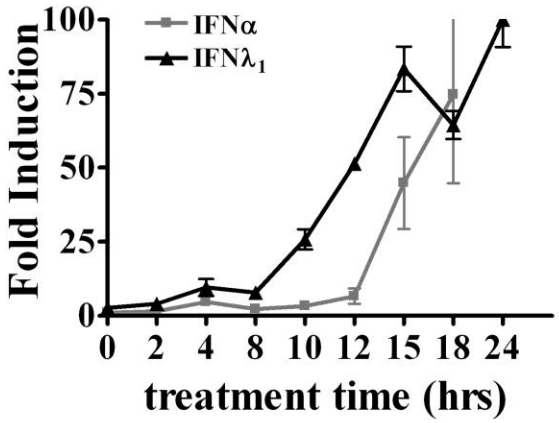

Figure 51: Evaluation of IFN expression over time in etoposide-treated cells.

THP1 cells were treated with etoposide for the times indicated. Quantitative RT-PCR was performed using primers specific most IFNα species or IFNλ_1. Data was analyzed using the LightCycler software and values were normalized to actin mRNA levels

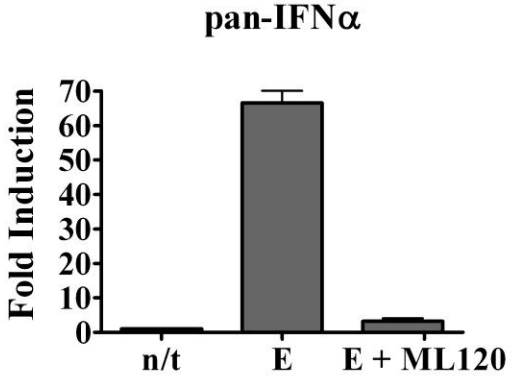

Figure 52: IFNα induction is NFκB dependent in etoposide-treated cells.

HeLa cells were treated with 40ug/mL of etoposide for 24 hours or first pretreated with the IKKβ inhibitor ML120 before etoposide treatment. Total RNA was isolated and used to synthesize cDNA. Real Time PCR was performed using primers specific to most IFNα subspecies. Data was analyzed using the LightCycler software and values were normalized to actin mRNA levels.

inhibition of NFκB diminished IFNα levels in etoposide-treated cells. This observation and as well as published data describing NFκB induction of IRF7 in TNFα-treated cells (113), lead to studying the role NFκB has on IRF7 expression in etoposide-treated cells.

The mRNA levels of IRF7 in etoposide-treated cells was studied when NFκB was inhibited with the IKKβ inhibitors BAY117085 and ML120. HeLa cells were treated with etoposide for 5 hours and, as indicated, cells were also pretreated with either BAY117085 or ML120. RNA was isolated and used in quantitative RT-PCR to measure IRF7 mRNA levels using primers specific to IRF7. Data was analyzed using the LightCycler software and values were normalized to actin mRNA levels using primers specific to actin (Figure 53). IRF7 was induced with etoposide treatment and its levels were diminished when NFκB activity was inhibited with the IKKβ inhibitors, strongly suggesting that IRF7 expression in etoposide-treated cells is NFκB dependent.

In addition to its role in activating the IRF7 gene, NFκB has also been implicated in the activation of the IRF1 gene (113, 152, 161, 192). Therefore, etoposide induced IRF1 expression was studied in cells wherein NFκB was inhibited. HeLa cells were pretreated with either IKKβ inhibitors BAY117085 or ML120 before treatment with etoposide. Quantitative RT-PCR was performed using primers specific to IRF1 (Figure 54). As with IRF7 (Figure 53), IRF1 mRNA levels decreased with NFκB inhibition, indicating that NFκB is not only responsible for IFN induction but also for IRF7 and IRF1 expression.

IRF7 partially rescues IFNα gene expression in cells treated with NFκB inhibitor.

The mRNA levels of IRF7, the transcription factor responsible for etoposide-induced IFNα (Figure 39 and 40), diminish with the use of NFκB inhibitors (Figure 52); and, despite not having an NFκB binding site in their promoters, etoposide-induced IFNα mRNA levels also decrease with the use of NFκB inhibitors. To determine whether the reduction of etoposide-induced IFNα in ML120 pretreated cells is due to the reduction of IRF7 levels, a "rescue" experiment was performed, measuring IFNα levels in etoposide/ML120-treated cells wherein IRF7 was reintroduced (Figure 55). HT1080 tetracycline-inducible IRF7-myc stable cells were treated with etoposide and/or ML120.

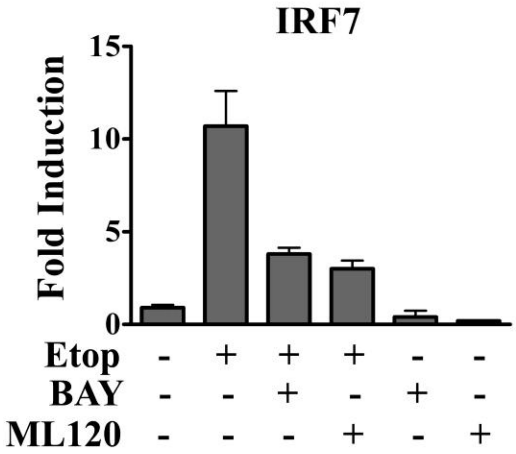

Figure 53: IRF7 expression is NFκB dependent in etoposide-treated cells.

HeLa cells were treated with etoposide for 5 hours. Where indicated, cells were also pretreated with IKKβ inhibitors BAY117085 or ML120 for 1 hour. Quantitative RT-PCR was performed using primers specific to IRF7. Data was analyzed using the LightCycler software and values were normalized to actin mRNA levels.

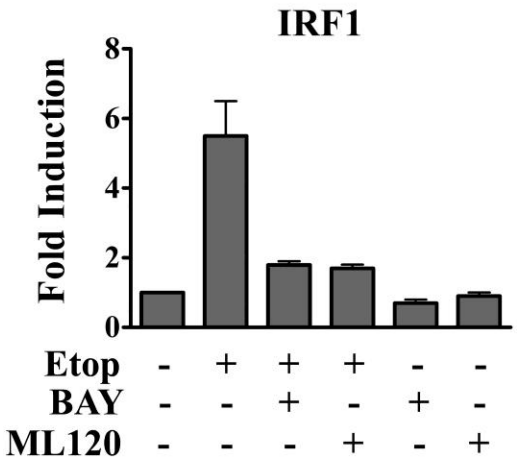

Figure 54: IRF1 expression is NFκB dependent in etoposide-treated cells.

HeLa cells were treated with etoposide for 5 hours. Where indicated, cells were also pretreated with IKKβ inhibitors BAY117085 or ML120 for 1 hour. Quantitative RT-PCR was performed using primers specific to IRF1. Data was analyzed using the LightCycler software and values were normalized to actin mRNA levels.

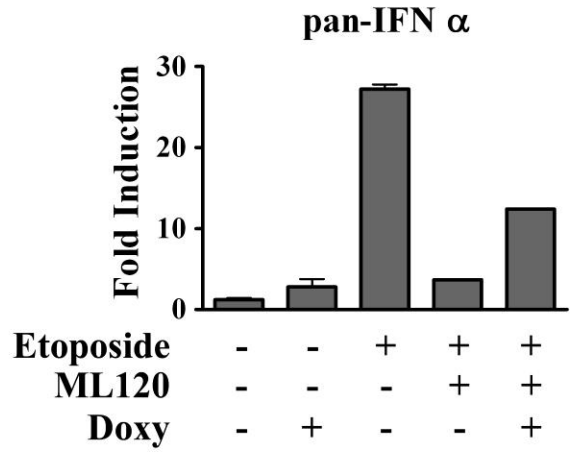

Figure 55: IRF7 rescues IFNα induction in etoposide-treated cells when NFκB is inhibited.

HT1080 tetracycline-inducible IRF7-myc stable cell line were treated with doxycycline, Etoposide or IKKβ inhibitor ML120 for 18 hours. Quantitative RT-PCR was performed using primers specific to most IFNα Data was analyzed using the LightCycler software and values were normalized to actin mRNA levels.

Where indicated, IRF7 was induced using doxycycline. Quantitative RT-PCR was performed using primers specific to most IFNα genes and data was analyzed using Light Cycler software. As previously shown, IFNα levels in etoposide-treated cells decrease with the use of the NFκB, ML120. However, when IRF7 is induced with doxycycline, IFNα gene expression returns to about 50% of its original expression. This data further indicates that IRF7 is responsible for IFNα induction in etoposide-treated cells.

In summary, NFκB is responsible for the induction of both the IRF1 and IRF7 genes in etoposide-treated cells. While IRF1, together with NFκB, induces the IFNλ_1 gene, IRF7 induces IFNα.

Part V: The role of ATM and p53 in etoposide induced IFN.

Etoposide-induced IFN levels decrease with ATM inhibition.

As indicated by the above data, NFκB is a major transcription factor in the etoposide-induced IFN signaling in cells. A linkage between DNA damage signaling and the NFκB activation pathway in cells undergoing genotoxic stress has been suggested (237). Upon DNA double-stranded breakage caused by etoposide, the nuclear protein kinase ATM phosphorylates and associates with NEMO, the regulatory subunit of the IKK complex. The NEMO-ATM complex translocates into the cytoplasm and interacts with the catalytic IKK subunits and activates NFκB signaling.

To investigate whether ATM signaling plays a role in IFN induction in etoposide-treated cells, an ATM inhibitor, AZ12622702, was utilized. RNA was isolated from untreated cells, cells treated with etoposide or AZ12622702, and cells concurrently treated with AZ12622702 and etoposide. cDNA was generated and quantitative RT-PCR was performed using primers specific to IFNλ_1 and primers recognizing most IFNα species (Figure 56). Data was analyzed using LightCycler software and values were normalized to actin. Compared to the etoposide treatment alone, both IFNα and IFNλ_1 mRNA levels decrease by about half with the use of the ATM inhibitor when treating cells with etoposide. This indicates that ATM signaling plays some role in the induction of IFN in etoposide-treated cells.

Lack of p53 inhibits ISG54 induction but not IFN induction in etoposide-treated cells.

Activation of p53 occurs in response to a number of cellular stresses, including DNA damage. Several forms of DNA damage have been shown to activate p53, including those generated by ionizing radiation, ultraviolet light, and chemicals such as etoposide (75). To determine whether p53 plays a role in etoposide-induced IFN signaling, ISG54 induction was studied by Western blot analysis in HCT116 p53 null cells and HCT116 wild type cells. Cells were treated with etoposide for 40 or 80 hours or with IFN for 18 hours, as a positive control. Cells lysates of untreated and treated cells were separated by SDS-PAGE and Western blot analysis with an ISG54 antibody was

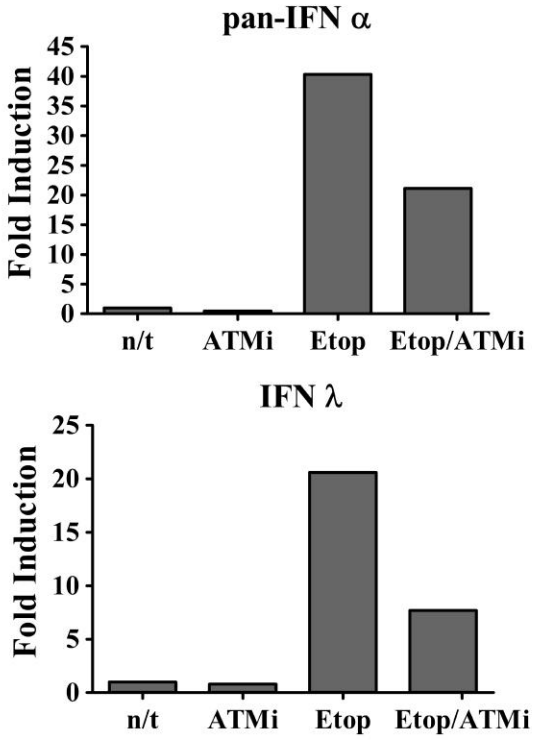

Figure 56. Inhibition of ATM reduces IFN response in etoposide treated cells.

Cells were treated with etoposide for 24 hours. Where indicated, cells were also pretreated with AZ12622702 ATM inhibitor for 1 hour. Quantitative RT-PCR was performed using primers specific to most IFNα or IFNλ_1. Data was analyzed using the LightCycler software and values were normalized to actin mRNA levels.

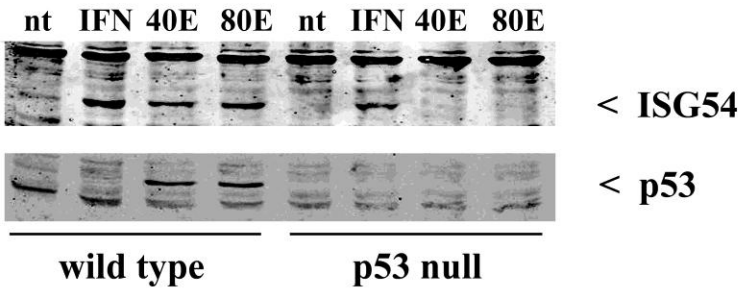

Figure 57: ISG54 is not induced in p53 null HCT116 cells in response to etoposide.

Wild type and p53 null HCT116 cells were treated with 40ug/mL or 80ug/mL etoposide for 24 hours or IFN for 18 hours. Cells lysates of treated and untreated cells were used in Western Blot analysis for ISG54 and p53.

performed (Figure 57). ISG54 was induced by IFN in both wild type and p53 null cells. However, with etoposide treatment, ISG54 was not induced in the p53 null cells, while its wild type parental cell line clearly induced ISG54 in response to etoposide treatments. This data suggests that p53 may play some role in interferon signaling in response to etoposide.

To determine whether the loss of p53 had an impact on IFN induction in etoposide-treated cells, IFNα levels in etoposide-treated HCT116 p53 null cells were compared to those of HCT116 wild type cells. RNA was isolated from untreated and 48 hour etoposide-treated HCT116 wild type and p53 null cells. cDNA was generated and quantitative RT-PCR was performed using primers recognizing most IFNα species (Figure 58). Data was analyzed using LightCycler software and values were normalized to actin. Compared to the wild type, the p53 null cells produced comparable levels of IFN in response to etoposide treatment.

p53 levels stabilize in etoposide-treated HeLa cells.

HeLa cells possess the E6 Human papillomavirus (HPV) protein, which targets p53 protein for degradation via the ubiquitin pathway (57, 178). Studies have shown that p53 protein levels in HPV-positive cervical cancer cells stabilize and increase with cisplatin treatments (56, 106, 107). In order to investigate whether etoposide had a similar effect on p53 protein levels, Western blot analysis of p53 was performed using etoposide-treated HeLa cell lysates. Hela cells were treated with etoposide for 24 hours. Cells lysates of untreated and treated cells were separated by SDS-PAGE and Western blot analysis with a p53 antibody was performed (Figure 59). p53 levels increased with etoposide treatment, suggesting that etoposide treatment stabilizes p53 protein levels, despite the presence of the E6 HPV protein.

NFκB subunit RelA continues to be phosphorylated on Serine 536 in etoposide-treated cells.

Studies suggest that p53 plays a role in NFκB activation (17, 172). p53 induces Ribosomal S6 Kinase 1 (RSK1) activation, which in turn promotes the phosphorylation of Serine 536 of RelA and activates NFκB transcriptional activation. To investigate

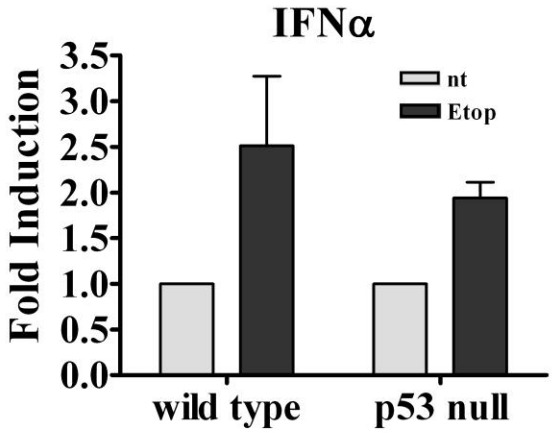

Figure 58: IFNα induction in etoposide treated p53 null cells is similar to those of wild type cells.

HCT116 p53 null or HCT116 wildtype cells were treated with etoposide for 48 hours. Quantitative RT-PCR was performed using primers specific to most IFNα species. Data was analyzed using the LightCycler software and values were normalized to actin mRNA levels.

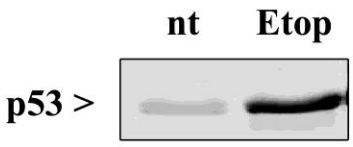

Figure 59: p53 protein levels increase in etoposide treated HeLa cells.

HeLa cells were left untreated or were treated with etoposide for 24 hours. p53 protein levels were evaluated by Western blot analysis, using whole cell lysates and an anti-p53 antibody.

whether NFκB phosphorylation is abrogated in etoposide-treated p53 null cells, Western blot analysis was performed using antibodies against phospho-Serine 536 RelA. Wild type and p53 null HCT116 cells were treated with etoposide as indicated or with TNFα, as a positive control. Cell lysates were incubated with an antibody against RelA and the immunocomplexes were separated by SDS-PAGE. Western blot analysis was then performed using antibodies again phopho-Serine 536 RelA. In both the wild type and the p53 null cells, RelA was phosphorylated by 24 hours of etoposide treatment. Since the p53 null cells show no deficiency in RelA phosphorylation on Serine 536, it is unlikely that the RSK1 kinase plays a role in the phosphorylation of RelA in response to etoposide treatments (Figure 60).

In summary, preliminary data suggests that ATM appears to play a role in IFN signaling in etoposide-treated cells. When ATM is inhibited, etoposide-induced IFN mRNA levels diminish. In cells lacking p53, etoposide-induced IFN signaling is also diminished, as indicated by the lack of ISG54 induction, an indicator of IFN signaling. However, IFN induction itself does not appear to be diminished in cells lacking p53.

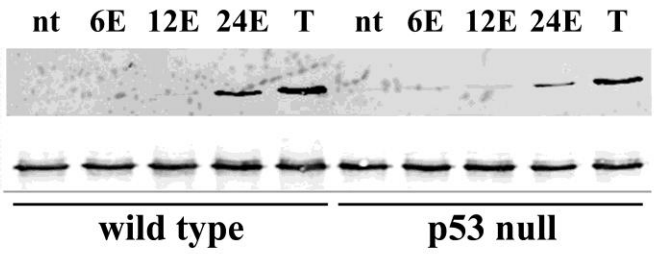

Figure 60: HCT116 p53 null cells are not deficent in RelA phosphorylation.

Wild type and p53 null HCT116 were treated with etoposide for 6, 12 or 24 hours, or treated with TNFα (T) for 2 hours. Cell lysates of treated and untreated (nt) cells were incubated with an antibody against RelA and the immunocomplexes were run on SDS-PAGE. Western blotting analysis was performed using anti-phosphoSerine 536 RelA or RelA antibodies.

DISCUSSION AND FUTURE DIRECTION

DNA damage as a stimulus for the antiviral IFN pathway.

Cells continually experience the threat of genetic damage by both external environmental agents and internal replicational and transcriptional errors (108). Consequently, the DNA damage response is crucial in maintaining genomic integrity against such insults to the DNA. This response not only initiates DNA repair machinery to repair the damage, it also activates a complex system of signaling pathways. These pathways can initiate cell cycle arrest, allow time for the repair of the DNA lesions by repair machinery, or commence apoptosis to clear the organism of a potentially tumorigenic threat (15, 48).

This dissertation begins to describe a novel observation of the convergence of the DNA damage response and IFN signaling pathways. It initiates speculations as to what role IFN plays in a host cell's response to genotoxic stresses. IFNs are well characterized for their antiproliferative, antiviral, and antibacterial effects in response to pathogenic stimuli, such as LPS, flagellin, viral dsRNA and ssRNA . However, specific viral DNA configurations also have been found to be stimuli for IFN production.

Viral infection and replication exposes the cell to exogenous genetic material that can activate IFN signaling through TLR and RLR signaling pathways (70). Furthermore, some viruses are known to stimulate DNA damage response pathways. Therefore, in addition to triggering the IFN response, viruses may also trigger the DNA damage response. For example, the ends of a DNA virus' genome may resemble the DSB of damaged DNA or viruses can generate single strand and double strand DNA breaks during their lytic replication cycle. Epstein-Barr virus, herpes simplex virus 1, and adenovirus are a few examples of DNA viruses that have been documented to activate a DNA damage response (101, 190). Also, the integration of retroviruses, such as HIV, produces a lesion in the host DNA (193, 194, 233).

In addition to developing strategies to block IFN signaling, viruses also have evolved mechanisms to inhibit activation or downstream function of the DNA damage response For example, the adenovirus genome encodes proteins that sequester and degrade the host's MRN complex, which is critical for the DNA damage response (41,

100, 201). These viruses may inhibit this pathway not only to block cell cycle arrest and apoptosis, but to block the antiviral functions of IFNs that are produced by DNA damage.

Possible non anti-viral role of IFN induction as a DNA damage response.

Although the interferon response is known more for its antiviral and antiproliferative activity, studies have suggested that IFN may also act as a tumor suppressor (175, 212). In fact, due to its anti-tumor activity, IFN has been used clinically to treat several types of cancers, including hairy cell leukemia, melanoma, Kaposi's sarcoma, osteosarcoma and colorectal carcinoma (47, 51, 88, 225, 234). It remains unclear as to how IFN functions in controlling tumor progression, but several mechanisms have been suggested. Interferon can trigger cellular senescence by stimulating the expression of certain senescence regulators (135, 198, 207), setting up a line of defense against tumor formation, by preventing the expansion of potentially malignant cells (135). Other studies suggest the anti-tumor effects of IFN are largely due to its ability to induce apoptosis in malignant cells (174, 217).

As cytokines, IFNs have a vital role in immunoregulatory function in addition to their antiviral role (94). Both type I and type III IFNs have been implicated in modulating the adaptive immune response by stimulating MHC class I expression to promote antigen presentation on tumor cells (98, 175) and aiding in the activation of Natural Killer (NK) cells and macrophages (120, 149). Together with its anti-proliferative and apoptotic properties, perhaps the role of IFN in the DNA damage response pathway involves the clearance of potential tumor cells in an NK cell-mediated manner, much like its role in limiting the dissemination of virus.

DNA damage activates IFN signaling.

This study begins by determining that DNA damage induces IFN signaling, independent of viral infection. IFNα and IFNλ, but not IFNβ, was detected by RT-PCR in etoposide-treated monocytes (Figures 20-22). Although IFN secretion was not measured directly, several experiments verified that the IFN was functional and actively transcribed. Active IFN signaling was observed by studying the activation of STAT1 and STAT2, two transcription factors involved in carrying out the IFN response. Both

STAT1 and STAT2 are tyrosine phosphorylated and accumulate in the nucleus with etoposide treatment, both indicators of STAT activation (Figures 18 and 19).

In addition, ISG54, an IFN-inducible gene and a common indicator of active IFN signaling was induced in etoposide-treated cells (Figure 15). Furthermore, the ISG15 promoter, an IFN-responsive promoter, was activated by etoposide treatment and it was determined that the ISRE enhancer was the etoposide responsive DNA element within the ISG15 promoter. In both experiments, IFN-activated STAT1 was required for promoter activation, as demonstrated with the diminishment of ISG15 and ISRE promoter activation in the U3A STAT -/- cells (Figures 16-17).

The active transcription of IFN genes in etoposide-treated cells was first studied by trying to determine whether the IFN promoters were activated. As expected, the IFNλ_1 gene promoter was activated substantially in etoposide-treated cells (Figure 26), supporting the IFNλ_1 RT-PCR data, wherein IFNλ_1 mRNA levels increased with etoposide treatment (Figure 22). However, the promoter activity of IFNα_{14} and IFNα_6 in response to etoposide was more difficult to access. Although RT-PCR experiments indicated that IFNα mRNA levels increased with etoposide treatment (Figure 21), the IFNα promoters remained inactive. Initially small fragments (~500pb) of the IFNα promoters were examined (data not shown) but did not respond to etoposide, despite being induction by viral infection. Suspecting that positive promoter elements further upstream were required for activation by etoposide, larger fragments (~4kB) were examined (Figure 25). Unfortunately, these larger fragments of the IFNα promoters were still unresponsive to etoposide treatment.

The possibility existed that the increase of IFNα mRNA was not due to active transcription of the gene, but an increase in stability of existing IFNα transcripts in the cytoplasm. This possibility was ruled out since IFNα mRNA levels increased in the nucleus (Figure 27a), a strong indicator of active transcription.

Given that IFNα transcripts are generated by the etoposide-treated cells, it is possible that the IFN-directed luciferase reporter assay was not sensitive enough to detect promoter activity. The induction of the IFNλ_1 gene depends primarily on NFκB, whereas the induction of the IFNα genes are dependent on the transcription factor IRF7 (Figures

39 and 40) (154). NFκB is present in the cell, whereas IRF7 must first be transcribed. This may explain why the IFNλ_1 promoter activity is detected by the luciferase assay, whereas IFNα promoter activity is not. Experimentally this is overcome with IRF7 overexpression. IFNα promoter activity is easily detected when IRF7 is over expressed and its activity is further enhanced with etoposide treatment (Figure 39).

Unlike virally infected cells, IFNβ is not activated in etoposide-treated cells.

The regulation of IFN expression in response to the DNA damage was investigated in this study and compared to the induction of IFNs associated with the antiviral response (70). The transcriptional induction of the IFN family is tightly regulated and involves various transcription factors and regulatory DNA sequences (30, 35, 117, 129, 153). IFNβ is the first IFN produced by infected cells and aids in potentiating the IFNα response (118). Its expression is regulated primarily by the IRF family of transcription factors, especially IRF3 (162, 229), in addition to several other transcription factors, including NFκB (233).

Curiously, IFNβ is not produced by etoposide-treated cells, suggesting a distinctive IFN response to DNA damage. In this, and in other studies (202), NFκB is clearly activated in etoposide-treated cells, as indicated by its nuclear accumulation, phosphorylation on Serine 536 and its ability to bind DNA (Figures 44-46). However, IRF3 is not activated in response to etoposide treatment (Figures 30 and 31), despite previous findings suggesting otherwise (81). Since IRF3 is part of the enhanceosome responsible for IFNβ expression and IFN production is impaired without its presence within the complex (117, 229), the lack of IRF3 activation in etoposide-treated cells serves as an explanation for the lack of IFNβ induction. It has been reported that IRF5 may play a role in IFNβ induction in response to specific viruses (14, 180). However, IRF5, like IRF3, is not activated in response to etoposide treatment (Figures 32 and 33).

NFκB is the master regulator of etoposide-induced IFNs.

The role of NFκB in IFNλ$_1$ expression.

Despite the lack of IFNβ induction, this study does proceed to show that NFκB plays a vital role in IFNλ$_1$ induction in response to DNA damage. It has been reported that IRF3 and NFκB regulate IFNλ$_1$ transcription, but NFκB alone is sufficient for its induction (67, 153, 154), thus explaining why IFNλ$_1$ but not IFNβ is induced in etoposide-treated cells (Figures 20 and 22). NFκB is essential for IFNλ$_1$ induction in response to etoposide treatment. Inhibition of NFκB by a dominant-negative IκB decreased IFNλ$_1$ promoter activity (Figure 47) and the inhibition of NFκB by ML120 diminished etoposide-induced IFNλ$_1$ (Figure 49).

Surprisingly, this study found that IFNλ$_1$ expression is also regulated by IRF1. Although it is the founding member of the IRF family and described as a mediator of IFN transcription, IRF1 has been shown to be a weak transcriptional activator (89) and its significance in type I IFN induction in response to virus has been dismissed (167, 171). Yet, in addition to being induced in etoposide-treated cells (Figure 34) (155), IRF1 binds the IRF binding site within the IFNλ$_1$ gene promoter (Figure 43). Furthermore, its overexpression increases the IFNλ$_1$ promoter activation in etoposide-treated cells (Figure 42). It was unexpected to find IRF1 involvement in the regulation of IFNλ$_1$ gene induction in response to etoposide treatment, but it is not unusual that NFκB and IRF1 would work together to stimulate gene expression. For example, NFκB and IRF1 both play a role in MHC class I and inducible nitric oxide syntase (iNOS) gene expression (89, 214, 215).

Another layer of NFκB regulation of the IFNλ$_1$ gene in etoposide-treated cells was determined by this study. While IRF1 is itself an IFN-inducible gene (45), other stimuli, such as TNFα, prolactin and various interleukins, also induce its expression (89). Since IRF1 induction in etoposide-treated cells precedes that of IFN (Figures 50 and 51), it was hypothesized that IRF1 is induced by some other mechanism. IRF1 mRNA levels decrease with the use of NFκB inhibitors ML120 and BAY (Figure 54), indicating that IRF1 induction in etoposide-treated cells is NFκB-dependent. However, once IFN is generated, late IRF1 expression may be amplified by IFN signaling, as there is a

significant increase of IRF1 expression at about 10-12 hours of etoposide treatment, when IFN levels begin to increase (Figure 50).

The role of NFκB in IFNα expression.

In virally infected cells, IFNα species are primarily regulated by IRF7, an IRF family member that is itself induced by IFN signaling and is responsible for the IFN induction of the secondary wave IFNs (118). Likewise, IRF7 is induced and activated in etoposide-treated cells (Figures34-38). Furthermore, its overexpression activates the $IFN\alpha_{14}$ promoter and enhances IFNα mRNA levels in cells treated with etoposide (Figures 39 and 40).

Despite not having NFκB binding sites within their promoters, IFNα expression in etoposide-treated cells appears to be NFκB dependent (Figure 52). This suggests that the transcription factor responsible for IFNα induction is NFκB dependent. Indeed, like IRF1, IRF7 expression in etoposide-treated cells is diminished with the use of NFκB inhibitors (Figure 53). Furthermore, overexpressing IRF7 rescues IFNα induction in etoposide-treated cells when NFκB is inhibited (Figure 54). As with IRF1 expression, late IRF7 expression may be amplified by IFN signaling, as there is a significant increase of IRF7 at about 10-12 hours of etoposide treatment, when IFN levels begin to increase (Figures 50 and 51).

Further investigation of distinctive IRF7 activation in etoposide-treated cells.

Our understanding of IRF7 activation in etoposide-treated cells needs further investigation. In virally infected cells, IRF7 is induced by IFN signaling (112, 118, 176) and IRF7 is activated by the serine/threonine kinases IKKε or TBK1 (42, 53, 185). It is unlikely that IRF7 activation is TBK1 or IKKε dependent since IRF7 phosphorylation was not demonstrated in etoposide-treated cells (Figure 37). IRF3, another substrate for TBK1 and IKKε, is not activated by etoposide treatment, also suggesting that TBK1 and IKKε do not play a role in IRF7 activation by etoposide.

Despite these observations, the possibility of IRF7 phosphorylation by TBK1 or IKKε has not been fully excluded and needs further review. If these kinases were to activate IRF7 but not IRF3, determining how TBK1 or IKKε discriminate between IRF7

and IRF3 in etoposide-treated cells would be of great interest. However, if IRF7 were to be phosphorylated in a TBK1/IKKε independent manner, identifying the kinase responsible and the exact sites of phosphorylation would be another potential area of study.

In addition to serine phosphorylation (22), IRF7 function is also regulated by K63-linked ubiquitination (58). This mode of activation seems to be a plausible explanation for the differential activation of IRF7 but not IRF3, since it was demonstrated that IRF7 is ubiquitinated in a K63 linkage manner in etoposide-treated cells (Figure 38). Identifying ubiquitination sites on IRF7 may be needed to evaluate how ubiquitination regulates IRF7 activity. Once these sites are identified, they may be mutated to inhibit IRF7 ubiquitination, allowing a better understanding of the role ubiquitination plays in DNA damage-induced IFN signaling.

IFN response to DNA damage is part of the ATM signaling pathway.

ATM is a major transducer of the DNA damage signaling pathway and mutations in the gene can impair a proper DNA damage repair response. Ataxia-telangiectasia patients, who possess mutations in the ATM gene, display cerebellar ataxia, oculocutaneous telangiectasia, immunodeficiency, and susceptibility to cancer (95, 169). The clinical manifestation of immunodeficiency may suggest a diminished IFN response. Therefore, it may be of clinical interest to examine levels of IFN production in ataxia-telangiectasia patients and consider the impact a deficient IFN response to DNA damage plays in this disease. A diminished IFN response to DNA damage that occurs through physiological processes may contribute to the immunodeficiency and tumor formation in ataxia-telangiectasia patients.

However, these studies have primarily focused on the immediate upstream regulation of the IFN genes. Future studies should be focused on the upstream DNA damage signaling pathways to discern how the DNA response and IFN signaling pathways converge. Preliminary data suggests that the IFN induction by etoposide treatment is ATM-dependent (Figure 56). A linkage between the ATM-dependent DNA damage signaling pathway and the NFκB activation pathway in cells undergoing genotoxic stress has been suggested (237). Upon DSB caused by etoposide, the nuclear

protein kinase ATM phosphorylates and associates with IKKγ, the regulatory subunit of the IKK complex. The IKKγ-ATM complex translocates into the cytoplasm and interacts with the catalytic IKK subunits, IKKα and IKKβ, and activates NFκB signaling.

Based on these observations, it could be speculated that the activation of NFκB by the ATM-IKKγ pathway results in NFκB-dependent IFN production in etoposide-treated cells. This proposed interferon arm of the ATM signaling pathway may be confirmed by utilizing IKKγ -/- mouse cells and ATM-/- mouse cells. If the ATM-IKKγ pathway is primarily responsible for the initial signaling pathways that lead to IFN gene expression by etoposide-induced DNA damage, diminished IFN gene expression levels in IKKγ -/- mouse and ATM -/- mouse cells would be expected. If IFN levels only mildly diminish in these knockout cells, it may be possible that yet another transducer is part of the IFN response to DNA damage.

Investigating whether IFN signaling is part of other DNA signaling pathways.

Etoposide induces DSB, which activates an ATM dependent IFN signaling pathway. However, etoposide also induces SSB (128). Furthermore, other DNA damaging agents with different modes of DNA damage also induced IFN (Figures 23 and 24) Camptothecin induces single stranded breaks through a ternary complex with DNA and topoisomerase I; adriamycin is a DNA intercalating agent that binds to topoisomerase II and causes DNA strand breaks; and mitomycin C alkylates DNA (7). Based on this observation, it is possible that other arms of the DNA signaling pathway also activate IFN signaling. By inhibiting DNA damage signaling proteins such as ATR and DNAPK, it may be possible to test this hypothesis.

The role of p53 in the IFN signaling pathway of etoposide-treated cells.

The tumor suppressor p53 induces genes that promote cell cycle arrest and/or apoptosis as a DNA damage response via the ATM, ATR and DNA-PK signaling pathways (2). Etoposide treatment induces and activates p53 (75) and its possible role in IFN induction in etoposide-treated cells was briefly studied.

Initially it was believed that p53 played no role in activating the etoposide-induced IFN response. The transformed cell line HeLa possesses an HPV E6 oncogene

that targets p53 protein for degradation (139) and it was still able to induce IFN in etoposide-treated cells. However, studies have shown that p53 protein levels increase with treatment of the DNA damaging agent cisplastin (56). Upon further study, it was confirmed that p53 protein levels stabilized in HeLa cells when treated with etoposide (Figure 59) by an unknown mechanism, despite the presence of HPV E6. This observation prompted us to investigate whether p53 played some role in IFN induction in etoposide-treated cells.

ISG54, an indicator of active IFN signaling, was not induced in cells lacking p53 (Figure 57). However, when etoposide-induced IFN levels were studied in the p53 null cells and compared to its wild type parental line, IFN levels were only mildly diminished (Figure 58). This paradoxical observation is potentially explained by p53's transcriptional role in IRF9 induction (140). IRF9 is part of the ISGF3 complex responsible for the induction of the ISGs that confer the antiviral response (196, 199). p53 has been reported to enhance IRF9 expression, potentiating IFN signaling to the ISGs (140). Since ISG54 levels are diminished with the p53 knockout, p53 may play a similar role in potentiating the IFN response in etoposide-treated cells.

Studies suggest that p53 plays a role in NFκB activation (17, 172). p53 induces RSK1 activation, which in turn promotes the phosphorylation of Serine 536 of RelA and activates NFκB transcriptional activation. However, this study found that p53 null cells show no deficiency in RelA phosphorylation on Serine 536, and it is unlikely that the RSK1 kinase plays a role in the phosphorylation of RelA in response to etoposide treatments (Figure 60).

Identifying a cytoplasmic DNA sensor that triggers IFN induction as a response to DNA damage.

The innate immune system uses sensors, such as TLR and RLR, to recognize and react to pathogenic nucleic acids, including DNA. For example, endosomal membrane bound TLR9 induces IFN in response to unmethylated CpG dsDNA. However, dsDNA introduced directly into the cytoplasm can induce activation of interferon genes independently of TLR and RLR signaling (200). It is conceivable that DNA may "spill over" into the cytoplasm after DNA damage and induce IFN, especially if the cell

undergoes apoptosis and the nuclear membrane has begun to disintegrate. Identifying a cytoplasmic DNA sensor could be a novel form of DNA damage signaling activation.

DAI was described as a potential cytoplasmic DNA sensor that binds DNA and activates IFN gene expression (208, 209). Discrimination between "self" and "non-self" DNA by DAI is based on cellular localization rather than the chemical features of the DNA source (242), making it a viable candidate for being a cytoplasmic DNA damage sensor. DAI induction of IFNβ is dependent on IRF3 and TBK1 or IKKε. Although etoposide-induced IFN is more dependent on IRF7 and IRF1, it may still be worthwhile to study the effect DAI knockdown has on the DNA damage IFN response. NFκB is activated in the DAI signaling pathway, but the role of NFκB in DAI-dependent IFNβ induction is questionable (200). NFκB is activated in etoposide-treated cells and plays a crucial role in IFNα and IFNλ induction. Perhaps, DAI activation of NFκB may differentially activate IFNα and IFNλ signaling in response to etoposide.

The knockdown of DAI does not fully diminish the IFN response to DNA and DAI knockout cells are not deficient in IFN signaling in response to cytoplasmic DNA (209). These observations suggest the possibility of alternative DNA sensing pathways and the existence of another unique dsDNA sensor in the cytoplasm. Other pathways for inducing IFN in response to cytoplasmic DNA have been described. Polymerase III and STING have both been described as playing a role in the dsDNA IFN response. However, as in the DAI signaling pathway, these IFN signaling pathways are also TBK and IRF3 dependent (243).

Working Model of the IFN response to DNA damage.

This study proposes that the induction of IFN is yet another arm of the ATM DNA damage signaling pathway (Figure 61). DSB, such as those created by etoposide, triggers the ATM-dependent DNA damage signaling response. ATM phosphorylates and associates with IKKγ, which proceeds to activate the catalytic IKK subunits, IKKα and IKKβ. The activated IKK complex phosphorylates IκB, the inhibitor of NFκB, and is then ubiquitinated and degraded, releasing NFκB to bind its target gene promoters.

Once activated, NFκB induces IRF1 and, together with IRF1, it activates IFNλ_1 gene transcription. Concurrently, NFkB induces IRF7 and IRF7, in turn, may induce various IFNα subspecies. As in the virally induced IFN pathway, the IFN species can continue to then prime and potentiate the IFN response.

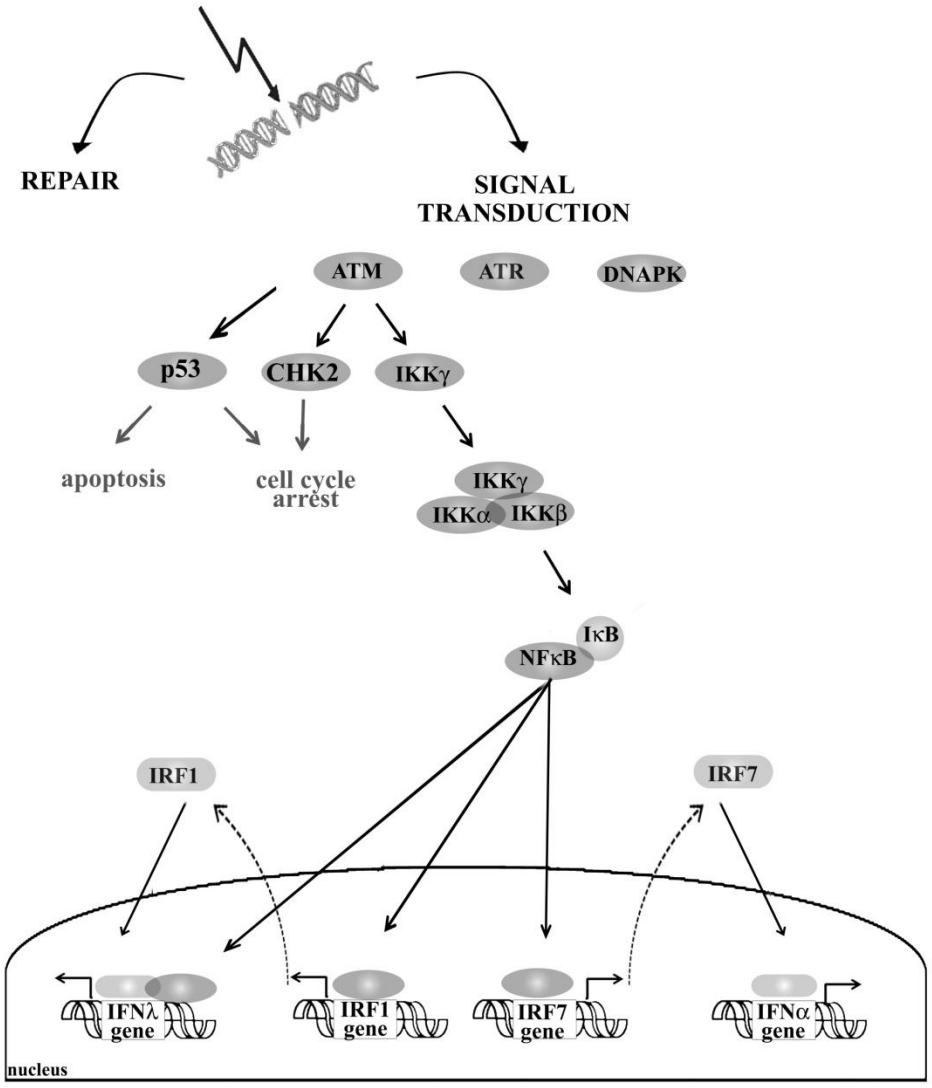

Figure 61: IFN signaling is part of the DNA damage response.

DNA damage induces DNA repair and DNA signal transduction pathways, mediated by ATM, ATR and DNAPK. DSB activate the ATM signaling pathway that results in cell cycle arrest and/or apoptosis. In addition to these pathways, the DSB created by etoposide activates IFN signaling through NFκB activation.

ATM phosphorylates and associates with IKKγ, which proceeds to activate the IKK complex. Once the IKK complex phosphorylates IκB, targeting it for degradation, NFκB is released and induces the IRF1 gene. Together with IRF1, NFκB activates IFNλ_1 gene transcription. Concurrently, NFκB induces IRF7, which induces the IFNα genes.

REFERENCES

1. **Ablasser, A., F. Bauernfeind, G. Hartmann, E. Latz, K. A. Fitzgerald, and V. Hornung.** 2009. RIG-I-dependent sensing of poly(dA:dT) through the induction of an RNA polymerase III-transcribed RNA intermediate. Nat Immunol **10:**1065-72.
2. **Abraham, R. T.** 2001. Cell cycle checkpoint signaling through the ATM and ATR kinases. Genes Dev **15:**2177-96.
3. **Alderton, G. K., H. Joenje, R. Varon, A. D. Borglum, P. A. Jeggo, and M. O'Driscoll.** 2004. Seckel syndrome exhibits cellular features demonstrating defects in the ATR-signalling pathway. Hum Mol Genet **13:**3127-38.
4. **Ank, N., M. B. Iversen, C. Bartholdy, P. Staeheli, R. Hartmann, U. B. Jensen, F. Dagnaes-Hansen, A. R. Thomsen, Z. Chen, H. Haugen, K. Klucher, and S. R. Paludan.** 2008. An important role for type III interferon (IFN-lambda/IL-28) in TLR-induced antiviral activity. J Immunol **180:**2474-85.
5. **Ank, N., H. West, C. Bartholdy, K. Eriksson, A. R. Thomsen, and S. R. Paludan.** 2006. Lambda interferon (IFN-lambda), a type III IFN, is induced by viruses and IFNs and displays potent antiviral activity against select virus infections in vivo. J Virol **80:**4501-9.
6. **Ank, N., H. West, and S. R. Paludan.** 2006. IFN-lambda: novel antiviral cytokines. J Interferon Cytokine Res **26:**373-9.
7. **Aoki, R., Kavanagh, J.J.** 2004. Antineoplastic Agents: Classification and Mechanisms of Action, p. 1-12. *In* P. B. P. Roberto Angioli, John J. Kavanagh, Sergio Pecorelli, Manuel Penalver (ed.), Chemotherapy for Gynecological Neoplasms: Current Therapy and Novel Approaches, 1 ed. Marcel Dekker, New York, NY.
8. **Au, W. C., P. A. Moore, D. W. LaFleur, B. Tombal, and P. M. Pitha.** 1998. Characterization of the interferon regulatory factor-7 and its potential role in the transcription activation of interferon A genes. J Biol Chem **273:**29210-7.
9. **Au, W. C., W. S. Yeow, and P. M. Pitha.** 2001. Analysis of functional domains of interferon regulatory factor 7 and its association with IRF-3. Virology **280:**273-82.
10. **Bakkenist, C. J., and M. B. Kastan.** 2003. DNA damage activates ATM through intermolecular autophosphorylation and dimer dissociation. Nature **421:**499-506.
11. **Baldwin, E. L., and N. Osheroff.** 2005. Etoposide, topoisomerase II and cancer. Curr Med Chem Anticancer Agents **5:**363-72.
12. **Banninger, G., and N. C. Reich.** 2004. STAT2 nuclear trafficking. J Biol Chem **279:**39199-206.
13. **Barnes, B., B. Lubyova, and P. M. Pitha.** 2002. On the role of IRF in host defense. J Interferon Cytokine Res **22:**59-71.
14. **Barnes, B. J., P. A. Moore, and P. M. Pitha.** 2001. Virus-specific activation of a novel interferon regulatory factor, IRF-5, results in the induction of distinct interferon alpha genes. J Biol Chem **276:**23382-90.

15. **Bartkova, J., Z. Horejsi, K. Koed, A. Kramer, F. Tort, K. Zieger, P. Guldberg, M. Sehested, J. M. Nesland, C. Lukas, T. Orntoft, J. Lukas, and J. Bartek.** 2005. DNA damage response as a candidate anti-cancer barrier in early human tumorigenesis. Nature **434:**864-70.
16. **Bekisz, J., H. Schmeisser, J. Hernandez, N. D. Goldman, and K. C. Zoon.** 2004. Human interferons alpha, beta and omega. Growth Factors **22:**243-51.
17. **Bohuslav, J., L. F. Chen, H. Kwon, Y. Mu, and W. C. Greene.** 2004. p53 induces NF-kappaB activation by an IkappaB kinase-independent mechanism involving phosphorylation of p65 by ribosomal S6 kinase 1. J Biol Chem **279:**26115-25.
18. **Brockman, J. A., D. C. Scherer, T. A. McKinsey, S. M. Hall, X. Qi, W. Y. Lee, and D. W. Ballard.** 1995. Coupling of a signal response domain in I kappa B alpha to multiple pathways for NF-kappa B activation. Mol Cell Biol **15:**2809-18.
19. **Brown, E. J., and D. Baltimore.** 2000. ATR disruption leads to chromosomal fragmentation and early embryonic lethality. Genes Dev **14:**397-402.
20. **Buss, H., A. Dorrie, M. L. Schmitz, E. Hoffmann, K. Resch, and M. Kracht.** 2004. Constitutive and interleukin-1-inducible phosphorylation of p65 NF-{kappa}B at serine 536 is mediated by multiple protein kinases including I{kappa}B kinase (IKK)-{alpha}, IKK{beta}, IKK{epsilon}, TRAF family member-associated (TANK)-binding kinase 1 (TBK1), and an unknown kinase and couples p65 to TATA-binding protein-associated factor II31-mediated interleukin-8 transcription. J Biol Chem **279:**55633-43.
21. **Cai, R. R., B. Carpick, R. F. Chun, K. T. Jeang, and B. R. G. Williams.** 2000. HIV-I TAT inhibits PKR activity by both RNA-dependent and RNA-independent mechanisms. Archives of Biochemistry and Biophysics **373:**361-367.
22. **Caillaud, A., A. G. Hovanessian, D. E. Levy, and I. J. Marie.** 2005. Regulatory serine residues mediate phosphorylation-dependent and phosphorylation-independent activation of interferon regulatory factor 7. J Biol Chem **280:**17671-7.
23. **Caldecott, K. W.** 2008. Single-strand break repair and genetic disease. Nat Rev Genet **9:**619-31.
24. **Carroll, S. S., E. Chen, T. Viscount, J. Geib, M. K. Sardana, J. Gehman, and L. C. Kuo.** 1996. Cleavage of oligoribonucleotides by the 2',5'-oligoadenylate-dependent ribonuclease L. J Biol Chem **271:**4988-92.
25. **Chen, C. G., J. Malliaros, M. Katerelos, A. J. d'Apice, and M. J. Pearse.** 1996. Inhibition of NF-kappaB activation by a dominant-negative mutant of IkappaBalpha. Mol Immunol **33:**57-61.
26. **Chen, J., E. Baig, and E. N. Fish.** 2004. Diversity and relatedness among the type I interferons. J Interferon Cytokine Res **24:**687-98.
27. **Cheng, T.-F.** 2006. Characterization of IRF-5 in the Innate Immune System. Stony Brook University, Stony Brook.
28. **Cheng, T. F., S. Brzostek, O. Ando, S. Van Scoy, K. P. Kumar, and N. C. Reich.** 2006. Differential activation of IFN regulatory factor (IRF)-3 and IRF-5 transcription factors during viral infection. J Immunol **176:**7462-70.

29. **Chiu, Y. H., J. B. Macmillan, and Z. J. Chen.** 2009. RNA polymerase III detects cytosolic DNA and induces type I interferons through the RIG-I pathway. Cell **138:**576-91.
30. **Civas, A., M. L. Island, P. Genin, P. Morin, and S. Navarro.** 2002. Regulation of virus-induced interferon-A genes. Biochimie **84:**643-54.
31. **Cliby, W. A., C. J. Roberts, K. A. Cimprich, C. M. Stringer, J. R. Lamb, S. L. Schreiber, and S. H. Friend.** 1998. Overexpression of a kinase-inactive ATR protein causes sensitivity to DNA-damaging agents and defects in cell cycle checkpoints. EMBO J **17:**159-69.
32. **Czornak, K., S. Chughtai, and K. H. Chrzanowska.** 2008. Mystery of DNA repair: the role of the MRN complex and ATM kinase in DNA damage repair. J Appl Genet **49:**383-96.
33. **Daly, C., and N. C. Reich.** 1995. Characterization of specific DNA-binding factors activated by double-stranded RNA as positive regulators of interferon alpha/beta-stimulated genes. J Biol Chem **270:**23739-46.
34. **Darnell, J. E., Jr.** 1998. Studies of IFN-induced transcriptional activation uncover the Jak-Stat pathway. J Interferon Cytokine Res **18:**549-54.
35. **Doly, J., A. Civas, S. Navarro, and G. Uze.** 1998. Type I interferons: expression and signalization. Cell Mol Life Sci **54:**1109-21.
36. **Doyle, S. E., H. Schreckhise, K. Khuu-Duong, K. Henderson, R. Rosler, H. Storey, L. Yao, H. Liu, F. Barahmand-pour, P. Sivakumar, C. Chan, C. Birks, D. Foster, C. H. Clegg, P. Wietzke-Braun, S. Mihm, and K. M. Klucher.** 2006. Interleukin-29 uses a type 1 interferon-like program to promote antiviral responses in human hepatocytes. Hepatology **44:**896-906.
37. **Dumoutier, L., A. Tounsi, T. Michiels, C. Sommereyns, S. V. Kotenko, and J. C. Renauld.** 2004. Role of the interleukin (IL)-28 receptor tyrosine residues for antiviral and antiproliferative activity of IL-29/interferon-lambda 1: similarities with type I interferon signaling. J Biol Chem **279:**32269-74.
38. **Durocher, D., and S. P. Jackson.** 2001. DNA-PK, ATM and ATR as sensors of DNA damage: variations on a theme? Curr Opin Cell Biol **13:**225-31.
39. **Ealick, S. E., W. J. Cook, S. Vijaykumar, M. Carson, T. L. Nagabhushan, P. P. Trotta, and C. E. Bugg.** 1991. 3-Dimensional Structure of Recombinant Human Interferon-Gamma. Science **252:**698-702.
40. **Eker, A. P., C. Quayle, I. Chaves, and G. T. van der Horst.** 2009. DNA repair in mammalian cells: Direct DNA damage reversal: elegant solutions for nasty problems. Cell Mol Life Sci **66:**968-80.
41. **Evans, J. D., and P. Hearing.** 2005. Relocalization of the Mre11-Rad50-Nbs1 complex by the adenovirus E4 ORF3 protein is required for viral replication. Journal of Virology **79:**6207-6215.
42. **Fitzgerald, K. A., S. M. McWhirter, K. L. Faia, D. C. Rowe, E. Latz, D. T. Golenbock, A. J. Coyle, S. M. Liao, and T. Maniatis.** 2003. IKKepsilon and TBK1 are essential components of the IRF3 signaling pathway. Nat Immunol **4:**491-6.
43. **Ford, E., and D. Thanos.** The transcriptional code of human IFN-beta gene expression. Biochim Biophys Acta **1799:**328-336.

44. **Fujita, F., Y. Taniguchi, T. Kato, Y. Narita, A. Furuya, T. Ogawa, H. Sakurai, T. Joh, M. Itoh, M. Delhase, M. Karin, and M. Nakanishi.** 2003. Identification of NAP1, a regulatory subunit of IkappaB kinase-related kinases that potentiates NF-kappaB signaling. Mol Cell Biol **23:**7780-93.
45. **Fujita, T., L. F. Reis, N. Watanabe, Y. Kimura, T. Taniguchi, and J. Vilcek.** 1989. Induction of the transcription factor IRF-1 and interferon-beta mRNAs by cytokines and activators of second-messenger pathways. Proc Natl Acad Sci U S A **86:**9936-40.
46. **Gale, M. J., M. J. Korth, N. M. Tang, S. L. Tan, D. A. Hopkins, T. E. Dever, S. J. Polyak, D. R. Gretch, and M. G. Katze.** 1997. Evidence that hepatitis C virus resistance to interferon is mediated through repression of the PKR protein kinase by the nonstructural 5A protein. Virology **230:**217-227.
47. **Goldstein, D., and J. Laszlo.** 1988. The role of interferon in cancer therapy: a current perspective. CA Cancer J Clin **38:**258-77.
48. **Gorgoulis, V. G., L. V. Vassiliou, P. Karakaidos, P. Zacharatos, A. Kotsinas, T. Liloglou, M. Venere, R. A. Ditullio, Jr., N. G. Kastrinakis, B. Levy, D. Kletsas, A. Yoneta, M. Herlyn, C. Kittas, and T. D. Halazonetis.** 2005. Activation of the DNA damage checkpoint and genomic instability in human precancerous lesions. Nature **434:**907-13.
49. **Grandvaux, N., B. R. tenOever, M. J. Servant, and J. Hiscott.** 2002. The interferon antiviral response: from viral invasion to evasion. Curr Opin Infect Dis **15:**259-67.
50. **Gray, P. W., and D. V. Goeddel.** 1982. Structure of the human immune interferon gene. Nature **298:**859-63.
51. **Gutterman, J. U.** 1994. Cytokine therapeutics: lessons from interferon alpha. Proc Natl Acad Sci U S A **91:**1198-205.
52. **Hande, K. R.** 1998. Etoposide: four decades of development of a topoisomerase II inhibitor. Eur J Cancer **34:**1514-21.
53. **Honda, K., and T. Taniguchi.** 2006. IRFs: master regulators of signalling by Toll-like receptors and cytosolic pattern-recognition receptors. Nat Rev Immunol **6:**644-58.
54. **Honda, K., H. Yanai, H. Negishi, M. Asagiri, M. Sato, T. Mizutani, N. Shimada, Y. Ohba, A. Takaoka, N. Yoshida, and T. Taniguchi.** 2005. IRF-7 is the master regulator of type-I interferon-dependent immune responses. Nature **434:**772-7.
55. **Hu, R., Y. Gan, J. Liu, D. Miller, and K. C. Zoon.** 1993. Evidence for multiple binding sites for several components of human lymphoblastoid interferon-alpha. J Biol Chem **268:**12591-5.
56. **Huang, H., S. Y. Huang, T. T. Chen, J. C. Chen, C. L. Chiou, and T. M. Huang.** 2004. Cisplatin restores p53 function and enhances the radiosensitivity in HPV16 E6 containing SiHa cells. J Cell Biochem **91:**756-65.
57. **Huibregtse, J. M., M. Scheffner, and P. M. Howley.** 1993. Localization of the E6-AP regions that direct human papillomavirus E6 binding, association with p53, and ubiquitination of associated proteins. Mol Cell Biol **13:**4918-27.

58. **Huye, L. E., S. Ning, M. Kelliher, and J. S. Pagano.** 2007. Interferon regulatory factor 7 is activated by a viral oncoprotein through RIP-dependent ubiquitination. Mol Cell Biol **27:**2910-8.
59. **Ihle, J. N.** 2001. The Stat family in cytokine signaling. Curr Opin Cell Biol **13:**211-7.
60. **Imbert, T. F.** 1998. Discovery of podophyllotoxins. Biochimie **80:**207-22.
61. **Iqbal, M., E. Poole, S. Goodbourn, and J. W. McCauley.** 2004. Role for bovine viral diarrhea virus Erns glycoprotein in the control of activation of beta interferon by double-stranded RNA. J Virol **78:**136-45.
62. **Isaacs, A., and J. Lindenmann.** 1957. Virus interference. I. The interferon. Proc R Soc Lond B Biol Sci **147:**258-67.
63. **Isaacs, A., J. Lindenmann, and R. C. Valentine.** 1957. Virus interference. II. Some properties of interferon. Proc R Soc Lond B Biol Sci **147:**268-73.
64. **Ishii, K. J., C. Coban, H. Kato, K. Takahashi, Y. Torii, F. Takeshita, H. Ludwig, G. Sutter, K. Suzuki, H. Hemmi, S. Sato, M. Yamamoto, S. Uematsu, T. Kawai, O. Takeuchi, and S. Akira.** 2006. A Toll-like receptor-independent antiviral response induced by double-stranded B-form DNA. Nat Immunol **7:**40-8.
65. **Ishikawa, H., and G. N. Barber.** 2008. STING is an endoplasmic reticulum adaptor that facilitates innate immune signalling. Nature **455:**674-8.
66. **Ishikawa, H., Z. Ma, and G. N. Barber.** 2009. STING regulates intracellular DNA-mediated, type I interferon-dependent innate immunity. Nature **461:**788-92.
67. **Iversen, M. B., N. Ank, J. Melchjorsen, and S. R. Paludan.** Expression of type III IFN in the vaginal mucosa is mediated primarily by DCs and displays stronger dependence on NF-{kappa}B than type I IFNs. J Virol.
68. **Iwamura, T., M. Yoneyama, K. Yamaguchi, W. Suhara, W. Mori, K. Shiota, Y. Okabe, H. Namiki, and T. Fujita.** 2001. Induction of IRF-3/-7 kinase and NF-kappaB in response to double-stranded RNA and virus infection: common and unique pathways. Genes Cells **6:**375-88.
69. **Jackson, S. P.** 2002. Sensing and repairing DNA double-strand breaks. Carcinogenesis **23:**687-96.
70. **Jefferies, C. A., and K. A. Fitzgerald.** 2005. Interferon gene regulation: not all roads lead to Tolls. Trends Mol Med **11:**403-11.
71. **Jenkins, K. A., and A. Mansell.** TIR-containing adaptors in Toll-like receptor signalling. Cytokine **49:**237-44.
72. **Jiang, X., N. Takahashi, N. Matsui, T. Tetsuka, and T. Okamoto.** 2003. The NF-kappa B activation in lymphotoxin beta receptor signaling depends on the phosphorylation of p65 at serine 536. J Biol Chem **278:**919-26.
73. **John, J., R. McKendry, S. Pellegrini, D. Flavell, I. M. Kerr, and G. R. Stark.** 1991. Isolation and characterization of a new mutant human cell line unresponsive to alpha and beta interferons. Mol Cell Biol **11:**4189-95.
74. **Kanerva, M., K. Melen, A. Vaheri, and I. Julkunen.** 1996. Inhibition of puumala and tula hantaviruses in vero cells by MxA protein. Virology **224:**55-62.
75. **Karpinich, N. O., M. Tafani, R. J. Rothman, M. A. Russo, and J. L. Farber.** 2002. The course of etoposide-induced apoptosis from damage to DNA and p53 activation to mitochondrial release of cytochrome c. J Biol Chem **277:**16547-52.

76. **Karpusas, M., M. Nolte, C. B. Benton, W. Meier, W. N. Lipscomb, and S. Goelz.** 1997. The crystal structure of human interferon beta at 2.2-angstrom resolution. Proceedings of the National Academy of Sciences of the United States of America **94:**11813-11818.
77. **Kato, H., O. Takeuchi, S. Sato, M. Yoneyama, M. Yamamoto, K. Matsui, S. Uematsu, A. Jung, T. Kawai, K. J. Ishii, O. Yamaguchi, K. Otsu, T. Tsujimura, C. S. Koh, C. Reis e Sousa, Y. Matsuura, T. Fujita, and S. Akira.** 2006. Differential roles of MDA5 and RIG-I helicases in the recognition of RNA viruses. Nature **441:**101-5.
78. **Kawai, T., K. Takahashi, S. Sato, C. Coban, H. Kumar, H. Kato, K. J. Ishii, O. Takeuchi, and S. Akira.** 2005. IPS-1, an adaptor triggering RIG-I- and Mda5-mediated type I interferon induction. Nat Immunol **6:**981-8.
79. **Kelly, M., and J. L. Hartwell.** 1954. The biological effects and the chemical composition of podophyllin: a review. J Natl Cancer Inst **14:**967-1010.
80. **Kim, R., M. Emi, and K. Tanabe.** 2005. Caspase-dependent and -independent cell death pathways after DNA damage (Review). Oncol Rep **14:**595-9.
81. **Kim, T., T. Y. Kim, Y. H. Song, I. M. Min, J. Yim, and T. K. Kim.** 1999. Activation of interferon regulatory factor 3 in response to DNA-damaging agents. J Biol Chem **274:**30686-9.
82. **Klaus, W., B. Gsell, A. M. Labhardt, B. Wipf, and H. Senn.** 1997. The three-dimensional high resolution structure of human interferon alpha-2a determined by heteronuclear NMR spectroscopy in solution. Journal of Molecular Biology **274:**661-675.
83. **Kochs, G., and O. Haller.** 1998. Antiviral mechanism of interferon action: Human MxA protein interferes with transport of thogoto viral genomes into the cell nucleus. European Cytokine Network **9:**318-318.
84. **Kochs, G., C. Janzen, H. Hohenberg, and O. Haller.** 2002. Antivirally active MxA protein sequesters La Crosse virus nucleocapsid protein into perinuclear complexes. Proc Natl Acad Sci U S A **99:**3153-8.
85. **Komuro, A., and C. M. Horvath.** 2006. RNA- and virus-independent inhibition of antiviral signaling by RNA helicase LGP2. J Virol **80:**12332-42.
86. **Korn, A. P., D. R. Rose, and E. N. Fish.** 1994. Three-dimensional model of a human interferon-alpha consensus sequence. J Interferon Res **14:**1-9.
87. **Kotenko, S. V., G. Gallagher, V. V. Baurin, A. Lewis-Antes, M. Shen, N. K. Shah, J. A. Langer, F. Sheikh, H. Dickensheets, and R. P. Donnelly.** 2003. IFN-lambdas mediate antiviral protection through a distinct class II cytokine receptor complex. Nat Immunol **4:**69-77.
88. **Kovacs, J. A., L. Deyton, R. Davey, J. Falloon, K. Zunich, D. Lee, J. A. Metcalf, J. W. Bigley, L. A. Sawyer, K. C. Zoon, and et al.** 1989. Combined zidovudine and interferon-alpha therapy in patients with Kaposi sarcoma and the acquired immunodeficiency syndrome (AIDS). Ann Intern Med **111:**280-7.
89. **Kroger, A., M. Koster, K. Schroeder, H. Hauser, and P. P. Mueller.** 2002. Activities of IRF-1. J Interferon Cytokine Res **22:**5-14.
90. **Kumar, H., T. Kawai, H. Kato, S. Sato, K. Takahashi, C. Coban, M. Yamamoto, S. Uematsu, K. J. Ishii, O. Takeuchi, and S. Akira.** 2006.

Essential role of IPS-1 in innate immune responses against RNA viruses. J Exp Med **203:**1795-803.

91. **Kumar, K. P., K. M. McBride, B. K. Weaver, C. Dingwall, and N. C. Reich.** 2000. Regulated nuclear-cytoplasmic localization of interferon regulatory factor 3, a subunit of double-stranded RNA-activated factor 1. Mol Cell Biol **20:**4159-68.
92. **Kunz, C., Y. Saito, and P. Schar.** 2009. DNA Repair in mammalian cells: Mismatched repair: variations on a theme. Cell Mol Life Sci **66:**1021-38.
93. **Lavin, M. F., and Y. Shiloh.** 1997. The genetic defect in ataxia-telangiectasia. Annu Rev Immunol **15:**177-202.
94. **Le Bon, A., and D. F. Tough.** 2002. Links between innate and adaptive immunity via type I interferon. Curr Opin Immunol **14:**432-6.
95. **Lemaitre, B., E. Nicolas, L. Michaut, J. M. Reichhart, and J. A. Hoffmann.** 1996. The dorsoventral regulatory gene cassette spatzle/Toll/cactus controls the potent antifungal response in Drosophila adults. Cell **86:**973-83.
96. **Lewin, B.** 2000. Genes VII. Oxford University Press, Oxford ; New York.
97. **Li, K., E. Foy, J. C. Ferreon, M. Nakamura, A. C. Ferreon, M. Ikeda, S. C. Ray, M. Gale, Jr., and S. M. Lemon.** 2005. Immune evasion by hepatitis C virus NS3/4A protease-mediated cleavage of the Toll-like receptor 3 adaptor protein TRIF. Proc Natl Acad Sci U S A **102:**2992-7.
98. **Li, W., A. Lewis-Antes, J. Huang, M. Balan, and S. V. Kotenko.** 2008. Regulation of apoptosis by type III interferons. Cell Prolif **41:**960-79.
99. **Li, X., C. T. Ranjith-Kumar, M. T. Brooks, S. Dharmaiah, A. B. Herr, C. Kao, and P. Li.** 2009. The RIG-I-like receptor LGP2 recognizes the termini of double-stranded RNA. J Biol Chem **284:**13881-91.
100. **Lilley, C. E., C. T. Carson, A. R. Muotri, F. H. Gage, and M. D. Weitzman.** 2005. DNA repair proteins affect the lifecycle of herpes simplex virus 1. Proceedings of the National Academy of Sciences of the United States of America **102:**5844-5849.
101. **Lilley, C. E., M. S. Chaurushiya, and M. D. Weitzman.** Chromatin at the intersection of viral infection and DNA damage. Biochim Biophys Acta **1799:**319-27.
102. **Lilley, C. E., R. A. Schwartz, and M. D. Weitzman.** 2007. Using or abusing: viruses and the cellular DNA damage response. Trends Microbiol **15:**119-26.
103. **Lim, J. K., J. Xiong, N. Carrasco, and J. A. Langer.** 1994. Intrinsic ligand binding properties of the human and bovine alpha-interferon receptors. FEBS Lett **350:**281-6.
104. **Lin, R., Y. Mamane, and J. Hiscott.** 2000. Multiple regulatory domains control IRF-7 activity in response to virus infection. J Biol Chem **275:**34320-7.
105. **Liu, M., B. T. Hummer, X. Li, and B. A. Hassel.** 2004. Camptothecin induces the ubiquitin-like protein, ISG15, and enhances ISG15 conjugation in response to interferon. J Interferon Cytokine Res **24:**647-54.
106. **Liu, Y., Xing, H, Han, X, Shi, X, Liang, F, Chen, G, and Ma, D** 2005. The mechanism of cisplatin-induced apoptosis in HeLa cells Chinese Journal of Clinical Oncology **2:**866-869.

107. **Liu, Y. Q., H. Xing, X. B. Han, X. Y. Shi, F. Q. Liang, G. Cheng, Y. P. Lu, and D. Ma.** 2008. Apoptosis of HeLa cells induced by cisplatin and its mechanism. Journal of Huazhong University of Science and Technology-Medical Sciences **28:**197-199.
108. **Ljungman, M., and D. P. Lane.** 2004. Transcription - guarding the genome by sensing DNA damage. Nat Rev Cancer **4:**727-37.
109. **Lopez, S., R. Reeves, M. L. Island, M. T. Bandu, N. Christeff, J. Doly, and S. Navarro.** 1997. Silencer activity in the interferon-A gene promoters. J Biol Chem **272:**22788-99.
110. **Loseke, S., E. Grage-Griebenow, A. Wagner, K. Gehlhar, and A. Bufe.** 2003. Differential expression of IFN-alpha subtypes in human PBMC: evaluation of novel real-time PCR assays. J Immunol Methods **276:**207-22.
111. **Lovejoy, C. A., and D. Cortez.** 2009. Common mechanisms of PIKK regulation. DNA Repair (Amst) **8:**1004-8.
112. **Lu, R., W. C. Au, W. S. Yeow, N. Hageman, and P. M. Pitha.** 2000. Regulation of the promoter activity of interferon regulatory factor-7 gene. Activation by interferon snd silencing by hypermethylation. J Biol Chem **275:**31805-12.
113. **Lu, R., P. A. Moore, and P. M. Pitha.** 2002. Stimulation of IRF-7 gene expression by tumor necrosis factor alpha: requirement for NFkappa B transcription factor and gene accessibility. J Biol Chem **277:**16592-8.
114. **Madrid, L. V., M. W. Mayo, J. Y. Reuther, and A. S. Baldwin, Jr.** 2001. Akt stimulates the transactivation potential of the RelA/p65 Subunit of NF-kappa B through utilization of the Ikappa B kinase and activation of the mitogen-activated protein kinase p38. J Biol Chem **276:**18934-40.
115. **Mahaney, B. L., K. Meek, and S. P. Lees-Miller.** 2009. Repair of ionizing radiation-induced DNA double-strand breaks by non-homologous end-joining. Biochem J **417:**639-50.
116. **Malmgaard, L.** 2004. Induction and regulation of IFNs during viral infections. J Interferon Cytokine Res **24:**439-54.
117. **Maniatis, T., J. V. Falvo, T. H. Kim, T. K. Kim, C. H. Lin, B. S. Parekh, and M. G. Wathelet.** 1998. Structure and function of the interferon-beta enhanceosome. Cold Spring Harb Symp Quant Biol **63:**609-20.
118. **Marie, I., J. E. Durbin, and D. E. Levy.** 1998. Differential viral induction of distinct interferon-alpha genes by positive feedback through interferon regulatory factor-7. EMBO J **17:**6660-9.
119. **Marie, I., E. Smith, A. Prakash, and D. E. Levy.** 2000. Phosphorylation-induced dimerization of interferon regulatory factor 7 unmasks DNA binding and a bipartite transactivation domain. Mol Cell Biol **20:**8803-14.
120. **Matikainen, S., A. Paananen, M. Miettinen, M. Kurimoto, T. Timonen, I. Julkunen, and T. Sareneva.** 2001. IFN-alpha and IL-18 synergistically enhance IFN-gamma production in human NK cells: differential regulation of Stat4 activation and IFN-gamma gene expression by IFN-alpha and IL-12. Eur J Immunol **31:**2236-45.

121. **McBride, K. M., G. Banninger, C. McDonald, and N. C. Reich.** 2002. Regulated nuclear import of the STAT1 transcription factor by direct binding of importin-alpha. EMBO J **21:**1754-63.
122. **McBride, K. M., C. McDonald, and N. C. Reich.** 2000. Nuclear export signal located within theDNA-binding domain of the STAT1transcription factor. EMBO J **19:**6196-206.
123. **Medhurst, A. D., D. C. Harrison, S. J. Read, C. A. Campbell, M. J. Robbins, and M. N. Pangalos.** 2000. The use of TaqMan RT-PCR assays for semiquantitative analysis of gene expression in CNS tissues and disease models. J Neurosci Methods **98:**9-20.
124. **Medzhitov, R., P. Preston-Hurlburt, and C. A. Janeway, Jr.** 1997. A human homologue of the Drosophila Toll protein signals activation of adaptive immunity. Nature **388:**394-7.
125. **Memisoglu, A., and L. Samson.** 2000. Base excision repair in yeast and mammals. Mutat Res **451:**39-51.
126. **Mercurio, F., and A. M. Manning.** 1999. NF-kappaB as a primary regulator of the stress response. Oncogene **18:**6163-71.
127. **Meresse, P., E. Dechaux, C. Monneret, and E. Bertounesque.** 2004. Etoposide: Discovery and medicinal chemistry. Current Medicinal Chemistry **11:**2443-2466.
128. **Meresse, P., E. Dechaux, C. Monneret, and E. Bertounesque.** 2004. Etoposide: discovery and medicinal chemistry. Curr Med Chem **11:**2443-66.
129. **Mesplede, T., S. Navarro, P. Genin, P. Morin, M. L. Island, E. Bonnefoy, and A. Civas.** 2003. Positive and negative control of virus-induced interferon-A gene expression. Autoimmunity **36:**447-55.
130. **Meurs, E., K. Chong, J. Galabru, N. S. Thomas, I. M. Kerr, B. R. Williams, and A. G. Hovanessian.** 1990. Molecular cloning and characterization of the human double-stranded RNA-activated protein kinase induced by interferon. Cell **62:**379-90.
131. **Meylan, E., J. Curran, K. Hofmann, D. Moradpour, M. Binder, R. Bartenschlager, and J. Tschopp.** 2005. Cardif is an adaptor protein in the RIG-I antiviral pathway and is targeted by hepatitis C virus. Nature **437:**1167-72.
132. **Miller, D. M., C. M. Cebulla, and D. D. Sedmak.** 2000. Human cytomegalovirus inhibition of interferon signal transduction. Journal of Microbiology **38:**203-208.
133. **Miller, D. M., B. M. Rahill, J. M. Boss, M. D. Lairmore, J. E. Durbin, J. W. Waldman, and D. D. Sedmak.** 1998. Human cytomegalovirus inhibits major histocompatibility complex class II expression by disruption of the Jak/Stat pathway. J Exp Med **187:**675-83.
134. **Miyamoto, M., T. Fujita, Y. Kimura, M. Maruyama, H. Harada, Y. Sudo, T. Miyata, and T. Taniguchi.** 1988. Regulated expression of a gene encoding a nuclear factor, IRF-1, that specifically binds to IFN-beta gene regulatory elements. Cell **54:**903-13.
135. **Moiseeva, O., F. A. Mallette, U. K. Mukhopadhyay, A. Moores, and G. Ferbeyre.** 2006. DNA damage signaling and p53-dependent senescence after prolonged beta-interferon stimulation. Mol Biol Cell **17:**1583-92.

136. **Morin, P., J. Braganca, M. T. Bandu, R. Lin, J. Hiscott, J. Doly, and A. Civas.** 2002. Preferential binding sites for interferon regulatory factors 3 and 7 involved in interferon-A gene transcription. J Mol Biol **316:**1009-22.
137. **Morin, P., P. Genin, J. Doly, and A. Civas.** 2002. The virus-induced factor VIF differentially recognizes the virus-responsive modules of the mouse IFNA4 gene promoter. J Interferon Cytokine Res **22:**77-86.
138. **Mossman, K., C. Upton, R. M. Buller, and G. McFadden.** 1995. Species specificity of ectromelia virus and vaccinia virus interferon-gamma binding proteins. Virology **208:**762-9.
139. **Munger, K., M. Scheffner, J. M. Huibregtse, and P. M. Howley.** 1992. Interactions of HPV E6 and E7 oncoproteins with tumour suppressor gene products. Cancer Surv **12:**197-217.
140. **Munoz-Fontela, C., S. Macip, L. Martinez-Sobrido, L. Brown, J. Ashour, A. Garcia-Sastre, S. W. Lee, and S. A. Aaronson.** 2008. Transcriptional role of p53 in interferon-mediated antiviral immunity. J Exp Med **205:**1929-38.
141. **Myong, S., S. Cui, P. V. Cornish, A. Kirchhofer, M. U. Gack, J. U. Jung, K. P. Hopfner, and T. Ha.** 2009. Cytosolic viral sensor RIG-I is a 5'-triphosphate-dependent translocase on double-stranded RNA. Science **323:**1070-4.
142. **Nagano, Y., Y. Kojima, and Y. Sawai.** 1954. [Immunity and interference in vaccinia; inhibition of skin infection by inactivated virus.]. C R Seances Soc Biol Fil **148:**750-2.
143. **Nguyen, H., J. Hiscott, and P. M. Pitha.** 1997. The growing family of interferon regulatory factors. Cytokine Growth Factor Rev **8:**293-312.
144. **Ning, S., A. D. Campos, B. G. Darnay, G. L. Bentz, and J. S. Pagano.** 2008. TRAF6 and the three C-terminal lysine sites on IRF7 are required for its ubiquitination-mediated activation by the tumor necrosis factor receptor family member latent membrane protein 1. Mol Cell Biol **28:**6536-46.
145. **Ning, S., L. E. Huye, and J. S. Pagano.** 2005. Regulation of the transcriptional activity of the IRF7 promoter by a pathway independent of interferon signaling. J Biol Chem **280:**12262-70.
146. **Nouspikel, T.** 2009. DNA repair in mammalian cells : Nucleotide excision repair: variations on versatility. Cell Mol Life Sci **66:**994-1009.
147. **Nouspikel, T.** 2009. DNA repair in mammalian cells: So DNA repair really is that important? Cell Mol Life Sci **66:**965-7.
148. **Novick, D., B. Cohen, and M. Rubinstein.** 1994. The human interferon alpha/beta receptor: characterization and molecular cloning. Cell **77:**391-400.
149. **Numasaki, M., M. Tagawa, F. Iwata, T. Suzuki, A. Nakamura, M. Okada, Y. Iwakura, S. Aiba, and M. Yamaya.** 2007. IL-28 elicits antitumor responses against murine fibrosarcoma. J Immunol **178:**5086-98.
150. **O'Driscoll, M., and P. A. Jeggo.** 2003. Clinical impact of ATR checkpoint signalling failure in humans. Cell Cycle **2:**194-5.
151. **O'Driscoll, M., V. L. Ruiz-Perez, C. G. Woods, P. A. Jeggo, and J. A. Goodship.** 2003. A splicing mutation affecting expression of ataxia-telangiectasia and Rad3-related protein (ATR) results in Seckel syndrome. Nat Genet **33:**497-501.

152. **Ohmori, Y., R. D. Schreiber, and T. A. Hamilton.** 1997. Synergy between interferon-gamma and tumor necrosis factor-alpha in transcriptional activation is mediated by cooperation between signal transducer and activator of transcription 1 and nuclear factor kappaB. J Biol Chem **272:**14899-907.
153. **Onoguchi, K., M. Yoneyama, A. Takemura, S. Akira, T. Taniguchi, H. Namiki, and T. Fujita.** 2007. Viral infections activate types I and III interferon genes through a common mechanism. J Biol Chem **282:**7576-81.
154. **Osterlund, P. I., T. E. Pietila, V. Veckman, S. V. Kotenko, and I. Julkunen.** 2007. IFN regulatory factor family members differentially regulate the expression of type III IFN (IFN-lambda) genes. J Immunol **179:**3434-42.
155. **Pamment, J., E. Ramsay, M. Kelleher, D. Dornan, and K. L. Ball.** 2002. Regulation of the IRF-1 tumour modifier during the response to genotoxic stress involves an ATM-dependent signalling pathway. Oncogene **21:**7776-85.
156. **Parkinson, J., S. P. Lees-Miller, and R. D. Everett.** 1999. Herpes simplex virus type 1 immediate-early protein Vmw110 induces the proteasome-dependent degradation of the catalytic subunit of DNA-dependent protein kinase. Journal of Virology **73:**650-657.
157. **Paulus, C., S. Krauss, and M. Nevels.** 2006. A human cytomegalovirus antagonist of type IIFN-dependent signal transducer and activator of transcription signaling. Proceedings of the National Academy of Sciences of the United States of America **103:**3840-3845.
158. **Pavlovic, J., H. A. Arzet, H. P. Hefti, M. Frese, D. Rost, B. Ernst, E. Kolb, P. Staeheli, and O. Haller.** 1995. Enhanced Virus-Resistance of Transgenic Mice Expressing the Human Mxa Protein. Journal of Virology **69:**4506-4510.
159. **Pavlovic, J., T. Zurcher, O. Haller, and P. Staeheli.** 1990. Resistance to Influenza-Virus and Vesicular Stomatitis-Virus Conferred by Expression of Human Mxa Protein. Journal of Virology **64:**3370-3375.
160. **Peltomaki, P.** 2001. DNA mismatch repair and cancer. Mutat Res **488:**77-85.
161. **Pine, R.** 1997. Convergence of TNFalpha and IFNgamma signalling pathways through synergistic induction of IRF-1/ISGF-2 is mediated by a composite GAS/kappaB promoter element. Nucleic Acids Res **25:**4346-54.
162. **Pitha, P. M., W. C. Au, W. Lowther, Y. T. Juang, S. L. Schafer, L. Burysek, J. Hiscott, and P. A. Moore.** 1998. Role of the interferon regulatory factors (IRFs) in virus-mediated signaling and regulation of cell growth. Biochimie **80:**651-8.
163. **Powell, P. P., L. K. Dixon, and R. M. Parkhouse.** 1996. An IkappaB homolog encoded by African swine fever virus provides a novel mechanism for downregulation of proinflammatory cytokine responses in host macrophages. J Virol **70:**8527-33.
164. **Radhakrishnan, R., L. J. Walter, A. Hruza, P. Reichert, P. P. Trotta, T. L. Nagabhushan, and M. R. Walter.** 1996. Zinc mediated dimer of human interferon-alpha(2b) revealed by X-ray crystallography. Structure **4:**1453-1463.
165. **Reich, N., B. Evans, D. Levy, D. Fahey, E. Knight, Jr., and J. E. Darnell, Jr.** 1987. Interferon-induced transcription of a gene encoding a 15-kDa protein depends on an upstream enhancer element. Proc Natl Acad Sci U S A **84:**6394-8.

166. **Reich, N. C.** 2002. Nuclear/cytoplasmic localization of IRFs in response to viral infection or interferon stimulation. J Interferon Cytokine Res **22:**103-9.
167. **Reis, L. F., H. Ruffner, G. Stark, M. Aguet, and C. Weissmann.** 1994. Mice devoid of interferon regulatory factor 1 (IRF-1) show normal expression of type I interferon genes. EMBO J **13:**4798-806.
168. **Ronco, L. V., A. Y. Karpova, M. Vidal, and P. M. Howley.** 1998. Human papillomavirus 16 E6 oncoprotein binds to interferon regulatory factor-3 and inhibits its transcriptional activity. Genes Dev **12:**2061-72.
169. **Rothenfusser, S., N. Goutagny, G. DiPerna, M. Gong, B. G. Monks, A. Schoenemeyer, M. Yamamoto, S. Akira, and K. A. Fitzgerald.** 2005. The RNA helicase Lgp2 inhibits TLR-independent sensing of viral replication by retinoic acid-inducible gene-I. J Immunol **175:**5260-8.
170. **Rotman, G., and Y. Shiloh.** 1999. ATM: a mediator of multiple responses to genotoxic stress. Oncogene **18:**6135-44.
171. **Ruffner, H., L. F. Reis, D. Naf, and C. Weissmann.** 1993. Induction of type I interferon genes and interferon-inducible genes in embryonal stem cells devoid of interferon regulatory factor 1. Proc Natl Acad Sci U S A **90:**11503-7.
172. **Ryan, K. M., M. K. Ernst, N. R. Rice, and K. H. Vousden.** 2000. Role of NF-kappaB in p53-mediated programmed cell death. Nature **404:**892-7.
173. **Saito, T., R. Hirai, Y. M. Loo, D. Owen, C. L. Johnson, S. C. Sinha, S. Akira, T. Fujita, and M. Gale, Jr.** 2007. Regulation of innate antiviral defenses through a shared repressor domain in RIG-I and LGP2. Proc Natl Acad Sci U S A **104:**582-7.
174. **Sangfelt, O., S. Erickson, J. Castro, T. Heiden, S. Einhorn, and D. Grander.** 1997. Induction of apoptosis and inhibition of cell growth are independent responses to interferon-alpha in hematopoietic cell lines. Cell Growth Differ **8:**343-52.
175. **Sato, A., M. Ohtsuki, M. Hata, E. Kobayashi, and T. Murakami.** 2006. Antitumor activity of IFN-lambda in murine tumor models. J Immunol **176:**7686-94.
176. **Sato, M., N. Hata, M. Asagiri, T. Nakaya, T. Taniguchi, and N. Tanaka.** 1998. Positive feedback regulation of type I IFN genes by the IFN-inducible transcription factor IRF-7. FEBS Lett **441:**106-10.
177. **Satoh, T., H. Kato, Y. Kumagai, M. Yoneyama, S. Sato, K. Matsushita, T. Tsujimura, T. Fujita, S. Akira, and O. Takeuchi.** LGP2 is a positive regulator of RIG-I- and MDA5-mediated antiviral responses. Proc Natl Acad Sci U S A **107:**1512-7.
178. **Scheffner, M., J. M. Huibregtse, R. D. Vierstra, and P. M. Howley.** 1993. The HPV-16 E6 and E6-AP complex functions as a ubiquitin-protein ligase in the ubiquitination of p53. Cell **75:**495-505.
179. **Schneiderschaulies, S., J. Schneiderschaulies, A. Schuster, M. Bayer, J. Pavlovic, and V. Termeulen.** 1994. Cell-Type-Specific Mxa-Mediated Inhibition of Measles-Virus Transcription in Human Brain-Cells. Journal of Virology **68:**6910-6917.
180. **Schoenemeyer, A., B. J. Barnes, M. E. Mancl, E. Latz, N. Goutagny, P. M. Pitha, K. A. Fitzgerald, and D. T. Golenbock.** 2005. The interferon regulatory

factor, IRF5, is a central mediator of toll-like receptor 7 signaling. J Biol Chem **280:**17005-12.

181. **Schroder, K., P. J. Hertzog, T. Ravasi, and D. A. Hume.** 2004. Interferon-gamma: an overview of signals, mechanisms and functions. J Leukoc Biol **75:**163-89.
182. **Sen, G. C.** 2001. Viruses and interferons. Annu Rev Microbiol **55:**255-81.
183. **Seth, R. B., L. Sun, C. K. Ea, and Z. J. Chen.** 2005. Identification and characterization of MAVS, a mitochondrial antiviral signaling protein that activates NF-kappaB and IRF 3. Cell **122:**669-82.
184. **Severa, M., and K. A. Fitzgerald.** 2007. TLR-mediated activation of type I IFN during antiviral immune responses: fighting the battle to win the war. Curr Top Microbiol Immunol **316:**167-92.
185. **Sharma, S., B. R. tenOever, N. Grandvaux, G. P. Zhou, R. Lin, and J. Hiscott.** 2003. Triggering the interferon antiviral response through an IKK-related pathway. Science **300:**1148-51.
186. **Sheppard, P., W. Kindsvogel, W. Xu, K. Henderson, S. Schlutsmeyer, T. E. Whitmore, R. Kuestner, U. Garrigues, C. Birks, J. Roraback, C. Ostrander, D. Dong, J. Shin, S. Presnell, B. Fox, B. Haldeman, E. Cooper, D. Taft, T. Gilbert, F. J. Grant, M. Tackett, W. Krivan, G. McKnight, C. Clegg, D. Foster, and K. M. Klucher.** 2003. IL-28, IL-29 and their class II cytokine receptor IL-28R. Nat Immunol **4:**63-8.
187. **Shiloh, Y.** 1997. Ataxia-telangiectasia and the Nijmegen breakage syndrome: related disorders but genes apart. Annu Rev Genet **31:**635-62.
188. **Shiloh, Y.** 2001. ATM and ATR: networking cellular responses to DNA damage. Curr Opin Genet Dev **11:**71-7.
189. **Shiloh, Y., and G. Rotman.** 1996. Ataxia-telangiectasia and the ATM gene: linking neurodegeneration, immunodeficiency, and cancer to cell cycle checkpoints. J Clin Immunol **16:**254-60.
190. **Shirata, N., A. Kudoh, T. Daikoku, Y. Tatsumi, M. Fujita, T. Kiyono, Y. Sugaya, H. Isomura, K. Ishizaki, and T. Tsurumi.** 2005. Activation of ataxia telangiectasia-mutated DNA damage checkpoint signal transduction elicited by herpes simplex virus infection. Journal of Biological Chemistry **280:**30336-30341.
191. **Shirota, H., K. J. Ishii, H. Takakuwa, and D. M. Klinman.** 2006. Contribution of interferon-beta to the immune activation induced by double-stranded DNA. Immunology **118:**302-10.
192. **Sims, S. H., Y. Cha, M. F. Romine, P. Q. Gao, K. Gottlieb, and A. B. Deisseroth.** 1993. A novel interferon-inducible domain: structural and functional analysis of the human interferon regulatory factor 1 gene promoter. Mol Cell Biol **13:**690-702.
193. **Sinclair, A., S. Yarranton, and C. Schelcher.** 2006. DNA-damage response pathways triggered by viral replication. Expert Rev Mol Med **8:**1-11.
194. **Skalka, A. M., and R. A. Katz.** 2005. Retroviral DNA integration and the DNA damage response. Cell Death Differ **12 Suppl 1:**971-8.
195. **Smith, G. C., and S. P. Jackson.** 1999. The DNA-dependent protein kinase. Genes Dev **13:**916-34.

196. **Smith, P. L., G. Lombardi, and G. R. Foster.** 2005. Type I interferons and the innate immune response--more than just antiviral cytokines. Mol Immunol **42:**869-77.
197. **Sommereyns, C., S. Paul, P. Staeheli, and T. Michiels.** 2008. IFN-lambda (IFN-lambda) is expressed in a tissue-dependent fashion and primarily acts on epithelial cells in vivo. PLoS Pathog **4:**e1000017.
198. **Stadler, M., M. K. Chelbi-Alix, M. H. Koken, L. Venturini, C. Lee, A. Saib, F. Quignon, L. Pelicano, M. C. Guillemin, C. Schindler, and et al.** 1995. Transcriptional induction of the PML growth suppressor gene by interferons is mediated through an ISRE and a GAS element. Oncogene **11:**2565-73.
199. **Stark, G. R., I. M. Kerr, B. R. Williams, R. H. Silverman, and R. D. Schreiber.** 1998. How cells respond to interferons. Annu Rev Biochem **67:**227-64.
200. **Stetson, D. B., and R. Medzhitov.** 2006. Recognition of cytosolic DNA activates an IRF3-dependent innate immune response. Immunity **24:**93-103.
201. **Stracker, T. H., C. T. Carson, and M. D. Weitzman.** 2002. Adenovirus oncoproteins inactivate the Mre11-Rad50-NBS1 DNA repair complex. Nature **418:**348-352.
202. **Strozyk, E., B. Poppelmann, T. Schwarz, and D. Kulms.** 2006. Differential effects of NF-kappaB on apoptosis induced by DNA-damaging agents: the type of DNA damage determines the final outcome. Oncogene **25:**6239-51.
203. **Su, T. T.** 2006. Cellular responses to DNA damage: one signal, multiple choices. Annu Rev Genet **40:**187-208.
204. **Sun, Q., L. Sun, H. H. Liu, X. Chen, R. B. Seth, J. Forman, and Z. J. Chen.** 2006. The specific and essential role of MAVS in antiviral innate immune responses. Immunity **24:**633-42.
205. **Sun, W., Y. Li, L. Chen, H. Chen, F. You, X. Zhou, Y. Zhou, Z. Zhai, D. Chen, and Z. Jiang.** 2009. ERIS, an endoplasmic reticulum IFN stimulator, activates innate immune signaling through dimerization. Proc Natl Acad Sci U S A **106:**8653-8.
206. **Symons, J. A., A. Alcami, and G. L. Smith.** 1995. Vaccinia virus encodes a soluble type I interferon receptor of novel structure and broad species specificity. Cell **81:**551-60.
207. **Takaoka, A., S. Hayakawa, H. Yanai, D. Stoiber, H. Negishi, H. Kikuchi, S. Sasaki, K. Imai, T. Shibue, K. Honda, and T. Taniguchi.** 2003. Integration of interferon-alpha/beta signalling to p53 responses in tumour suppression and antiviral defence. Nature **424:**516-23.
208. **Takaoka, A., and T. Taniguchi.** 2008. Cytosolic DNA recognition for triggering innate immune responses. Adv Drug Deliv Rev **60:**847-57.
209. **Takaoka, A., Z. Wang, M. K. Choi, H. Yanai, H. Negishi, T. Ban, Y. Lu, M. Miyagishi, T. Kodama, K. Honda, Y. Ohba, and T. Taniguchi.** 2007. DAI (DLM-1/ZBP1) is a cytosolic DNA sensor and an activator of innate immune response. Nature **448:**501-5.
210. **Tan, S. L., and M. G. Katze.** 2000. HSV.com: Maneuvering the internetworks of viral neuropathogenesis and evasion of the host defense. Proceedings of the National Academy of Sciences of the United States of America **97:**5684-5686.

211. **Taniguchi, T., K. Ogasawara, A. Takaoka, and N. Tanaka.** 2001. IRF family of transcription factors as regulators of host defense. Annu Rev Immunol **19:**623-55.
212. **Taniguchi, T., and A. Takaoka.** 2002. The interferon-alpha/beta system in antiviral responses: a multimodal machinery of gene regulation by the IRF family of transcription factors. Curr Opin Immunol **14:**111-6.
213. **Tansey, W. P.** 2006. Detection of Ubiquitylated Proteins in Mammalian Cells, Cold Spring Harb Protocols. doi:10.1101/pdb.prot4616.
214. **Ten, R. M., V. Blank, O. Le Bail, P. Kourilsky, and A. Israel.** 1993. Two factors, IRF1 and KBF1/NF-kappa B, cooperate during induction of MHC class I gene expression by interferon alpha beta or Newcastle disease virus. C R Acad Sci III **316:**496-501.
215. **Tendler, D. S., C. Bao, T. Wang, E. L. Huang, E. A. Ratovitski, D. A. Pardoll, and C. J. Lowenstein.** 2001. Intersection of interferon and hypoxia signal transduction pathways in nitric oxide-induced tumor apoptosis. Cancer Res **61:**3682-8.
216. **Thomson, S. J., F. G. Goh, H. Banks, T. Krausgruber, S. V. Kotenko, B. M. Foxwell, and I. A. Udalova.** 2009. The role of transposable elements in the regulation of IFN-lambda1 gene expression. Proc Natl Acad Sci U S A **106:**11564-9.
217. **Thyrell, L., S. Erickson, B. Zhivotovsky, K. Pokrovskaja, O. Sangfelt, J. Castro, S. Einhorn, and D. Grander.** 2002. Mechanisms of Interferon-alpha induced apoptosis in malignant cells. Oncogene **21:**1251-62.
218. **Townsend, P. A., M. S. Cragg, S. M. Davidson, J. McCormick, S. Barry, K. M. Lawrence, R. A. Knight, M. Hubank, P. L. Chen, D. S. Latchman, and A. Stephanou.** 2005. STAT-1 facilitates the ATM activated checkpoint pathway following DNA damage. J Cell Sci **118:**1629-39.
219. **Tsai, M. H., J. A. Cook, G. V. Chandramouli, W. DeGraff, H. Yan, S. Zhao, C. N. Coleman, J. B. Mitchell, and E. Y. Chuang.** 2007. Gene expression profiling of breast, prostate, and glioma cells following single versus fractionated doses of radiation. Cancer Res **67:**3845-52.
220. **Uno, K., Y. Iwakura, and K. Ozato.** October 2005. Another Road to Interferon: Yasuichi Nagano's Journey, p. 9-13, International Society for Interferon and Cytokine Research, vol. 12, no.3.
221. **Upton, C., K. Mossman, and G. McFadden.** 1992. Encoding of a homolog of the IFN-gamma receptor by myxoma virus. Science **258:**1369-72.
222. **Venkataraman, T., M. Valdes, R. Elsby, S. Kakuta, G. Caceres, S. Saijo, Y. Iwakura, and G. N. Barber.** 2007. Loss of DExD/H box RNA helicase LGP2 manifests disparate antiviral responses. J Immunol **178:**6444-55.
223. **Viatour, P., M. P. Merville, V. Bours, and A. Chariot.** 2005. Phosphorylation of NF-kappaB and IkappaB proteins: implications in cancer and inflammation. Trends Biochem Sci **30:**43-52.
224. **Vilenchik, M. M., and A. G. Knudson.** 2003. Endogenous DNA double-strand breaks: production, fidelity of repair, and induction of cancer. Proc Natl Acad Sci U S A **100:**12871-6.

225. **Wadler, S., and E. L. Schwartz.** 1990. Antineoplastic activity of the combination of interferon and cytotoxic agents against experimental and human malignancies: a review. Cancer Res **50:**3473-86.
226. **Walter, M. R., W. Windsor, T. L. Nagabhushan, D. J. Lundell, C. A. Lunn, P. J. Zauodny, and S. K. Narula.** 1995. Crystal-Structure of a Complex between Interferon-Gamma and Its Soluble High-Affinity Receptor. Nature **376:**230-235.
227. **Wang, D., and A. S. Baldwin, Jr.** 1998. Activation of nuclear factor-kappaB-dependent transcription by tumor necrosis factor-alpha is mediated through phosphorylation of RelA/p65 on serine 529. J Biol Chem **273:**29411-6.
228. **Wang, Z., M. K. Choi, T. Ban, H. Yanai, H. Negishi, Y. Lu, T. Tamura, A. Takaoka, K. Nishikura, and T. Taniguchi.** 2008. Regulation of innate immune responses by DAI (DLM-1/ZBP1) and other DNA-sensing molecules. Proc Natl Acad Sci U S A **105:**5477-82.
229. **Wathelet, M. G., C. H. Lin, B. S. Parekh, L. V. Ronco, P. M. Howley, and T. Maniatis.** 1998. Virus infection induces the assembly of coordinately activated transcription factors on the IFN-beta enhancer in vivo. Mol Cell **1:**507-18.
230. **Weaver, B. K., O. Ando, K. P. Kumar, and N. C. Reich.** 2001. Apoptosis is promoted by the dsRNA-activated factor (DRAF1) during viral infection independent of the action of interferon or p53. FASEB J **15:**501-15.
231. **Weaver, B. K., K. P. Kumar, and N. C. Reich.** 1998. Interferon regulatory factor 3 and CREB-binding protein/p300 are subunits of double-stranded RNA-activated transcription factor DRAF1. Mol Cell Biol **18:**1359-68.
232. **Weichselbaum, R. R., H. Ishwaran, T. Yoon, D. S. Nuyten, S. W. Baker, N. Khodarev, A. W. Su, A. Y. Shaikh, P. Roach, B. Kreike, B. Roizman, J. Bergh, Y. Pawitan, M. J. van de Vijver, and A. J. Minn.** 2008. An interferon-related gene signature for DNA damage resistance is a predictive marker for chemotherapy and radiation for breast cancer. Proc Natl Acad Sci U S A **105:**18490-5.
233. **Weitzman, M. D., C. T. Carson, R. A. Schwartz, and C. E. Lilley.** 2004. Interactions of viruses with the cellular DNA repair machinery. DNA Repair (Amst) **3:**1165-73.
234. **Whelan, J., D. Patterson, M. Perisoglou, S. Bielack, N. Marina, S. Smeland, and M. Bernstein.** The role of interferons in the treatment of osteosarcoma. Pediatr Blood Cancer **54:**350-4.
235. **Wilkinson, D. E., and S. K. Weller.** 2006. Herpes simplex virus type I disrupts the ATR-dependent DNA-damage response during lytic infection. Journal of Cell Science **119:**2695-2703.
236. **Wreschner, D. H., J. W. McCauley, J. J. Skehel, and I. M. Kerr.** 1981. Interferon action--sequence specificity of the ppp(A2'p)nA-dependent ribonuclease. Nature **289:**414-7.
237. **Wu, Z. H., Y. Shi, R. S. Tibbetts, and S. Miyamoto.** 2006. Molecular linkage between the kinase ATM and NF-kappaB signaling in response to genotoxic stimuli. Science **311:**1141-6.
238. **Xu, L. G., Y. Y. Wang, K. J. Han, L. Y. Li, Z. Zhai, and H. B. Shu.** 2005. VISA is an adapter protein required for virus-triggered IFN-beta signaling. Mol Cell **19:**727-40.

239. **Yamaoka, K., P. Saharinen, M. Pesu, V. E. T. Holt, O. Silvennoinen, and J. J. O'Shea.** 2004. The Janus kinases (Jaks). Genome Biology **5:**-.
240. **Yang, J., Y. Yu, H. E. Hamrick, and P. J. Duerksen-Hughes.** 2003. ATM, ATR and DNA-PK: initiators of the cellular genotoxic stress responses. Carcinogenesis **24:**1571-80.
241. **Yasuda, K., P. Yu, C. J. Kirschning, B. Schlatter, F. Schmitz, A. Heit, S. Bauer, H. Hochrein, and H. Wagner.** 2005. Endosomal translocation of vertebrate DNA activates dendritic cells via TLR9-dependent and -independent pathways. J Immunol **174:**6129-36.
242. **Yoneyama, M., and T. Fujita.** 2007. Cytoplasmic double-stranded DNA sensor. Nat Immunol **8:**907-8.
243. **Yoneyama, M., and T. Fujita.** Recognition of viral nucleic acids in innate immunity. Rev Med Virol **20:**4-22.
244. **Yoneyama, M., and T. Fujita.** 2009. RNA recognition and signal transduction by RIG-I-like receptors. Immunol Rev **227:**54-65.
245. **Yoneyama, M., M. Kikuchi, K. Matsumoto, T. Imaizumi, M. Miyagishi, K. Taira, E. Foy, Y. M. Loo, M. Gale, Jr., S. Akira, S. Yonehara, A. Kato, and T. Fujita.** 2005. Shared and unique functions of the DExD/H-box helicases RIG-I, MDA5, and LGP2 in antiviral innate immunity. J Immunol **175:**2851-8.
246. **Yoneyama, M., M. Kikuchi, T. Natsukawa, N. Shinobu, T. Imaizumi, M. Miyagishi, K. Taira, S. Akira, and T. Fujita.** 2004. The RNA helicase RIG-I has an essential function in double-stranded RNA-induced innate antiviral responses. Nat Immunol **5:**730-7.
247. **Zhong, B., Y. Yang, S. Li, Y. Y. Wang, Y. Li, F. Diao, C. Lei, X. He, L. Zhang, P. Tien, and H. B. Shu.** 2008. The adaptor protein MITA links virus-sensing receptors to IRF3 transcription factor activation. Immunity **29:**538-50.
248. **Zhong, H., H. SuYang, H. Erdjument-Bromage, P. Tempst, and S. Ghosh.** 1997. The transcriptional activity of NF-kappaB is regulated by the IkappaB-associated PKAc subunit through a cyclic AMP-independent mechanism. Cell **89:**413-24.
249. **Zhong, H., R. E. Voll, and S. Ghosh.** 1998. Phosphorylation of NF-kappa B p65 by PKA stimulates transcriptional activity by promoting a novel bivalent interaction with the coactivator CBP/p300. Mol Cell **1:**661-71.
250. **Zhou, Z., O. J. Hamming, N. Ank, S. R. Paludan, A. L. Nielsen, and R. Hartmann.** 2007. Type III interferon (IFN) induces a type I IFN-like response in a restricted subset of cells through signaling pathways involving both the Jak-STAT pathway and the mitogen-activated protein kinases. J Virol **81:**7749-58.
251. **Zimonjic, D. B., L. J. Rezanka, C. H. Evans, M. H. Polymeropoulos, J. M. Trent, and N. C. Popescu.** 1995. Mapping of the immune interferon gamma gene (IFNG) to chromosome band 12q14 by fluorescence in situ hybridization. Cytogenet Cell Genet **71:**247-8.

Appendix A

Affymetrix DNA Microarray of Etoposide Treated Cells. Hec1B cells were treated with 40ug/mL etoposide for 52 hours and were analyzed with Affymetrix DNA microarrays to profile cellular genes induced in response to etoposide. Inductions were compared to Hec1B cells that were mock treated with DMSO.

	Gene Description		Fold
1	immunoglobulin lambda variable	AL021937	98.1
2	v-fos FBJ murine osteosarcoma viral oncogene homolog	K00650	49.3
3	dual specificity phosphatase 10	AB026436	48.5
4	nuclear receptor subfamily 4, group A, member 2	X75918	43.9
5	growth arrest and DNA-damage-inducible, beta	AF078077	42.3
6	protein MGC14376	AF070569	38.2
7	histone 2, H2aa	AI885852	37.1
8	mannosyl (alpha-1,6-)-glycoprotein beta-1,2-N-acetylglucosaminyltransferase	U15128	34.9
9	Histone H3.1	AL009179	30.1
10	zinc finger and BTB domain containing 1	AB023214	27.1
11	Human 28S ribosomal RNA gene	M27830	26.6
12	tubulin, alpha 3	X01703	26.6
13	histone 1, H2bd	AJ223353	25.5
14	mevalonate (diphospho) decarboxylase	U49260	23.5
15	nuclear receptor subfamily 4, group A, member 1	L13740	23.4
16	phosphoinositide-3-kinase, regulatory subunit, polypeptide 3 (p55, gamma)	D88532	23.1
17	diphtheria toxin receptor	M60278	22.5
18	distal-less homeo box 2	L07919	22.4
19	early growth response 3	X63741	20.0
20	GATA binding protein 2	M68891	19.5
21	tubulin, beta polypeptide	X79535	19.2
22	ectonucleotide pyrophosphatase/phosphodiesterase 2 (autotaxin)	L35594	17.0

23	jun B proto-oncogene	M29039	16.1
24	v-myb myeloblastosis viral oncogene homolog (avian)	U22376	15.7
25	nuclear receptor subfamily 4, group A, member 1	L13740	15.6
26	myeloid differentiation primary response gene (88)	U70451	15.3
27	human ortholog of rat Neuronal Pentraxin Receptor	AL008583	15.0
28	SKI-like	Z19588	15.0
29	similar to Ovis aries Y chromosome repeat region OY11.1	D87011	14.2
30	retinoblastoma 1 (including osteosarcoma)	L41870	13.9
31	P53 tumor suppressor {alternatively spliced, exon 9-10}	S66666	13.7
32	chemokine (C-X-C motif) receptor 4	L06797	13.6
33	Human 28S ribosomal RNA gene	M27830	13.3
34	gastrin	V00511	13.2
35	Homo sapiens cDNA: FLJ23438 fis, clone HRC13275.	W25892	13.0
36	cyclin E2	AF091433	12.5
37	cyclin-dependent kinase inhibitor 1C (p57, Kip2)	U22398	12.5
38	ALL1-fused gene from chromosome 1q	U16954	12.5
39	GATA binding protein 2	M68891	12.2
40	interleukin 13 receptor, alpha 1	Y10659	12.0
41	phosphatidylserine receptor	AB011157	11.9
42	msh homeo box homolog 1 (Drosophila)	M97676	11.7
43	serine/threonine kinase 17a (apoptosis-inducing)	AI961743	11.5
44	tumor necrosis factor, alpha-induced protein 6	M31165	11.4
45	serum/glucocorticoid regulated kinase	Y10032	11.2
46	GTP-binding protein	U69563	11.2
47	jun B proto-oncogene	X51345	11.1
48	H2A histone family, member O	L19779	10.9
49	KIAA1233 protein	AL109724	10.5
50	KIAA0716 gene product	AB018259	10.4
51	histone 1, H2bk	AJ223352	10.3

52	stathmin-like 2	D45352	10.2
53	connective tissue growth factor	X78947	9.9
54	Human DNA sequence from clone 465N24 on chromosome 1p35.1-36.13	AL031432	9.7
55	Homo sapiens cDNA: FLJ23438 fis, clone HRC13275.	W28729	9.6
56	transient receptor potential cation channel, subfamily C, member 1	X89066	9.2
57	aquaporin 3	N74607	9.0
58	distal-less homeo box 5	AC004774	8.9
59	dual specificity phosphatase 1	X68277	8.8
60	nuclear RNA export factor 1	AJ132712	8.7
61	GATA binding protein 2	M77810	8.7
62	postmeiotic segregation increased 2-like 5	D38502	8.7
63	growth arrest and DNA-damage-inducible, gamma	AI952982	8.6
64	transcription factor 8 (represses interleukin 2 expression)	D15050	8.3
65	gamma-aminobutyric acid (GABA) receptor, rho 1	M62400	8.3
66	interferon, alpha-inducible protein (clone IFI-15K)	M13755	8.1
67	ectodermal-neural cortex (with BTB-like domain)	AF059611	8.0
68	Homo sapiens apoptosis inhibitor survivin gene, complete cds	U75285	7.8
69	complement component 4 binding protein, alpha	M31452	7.5
70	DnaJ (Hsp40) homolog, subfamily B, member 4	U40992	7.5
71	regulator of G-protein signalling 2, 24kDa	L13463	7.4
72	dual-specificity tyrosine-(Y)-phosphorylation regulated kinase 3	Y12735	7.3
73	hypothetical protein CG003	U50534	6.9
74	2'-5'-oligoadenylate synthetase-like	AJ225089	6.9
75	vitamin D (1,25- dihydroxyvitamin D3) receptor	J03258	6.9
76	GATA binding protein 2	M77810	6.9
77	zinc finger protein 36, C3H type, homolog (mouse)	M92843	6.5
78	msh homeo box homolog 1 (Drosophila)	M97676	6.5
79	cysteine and glycine-rich protein 2	U57646	6.4
80	KIAA0469 gene product	AB007938	6.4

81	serine (or cysteine) proteinase inhibitor, clade I (neuroserpin), member 1	Z81326	6.4
82	PR domain containing 2, with ZNF domain	U23736	6.4
83	B-cell CLL/lymphoma 6 (zinc finger protein 51)	U00115	6.3
84	CDC-like kinase 1	M59287	6.3
85	tumor necrosis factor receptor superfamily, member 9	U03397	6.2
86	msh homeo box homolog 1 (Drosophila)	M97676	6.2
87	ribosomal protein L5	U66589	6.1
88	dihydrolipoamide branched chain transacylase	M19301	6.0
89	target of myb1 (chicken)	Z82244	6.0
90	tubulin, beta, 4	U47634	5.9
91	interferon, alpha-inducible protein (clone IFI-15K)	AA203213	5.8
92	protocadherin 9	AI524125	5.8
93	solute carrier family 12 (sodium/chloride transporters), member 3	X91220	5.7
94	nuclear receptor subfamily 4, group A, member 3	D78579	5.7
95	bromodomain and PHD finger containing, 1	M91585	5.7
96	chromosome 12 open reading frame 22	AF052105	5.6
97	Ras association (RalGDS/AF-6) domain family 1	AF061836	5.5
98	phorbol-12-myristate-13-acetate-induced protein 1	D90070	5.5
99	growth arrest and DNA-damage-inducible, beta	N95168	5.5
100	FBJ murine osteosarcoma viral oncogene homolog B	L49169	5.4
101	glutamate-ammonia ligase (glutamine synthase)	X59834	5.3
102	bromodomain containing 2	S78771	5.3
103	ubiquitin-conjugating enzyme E2D 1	AF020761	5.3
104	ras homolog gene family, member E	S82240	5.3
105	H.sapiens genes for histones H2B.1 and H2A	X57985	5.3
106	nuclear receptor subfamily 4, group A, member 2	S77154	5.3
107	GT198, complete ORF	L38933	5.3
108	peptidylprolyl isomerase E (cyclophilin E)	AF042386	5.2
109	growth arrest and DNA-damage-inducible, alpha	M60974	5.2

110	ubiquitin specific protease 11	U44839	5.2
111	vascular adhesion protein 1	U39447	5.1
112	BCL2-related 11, isoform 6	AI971169	5.0
113	Human Xq28 cosmid, creatine transporter (SLC6A8) gene	U36341	5.0
114	annexin A13	Z11502	5.0
115	tubulin-specific chaperone c	U61234	5.0
116	protein phosphatase 1, regulatory (inhibitor) subunit 15A	U83981	5.0
117	H2A histone family, member N	Z98744	5.0
118	tumor suppressing subtransferable candidate 3	AF001294	5.0
119	Homo sapiens AOC2 gene for retina-specific amine oxidase	AB012943	5.0
120	Mdm4, transformed 3T3 cell double minute 4	AF007111	4.8
121	hypothetical protein FLJ23053	W27519	4.8
122	heat shock 70kD protein 1B	M59830	4.8
123	GTP binding protein overexpressed in skeletal muscle	U10550	4.7
124	phosphoinositide-3-kinase, regulatory subunit, polypeptide 3	D88532	4.7
125	beta-2-microglobulin	S82297	4.7
126	hematopoietic cell-specific Lyn substrate 1	X16663	4.7
127	cyclin G2	U47414	4.7
128	cathepsin L2	AB001928	4.7
129	nucleoside phosphorylase	X00737	4.6
130	Kruppel-like factor 4 (gut)	U70663	4.5
131	cyclin E1	M74093	4.5
132	beta-2-microglobulin	AB021288	4.5
133	KIAA0570 gene product	AL050376	4.5
134	hemopoietic cell kinase	M16592	4.5
135	Human calmodulin (CALM1) gene	U12022	4.5
136	cyclin-dependent kinase inhibitor 1A (p21, Cip1)	U03106	4.4
137	bK447C4.1 (novel MAFF (v-maf musculoaponeurotic fibrosarcoma oncogene F)	AL021977	4.4
138	HMBA-inducible	AB021179	4.4

139	RCD1 required for cell differentiation1 homolog	D87957	4.4
140	smoothelin	Y13492	4.3
141	Homo sapiens cDNA FLJ25670 fis, clone TST03752.	W27600	4.3
142	solute carrier family 25 (mitochondrial carrier; adenine nucleotide translocator)	J02966	4.3
143	bromodomain containing 2	S78771	4.3
144	interferon-induced protein with tetratricopeptide repeats 4	AF026939	4.3
145	RCD1 required for cell differentiation1 homolog (S. pombe)	D87957	4.3
146	beta-2-microglobulin	V00567	4.3
147	M-phase phosphoprotein 9	AL096751	4.3
148	TAF9 RNA polymerase II, TATA box binding protein (TBP)-associated factor, 32kDa	U21858	4.3
149	ras homolog gene family, member B	M12174	4.3
150	collagen, type VIII, alpha 1	X57527	4.2
151	putative transmembrane protein	U23070	4.2
152	Homo sapiens mRNA; cDNA DKFZp564I066 (from clone DKFZp564I066)	AL049331	4.2
153	ATP/GTP-binding protein	U73524	4.2
154	v-rel reticuloendotheliosis viral oncogene homolog A	L19067	4.1
155	growth hormone 2	J03071	4.1
156	MARCKS-like protein	X70326	4.1
157	MIR-7 [Homo sapiens], mRNA sequence	AF004230	4.1
158	hyaluronoglucosaminidase 1	U03056	4.1
159	zinc finger protein 211	U38904	4.1
160	NAD kinase	AL031282	4.1
161	transcription elongation factor B (SIII), polypeptide 3	L47345	4.1
162	adhesion regulating molecule 1	D64154	4.1
163	cyclin E1	M73812	4.0
164	4-hydroxyphenylpyruvate dioxygenase	D31628	4.0
165	isopentenyl-diphosphate delta isomerase	X17025	4.0
166	sterol-C4-methyl oxidase-like	U60205	4.0
167	fascin homolog 1, actin-bundling protein	U03057	4.0

168	fatty acid desaturase 3	AC004770	4.0
169	glypican 5	U66033	3.9
170	solute carrier family 6 (neurotransmitter transporter, serotonin), member 4	L05568	3.9
171	2,3-bisphosphoglycerate mutase	X04327	3.9
172	hypothetical protein MGC9651	W21884	3.9
173	pim-2 oncogene	U77735	3.9
174	selenoprotein W, 1	U67171	3.9
175	hypothetical protein MGC4701	AF040964	3.9
176	histone 1, H1c	AI189287	3.9
177	Sec15B protein	AB023136	3.9
178	dJ196E23.2 (HIV-1 transcriptional elongation factor TAT cofactor TAT-SF1)	Z97632	3.8
179	eukaryotic translation initiation factor 5	U49436	3.8
180	activity-regulated cytoskeleton-associated protein	D87468	3.8
181	immediate early protein	M62831	3.8
182	sialidase 1 (lysosomal sialidase)	AF040958	3.8
183	cyclin G2	U47414	3.8
184	protein kinase, AMP-activated, beta 2 non-catalytic subunit	AJ224538	3.8
185	nuclear factor of kappa light polypeptide gene enhancer in B-cells inhibitor	M69043	3.8
186	heterogeneous nuclear ribonucleoprotein A1	X79536	3.8
187	tp95h03.x1 Homo sapiens cDNA, 3 end	AI687419	3.8
188	Human MHC class I molecule (MICB) gene, complete cds	U65416	3.7
189	ephrin-A1	M57730	3.7
190	hypothetical protein F23149_1	AC005239	3.7
191	killer cell lectin-like receptor subfamily C, member 4	AJ001683	3.7
192	Homo sapiens clone 24694 mRNA sequence	AF070620	3.7
193	adrenomedullin	D14874	3.7
194	nuclear factor related to kappa B binding protein	X80878	3.7
195	ataxia telangiectasia mutated	U26455	3.6
196	histone 1, H2bn	AA873858	3.6

197	polymerase (DNA directed), gamma	U60325	3.6
198	ProSAPiP1 protein	AB011124	3.6
199	sphingomyelin phosphodiesterase 1, acid lysosomal (acid sphingomyelinase)	X59960	3.6
200	H2A histone family, member X	X14850	3.6
201	collagen, type VII, alpha 1	L02870	3.6
202	regulator of G-protein signalling 16	U70426	3.6
203	2',3'-cyclic nucleotide 3' phosphodiesterase	M19650	3.5
204	clusterin (complement lysis inhibitor)	M25915	3.5
205	PRP4 pre-mRNA processing factor 4 homolog (yeast)	AF016369	3.5
206	Human laminin S B3 chain (LAMB3) gene	U17760	3.5
207	transducer of ERBB2, 2	D64109	3.5
208	tubulin, beta, 5	X00734	3.5
209	tumor necrosis factor receptor superfamily, member 10d	AF029761	3.5
210	paternally expressed 10	AB028974	3.5
211	interferon regulatory factor 7	U53831	3.4
212	KIAA0404 protein	AB007864	3.4
213	phosphoprotein enriched in astrocytes 15	X86809	3.4
214	transforming growth factor beta-stimulated protein TSC-22	AJ222700	3.4
215	ring finger protein 1	AL031228	3.4
216	dynein, axonemal, heavy polypeptide 9	AB002355	3.4
217	nucleolar protein 5A (56kDa with KKE/D repeat)	Y12065	3.4
218	NDRG family member 4	AF007138	3.4
219	breast cancer metastasis-suppressor 1	AL050008	3.3
220	regulatory solute carrier protein, family 1, member 1	X82877	3.3
221	DnaJ (Hsp40) homolog, subfamily C, member 9	AI680675	3.3
222	KIAA0721 protein	AB018264	3.3
223	opioid growth factor receptor	AF109134	3.3
224	Human P3 gene	X12458	3.3
225	serine (or cysteine) proteinase inhibitor, clade E	M14083	3.3

226	pim-2 oncogene	U77735	3.3
227	cyclin D3	M92287	3.3
228	phosphoinositide-3-kinase, regulatory subunit, polypeptide 3 (p55, gamma)	D88532	3.3
229	eukaryotic translation initiation factor 4E binding protein 2	N73769	3.3
230	solute carrier family 9 (sodium/hydrogen exchanger), isoform 3 regulatory factor	AF015926	3.3
231	hypothetical protein FLJ11560	R48209	3.3
232	thromboxane A2 receptor	AC005175	3.3
233	KIAA0455 gene product	AB007924	3.3
234	bromodomain containing 8	X87613	3.3
235	Human synaptobrevin 1 (SYB1) gene	M36200	3.3
236	Homo sapiens Brutons tyrosine kinase (BTK), alpha-D-galactosidase A (GLA)	U78027	3.3
237	B-cell translocation gene 1, anti-proliferative	X61123	3.3
238	MHC class I polypeptide-related sequence A	X92841	3.2
239	ADP-ribosylation factor-like 6 interacting protein	D31885	3.2
240	TAF7 RNA polymerase II, TATA box binding protein (TBP)-associated factor	U18062	3.2
241	BTG family, member 2	U72649	3.2
242	DnaJ (Hsp40) homolog, subfamily A, member 1	L08069	3.2
243	bromodomain containing 2	D42040	3.2
244	trophoblast glycoprotein	Z29083	3.2
245	homeo box A7	AJ005814	3.2
246	tumor suppressing subtransferable candidate 3	AF035444	3.2
247	karyopherin alpha 2 (RAG cohort 1, importin alpha 1)	U28386	3.2
248	Human pTR5 mRNA for repetitive sequence	X15674	3.2
249	RNA polymerase I transcription factor RRN3	AA213789	3.2
250	odd-skipped-related 2A protein	AI126171	3.2
251	KIAA0176 protein	D79998	3.1
252	jun D proto-oncogene	X56681	3.1
253	purine-rich element binding protein A	M96684	3.1
254	methyl-CpG binding domain protein 1	Y10746	3.1

255	transducer of ERBB2, 1	D38305	3.1
256	CDC6 cell division cycle 6 homolog (S. cerevisiae)	U77949	3.1
257	dual-specificity tyrosine-(Y)-phosphorylation regulated kinase 1A	D86550	3.1
258	amiloride binding protein 1	U11863	3.1
259	aminolevulinate, delta-, synthase 1	Y00451	3.1
260	carbonic anhydrase II	J03037	3.1
261	CDC20 cell division cycle 20 homolog (S. cerevisiae)	U05340	3.1
262	H2B histone family, member H	Z80780	3.1
263	caveolin 3	AF043101	3.1
264	ISL1 transcription factor, LIM/homeodomain, (islet-1)	U07559	3.0
265	glutamate receptor, ionotropic, kainate 5	AA977136	3.0
266	dJ150O5.2 (Inhibitor of DNA binding 3)	AL021154	3.0
267	gene predicted from cDNA	D14811	3.0
268	ribosomal protein L12	AL021366	3.0
269	myomesin (M-protein) 2, 165kDa	X69089	3.0
270	PL6 protein	U09584	3.0
271	microtubule-associated protein 1 light chain 3 beta	W28807	3.0
272	proteasome (prosome, macropain) 26S subunit, non-ATPase, 2	D78151	3.0
273	KIAA0935 protein	AB023152	3.0
274	protein phosphatase 2, regulatory subunit B (B56), beta isoform	L42374	3.0
275	Human slow twitch skeletal muscle	M37984	3.0
276	histone 1, H3d	N35832	3.0
277	translation factor sui1 homolog	AF064607	3.0
278	Wolfram syndrome 1 (wolframin)	AF084481	3.0
279	microtubule-associated protein 1 light chain 3 beta	W27998	3.0
280	v-jun sarcoma virus 17 oncogene homolog (avian)	J04111	3.0
281	bromodomain containing 8	AW020536	3.0
282	RNA binding motif protein 4	U89505	3.0
283	jun D proto-oncogene	X56681	3.0

284	hypothetical protein LOC162427	L38935	2.9
285	Bacteriophage P1 cre recombinase protein	X03453	2.9
286	retinoic acid receptor responder	AF060228	2.9
287	Human 26S protease subunit S5a mRNA, complete cds	U51007	2.9
288	KIAA0542 gene product	AB011114	2.9
289	B subtilis dapB, jojF, jojG genes corresponding to nucleotides 1358-3197 of L38	L38424	2.9
290	autoantigen	L26339	2.9
291	postmeiotic segregation increased 2-like 1	D38435	2.9
292	interleukin enhancer binding factor 2, 45kDa	U10323	2.9
293	ubiquitin-conjugating enzyme E2C	U73379	2.9
294	proteasome (prosome, macropain) inhibitor subunit 1 (PI31)	D88378	2.9
295	Homo sapiens GLC1A	Z97171	2.9
296	Homo sapiens cDNA FLJ38383 fis, clone FEBRA2003726.	AI827895	2.9
297	zinc finger protein 297B	AB007874	2.9
298	Src-like-adaptor	D89077	2.9
299	dystrophia myotonica-containing WD repeat motif	L19267	2.9
300	Kruppel-type zinc finger (C2H2)	AB011414	2.9
301	fragile X mental retardation, autosomal homolog 2	U31501	2.9
302	E coli bioC protein	J04423	2.9
303	Human DNA sequence from clone 833B7 on chromosome 22q12.3-13.2	AL008637	2.9
304	cancer/testis antigen 1	U87459	2.9
305	protocadherin gamma subfamily B, 7	D88799	2.9
306	MADS box transcription enhancer factor 2, polypeptide D	L16794	2.9
307	fibronectin leucine rich transmembrane protein 1	AF007139	2.8
308	cysteine-rich, angiogenic inducer, 61	Y11307	2.8
309	TSPY-like	AF042181	2.8
310	E coli bioD gene dethiobiotin synthetase	J04423	2.8
311	cyclin T1	AF048730	2.8
312	sterol-C4-methyl oxidase-like	AI535653	2.8

313	ferredoxin reductase	J03826	2.8
314	telomeric repeat binding factor 2, interacting protein	W28865	2.8
315	clone FFE-7 type II inosine monophosphate dehydrogenase (IMPDH2)	L33842	2.8
316	lung type-I cell membrane-associated glycoprotein	AI660929	2.8
317	thiosulfate sulfurtransferase (rhodanese)	D87292	2.8
318	stratifin	X57348	2.8
319	DKFZP434J214 protein	AL080156	2.8
320	ZW10 interactor	AF067656	2.8
321	sialyltransferase	U14550	2.8
322	activating transcription factor 3	L19871	2.8
323	cell division cycle 2-like 1 (PITSLRE proteins)	W32483	2.8
324	cyclin-dependent kinase 2	M68520	2.8
325	phosphodiesterase 8B	AF079529	2.8
326	NADH dehydrogenase (ubiquinone) 1 alpha subcomplex, 2, 8kDa	AF047185	2.7
327	cyclin D3	M92287	2.7
328	prefoldin 5	D89667	2.7
329	Homo sapiens insulin induced protein 1 (INSIG1) gene	U96876	2.7
330	Bacteriophage P1 cre recombinase protein	X03453	2.7
331	proline rich 2	U03105	2.7
332	microfibrillar-associated protein 1	U04209	2.7
333	tubulin, beta, 5	X00734	2.7
334	bladder cancer associated protein	AL049288	2.7
335	interleukin 1, alpha	M28983	2.7
336	cyclin A2	X51688	2.7
337	cyclin-dependent kinase inhibitor 2D (p19, inhibits CDK4)	U40343	2.7
338	Human clone 23933 mRNA sequence	U79273	2.7
339	splicing factor 3b, subunit 4, 49kD	L35013	2.7
340	zinc finger protein 183 (RING finger, C3HC4 type)	X98253	2.7
341	TIF1beta zinc finger protein [Homo sapiens], mRNA sequence	X97548	2.7

342	DKFZP434C171 protein	AL080169	2.7
343	E coli bioC protein	J04423	2.7
344	adrenergic, beta-2-, receptor, surface	M15169	2.7
345	bladder cancer associated protein	AL049288	2.7
346	lysophospholipase I	D84064	2.7
347	unc-51-like kinase 1	AF045458	2.7
348	proliferating cell nuclear antigen	M15796	2.7
349	nucleolar protein 1, 120kDa	X55504	2.7
350	proteasome (prosome, macropain) 26S subunit	D67025	2.7
351	requiem, apoptosis response zinc finger gene	AF001433	2.7
352	pituitary tumor-transforming 1	AA203476	2.7
353	jun D proto-oncogene	X56681	2.6
354	zinc finger protein 12	AI434146	2.6
355	cyclin-dependent kinase inhibitor 1C (p57, Kip2)	U22398	2.6
356	proteasome (prosome, macropain) 26S subunit, ATPase, 4	AF020736	2.6
357	GDP dissociation inhibitor 1	X79353	2.6
358	TAF13 RNA polymerase II, TATA box binding protei (TBP)-associated factor, 18kDa	X84003	2.6
359	golgi autoantigen, golgin subfamily a, 2	L06147	2.6
360	DnaJ (Hsp40) homolog, subfamily A, member 1	L08069	2.6
361	glyceraldehyde-3-phosphate dehydrogenase, testis-specific	AJ005371	2.6
362	PRP4 pre-mRNA processing factor 4 homolog (yeast)	AI184802	2.6
363	cadherin, EGF LAG seven-pass G-type receptor 3	AB011536	2.6
364	H2B histone family, member E	Z83738	2.6
365	Human mRNA for general transcription factor IIB	X59268	2.6
366	zinc finger protein 36 (KOX 18)	U09848	2.6
367	ADP-ribosyltransferase (NAD+; poly(ADP-ribose) polymerase)-like 2	AJ236876	2.6
368	Human gene for creatine kinase B (EC 2.7.3.2)	X15334	2.6
369	connector enhancer of KSR-like	AF100153	2.6
370	Tax interaction protein 1	U90913	2.6

371	sperm associated antigen 5	AF063308	2.6
372	three prime repair exonuclease 1	AJ243797	2.6
373	DnaJ (Hsp40) homolog, subfamily B, member 9	AL080081	2.6
374	myeloid cell leukemia sequence 1 (BCL2-related)	L08246	2.6
375	leucine-rich acidic nuclear protein like	AA913812	2.6
376	solute carrier family 35 (UDP-galactose transporter), member 2	D84454	2.6
377	serum-inducible kinase	AF059617	2.6
378	matrix Gla protein	AI953789	2.6
379	polymerase I and transcript release factor	AL050224	2.6
380	G protein pathway suppressor 2	U28963	2.6
381	collagen, type XVI, alpha 1	M92642	2.6
382	hypothetical protein FLJ21168	AI393342	2.5
383	DKFZP586B0923 protein	AL050190	2.5
384	cyclin A1	U66838	2.5
385	melanoma antigen, family A, 5	U10689	2.5
386	major histocompatibility complex, class I, A	D32129	2.5
387	fucosidase, alpha-L- 1, tissue	M29877	2.5
388	Homo sapiens mRNA; cDNA DKFZp586F2224	AI655015	2.5
389	tissue inhibitor of metalloproteinase 1	D11139	2.5
390	H.sapiens PAX7 gene, exon 1	X96744	2.5
391	RAD9 homolog (S. pombe)	U53174	2.5
392	high-mobility group box 2	X62534	2.5
393	E coli bioD gene dethiobiotin synthetase	J04423	2.5
394	SNARE protein Ykt6	U95735	2.5
395	histone 1, H2bc	AI688098	2.5
396	ae93d06.s1 Homo sapiens cDNA, 3 end	AA780435	2.5
397	protein tyrosine phosphatase, non-receptor type 6	X62055	2.5
398	interferon regulatory factor 1	L05072	2.5
399	early growth response 1	X52541	2.5

400	chromosome 14 open reading frame 3	AJ243310	2.5
401	aldolase C, fructose-bisphosphate	AF054987	2.5
402	tubulin, beta, 2	X02344	2.5
403	dJ97D16.4 (Histone H2B)	AL009179	2.5
404	chromosome 3p21.1 gene sequence	L13434	2.5
405	KIAA0907 protein	AB020714	2.5
406	caspase 7, apoptosis-related cysteine protease	U67319	2.5
407	cysteine and glycine-rich protein 1	M33146	2.5
408	unc-119 homolog (C. elegans)	U40998	2.5
409	Homo sapiens, clone IMAGE:3914313, mRNA	W25984	2.5
410	cathepsin L	X12451	2.5
411	proteasome (prosome, macropain) inhibitor subunit 1 (PI31)	D88378	2.5
412	diacylglycerol O-acyltransferase homolog 1 (mouse)	AF059202	2.5
413	male-enhanced antigen	M27937	2.5
414	Chromosome 22q13 BAC Clone CIT987SK-384D8 complete sequence	U62317	2.5
415	T-cell, immune regulator 1, ATPase, H+ transporting, lysosomal V0 protein a	U45285	2.5
416	DKFZP586O0120 protein	AL050157	2.5
417	CDC-like kinase 3	L29217	2.5
418	neuropilin 2	AF016098	2.5
419	paired-like homeodomain transcription factor 2	AF048722	2.5
420	zinc finger protein 134 (clone pHZ-15)	U09412	2.4
421	keratin 8	X74929	2.4
422	frizzled homolog 7 (Drosophila)	AB017365	2.4
423	G protein-coupled receptor 30	AF015257	2.4
424	FLN29 gene product	AB007447	2.4
425	fatty acid binding protein 5 (psoriasis-associated)	M94856	2.4
426	H2A histone family, member G	Z80776	2.4
427	Homo sapiens cDNA FLJ36527 fis, clone TRACH2003941.	AI761647	2.4
428	KIAA1100 protein	AB029023	2.4

429	chromosome 3 open reading frame 4	AL080097	2.4
430	Homo sapiens mRNA full length insert cDNA clone EUROIMAGE 51358.	AL109700	2.4
431	H2B histone family, member K	Z80782	2.4
432	Human Chromosome 16 BAC clone CIT987SK-A-270G1	AF001549	2.4
433	thioesterase, adipose associated	AB014607	2.4
434	protein tyrosine phosphatase, receptor type, f polypeptide (PTPRF)	AB014554	2.4
435	syndecan binding protein (syntenin)	AF000652	2.4
436	Human DLX-2 (Dlx2) mRNA, complete cds	U51003	2.4
437	inhibitor of DNA binding 1, dominant negative helix-loop-helix protein	X77956	2.4
438	RecQ protein-like (DNA helicase Q1-like)	L36140	2.4
439	zinc finger protein 384	U80760	2.4
440	phosphatidylserine decarboxylase	AL050371	2.4
441	Homo sapiens very long chain acyl-CoA dehydrogenase gene	L46590	2.4
442	chromosome 14 open reading frame 11	AI057607	2.4
443	thousand and one amino acid protein kinase	AB020688	2.4
444	GCN5 general control of amino-acid synthesis 5-like 2 (yeast)	AF029777	2.4
445	SNARE protein Ykt6	U95735	2.4
446	modulator of apoptosis 1	AI670788	2.4
447	butyrophilin, subfamily 2, member A1	U90543	2.4
448	cathepsin Z	AF032906	2.4
449	Huntingtin interacting protein E	AF049611	2.4
450	upstream transcription factor 2, c-fos interacting	AD000684	2.4
451	E coli bioB gene biotin synthetase	J04423	2.4
452	procollagen-proline, 2-oxoglutarate 4-dioxygenase alpha	U90441	2.4
453	BAI1-associated protein 2	AB015019	2.4
454	nebulin	X83957	2.4
455	stratifin	X57348	2.4
456	hypothetical protein BC004544	AI928387	2.4
457	importin 13	AB018267	2.4

458	M-phase phosphoprotein 10	X98494	2.4
459	TSC-22-like	AJ133115	2.4
460	5-hydroxytryptamine (serotonin) receptor 3A	D49394	2.3
461	forkhead box G1A	X74143	2.3
462	nucleolar cysteine-rich protein	H82458	2.3
463	death-associated protein 6	AB015051	2.3
464	Sec23 homolog B (S. cerevisiae)	X97065	2.3
465	DEAD/H (Asp-Glu-Ala-Asp/His) box polypeptide 38	D86977	2.3
466	RecQ protein-like 4	AB006532	2.3
467	nucleoporin 62kDa	X58521	2.3
468	adaptor-related protein complex 1, sigma 2 subunit	AF091077	2.3
469	transmembrane protein 5	AB015633	2.3
470	serine (or cysteine) proteinase inhibitor, clade E	AI743134	2.3
471	Homo sapiens mRNA from chromosome 5q21-22	AB002449	2.3
472	dual-specificity tyrosine-(Y)-phosphorylation regulated kinase 1A	D86550	2.3
473	nuclear receptor subfamily 1, group D, member 1	X72631	2.3
474	sex comb on midleg-like 2 (Drosophila)	Y18004	2.3
475	zyxin	X95735	2.3
476	BAI1-associated protein 1	W26805	2.3
477	DnaJ (Hsp40) homolog, subfmaily B, member 1	D85429	2.3
478	GABA(A) receptor-associated protein like 1	W28281	2.3
479	smoothelin	AI888563	2.3
480	Kruppel-like factor 5 (intestinal)	D14520	2.3
481	Homo sapiens mRNA; cDNA DKFZp586M0723	AL050227	2.3
482	Human hbc647 mRNA sequence.	U68494	2.3
483	DNA segment on chromosome X and Y (unique) 155 expressed sequence	L03426	2.3
484	cytokine-inducible kinase	U56998	2.3
485	cholecystokinin	AW043690	2.3
486	small nuclear RNA activating complex, polypeptide 5, 19kDa	AI557062	2.3

487	ATPase, H+ transporting, lysosomal interacting protein 1	D16469	2.3
488	leucine-rich acidic nuclear protein like	W25866	2.3
489	period homolog 2 (Drosophila)	AB002345	2.3
490	epoxide hydrolase 1, microsomal (xenobiotic)	L25879	2.3
491	xeroderma pigmentosum, complementation group C	D21089	2.3
492	TAF13 RNA polymerase II	X84003	2.3
493	DiGeorge syndrome critical region gene 14	L77566	2.3
494	testis-specific kinase 1	D50863	2.3
495	modulator recognition factor I	M62324	2.3
496	phosphoinositide-3-kinase, regulatory subunit, polypeptide 3 (p55, gamma)	D88532	2.3
497	small nuclear ribonucleoprotein 70kDa polypeptide (RNP antigen)	X06815	2.3
498	proteasome (prosome, macropain) activator subunit 2 (PA28 beta)	D45248	2.3
499	E coli bioB gene biotin synthetase	J04423	2.3
500	chitinase 1 (chitotriosidase)	U29615	2.3
501	thromboxane A2 receptor	AC005175	2.3
502	H2B histone family, member R	X00088	2.3
503	neuromedin B	AI985272	2.3
504	tumor necrosis factor receptor superfamily, member 25	Y09392	2.3
505	ATPase, H+ transporting, lysosomal interacting protein 2	W27971	2.3
506	cyclin-dependent kinase 9 (CDC2-related kinase)	X80230	2.3
507	myeloid cell leukemia sequence 1 (BCL2-related)	L08246	2.3
508	sterol-C5-desaturase (ERG3 delta-5-desaturase homolog, fungal)-like	AB016247	2.3
509	EH-domain containing 1	AF001434	2.3
510	Cbp/p300-interacting transactivator, with Glu/Asp-rich carboxy-terminal domain,	U65093	2.2
511	cutaneous T-cell lymphoma-associated tumor antigen se20-4	AB015345	2.2
512	proteasome (prosome, macropain) 26S subunit, ATPase, 5	AF035309	2.2
513	cyclin A2	X51688	2.2
514	golgi associated, gamma adaptin ear containing, ARF binding protein 3	D63876	2.2
515	Homo sapiens DMR-N9, partial cds; and myotonic dystrophy kinase (DM kinase)	L08835	2.2

516	RNA polymerase I subunit	AF008442	2.2
517	SOCS box-containing WD protein SWiP-1	W26496	2.2
518	syntaxin binding protein 2	AB002559	2.2
519	CD2 antigen (cytoplasmic tail) binding protein 2	AF104222	2.2
520	v-rel reticuloendotheliosis viral oncogene homolog A, nuclear factor of kappa li	L19067	2.2
521	secretory granule, neuroendocrine protein 1 (7B2 protein)	Y00757	2.2
522	Human endogenous retrovirus mRNA for ORF	X72790	2.2
523	death-associated protein kinase 3	AB007144	2.2
524	homocysteine-inducible, endoplasmic reticulum stress-inducible, ubiquitin-like d	AF055001	2.2
525	cell division cycle 25A	M81933	2.2
526	cyclin-dependent kinase 2	M68520	2.2
527	ATP-binding cassette, sub-family F (GCN20), member 3	U66685	2.2
528	suppressor of Ty 5 homolog (S. cerevisiae)	AF040253	2.2
529	COP9 homolog	U51205	2.2
530	nuclear cap binding protein subunit 2, 20kDa	D59253	2.2
531	proteasome (prosome, macropain) 26S subunit, non-ATPase, 7 (Mov34 homolog)	D50063	2.2
532	ubiquitin-specific protease otubain 1	AL096714	2.2
533	E2F transcription factor 1	M96577	2.2
534	similar to hypothetical protein DKFZp564N123.1 - human	AL050297	2.2
535	ribonuclease P (14kD)	AF001175	2.2
536	tubulin, alpha 1 (testis specific)	X06956	2.2
537	v-rel reticuloendotheliosis viral oncogene homolog A	U33838	2.2
538	mitogen-activated protein kinase kinase kinase 11	L32976	2.2
539	KIAA0708 protein	AB014608	2.2
540	emopamil binding protein (sterol isomerase)	Z37986	2.2
541	solute carrier family 22 (organic cation transporter)	AF037066	2.2
542	cytochrome P450, family 1, subfamily B, polypeptide 1	U03688	2.2
543	Human transcription factor, forkhead related activator 4 (FREAC-4) gene	U59831	2.2
544	pleiomorphic adenoma gene-like 2	D83784	2.2

545	CDC42 effector protein (Rho GTPase binding) 3	AF094521	2.2
546	protein kinase C, delta	D10495	2.2
547	hypothetical protein FLJ90798	AL049949	2.2
548	frizzled homolog 2 (Drosophila)	L37882	2.2
549	RUN and SH3 domain containing 1	AB026894	2.1
550	zinc finger protein 266	AA868898	2.1
551	DnaJ (Hsp40) homolog, subfamily B, member 4	U40992	2.1
552	cysteine-rich protein 2	D42123	2.1
553	ATPase, H+ transporting, lysosomal 16kDa, V0 subunit c	M62762	2.1
554	phosphoglucomutase 3	AA001791	2.1
555	stem-loop (histone) binding protein	U75679	2.1
556	chorionic gonadotropin, beta polypeptide	J00117	2.1
557	amyloid beta (A4) precursor-like protein 1	U48437	2.1
558	polymerase I and transcript release factor	AF000421	2.1
559	matrilin 3	AJ001047	2.1
560	putative translation initiation factor	AJ012375	2.1
561	heat shock 90kDa protein 1, alpha	X15183	2.1
562	proteasome 26S subunit, non-ATPase, 7	D50063	2.1
563	metallothionein 1X	AA224832	2.1
564	myeloid/lymphoid or mixed-lineage leukemia 4	AJ007041	2.1
565	peptidylprolyl isomerase F (cyclophilin F)	M80254	2.1
566	inhibitor of DNA binding 1	X77956	2.1
567	mitochondrial ribosomal protein L49	U39400	2.1
568	hypothetical protein FLJ90005	W27419	2.1
569	transmembrane 9 superfamily member 1	U94831	2.1
570	engrailed homolog 2	AI094859	2.1
571	ubiquitin specific protease 5 (isopeptidase T)	U47927	2.1
572	hypothetical protein FLJ14639	AA152202	2.1
573	tubulin, gamma 1	M61764	2.1

574	H2B histone family, member G	Z80779	2.1
575	follistatin-like 3 (secreted glycoprotein)	U76702	2.1
576	RNA binding protein S1, serine-rich domain	L37368	2.1
577	polymerase (DNA directed), epsilon 3 (p17 subunit)	AF070640	2.1
578	Mouse Mammary Turmor Virus Receptor homolog 1	AF052151	2.1
579	zinc finger protein 37a (KOX 21)	X69115	2.1
580	hypothetical protein MGC34648	AL035307	2.1
581	melanoma antigen, family D, 1	W26633	2.1
582	legumain	D55696	2.1
583	nucleoporin-like protein 1	U97198	2.1
584	histone 1, H2ag	L19778	2.1
585	proline-rich protein HaeIII subfamily 1	AI864120	2.1
586	Human nonmuscle	M22919	2.1
587	dynein, cytoplasmic, light polypeptide 1	AI540958	2.1
588	bromodomain containing 8	AF016270	2.1
589	N-acetyltransferase 1 (arylamine N-acetyltransferase)	D90041	2.1
590	potassium voltage-gated channel, shaker-related subfamily	L39833	2.1
591	tumor suppressor deleted in oral cancer-related 1	AF089814	2.1
592	Rhesus blood group, CcEe antigens	X63096	2.1
593	GLI-Kruppel family member HKR3	L16896	2.0
594	delta sleep inducing peptide, immunoreactor	Z50781	2.0
595	single-minded homolog 2 (Drosophila)	U80457	2.0
596	peripherin	L14565	2.0
597	heat shock 90kD protein 1, beta	J04988	2.0
598	cytochrome b5 reductase 1 (B5R.1)	AF091084	2.0
599	ortholog of mouse TPR-containing, SH2-binding phosphoprotein	D63875	2.0
600	Lutheran blood group (Auberger b antigen included)	X83425	2.0
601	Homo sapiens mRNA; cDNA DKFZp566E183	AL049354	2.0
602	EGF-containing fibulin-like extracellular matrix protein 2	AF093119	2.0

603	delta sleep inducing peptide, immunoreactor	AI635895	2.0
604	chaperonin containing TCP1, subunit 6A (zeta 1)	L27706	2.0
605	coagulation factor III (thromboplastin, tissue factor)	J02931	2.0
606	phosphatidylinositol polyphosphate 5-phosphatase type IV	U45974	2.0
607	KIAA0111 gene product	D21853	2.0
608	Homo sapiens clk2 kinase (CLK2)	AF023268	2.0
609	mannose-P-dolichol utilization defect 1	AF038961	2.0
610	nuclear cap binding protein subunit 2, 20kDa	AA149428	2.0
611	protein kinase D2	AL050147	2.0
612	1-acylglycerol-3-phosphate O-acyltransferase 2	U56418	2.0
613	cell division cycle 2, G1 to S and G2 to M	X05360	2.0
614	bystin-like	L36720	2.0
615	nucleosome assembly protein 1-like 3	D50370	2.0
616	degenerative spermatocyte homolog, lipid desaturase (Drosophila)	AF002668	2.0
617	Bacteriophage P1 cre recombinase protein	X03453	2.0
618	Human gene for creatine kinase B (EC 2.7.3.2)	X15334	2.0
619	quiescin Q6	L42379	2.0
620	butyrophilin, subfamily 3, member A1	U90552	2.0
621	hematopoietically expressed homeobox	L16499	2.0
622	Human gene for C1-inhibitor	X54486	2.0
623	Homo sapiens alpha tubulin (TUBA2) gene, partial cds	AF005392	2.0
624	S100 calcium binding protein A2	M87068	2.0
625	arsenate resistance protein ARS2	AL096723	2.0
626	Human hydroxymethylglutaryl-CoA lyase (HMGCL) gene	U49719	2.0
627	forkhead box M1	U74612	2.0
628	zinc finger protein 266	AA868898	2.0
629	RAE1 RNA export 1 homolog (S. pombe)	U84720	2.0
630	H3 histone, family 3B (H3.3B)	Z48950	2.0
631	glycoprotein Ib (platelet), alpha polypeptide	J02940	2.0

632	Notch homolog 4 (Drosophila)	U95299	2.0
633	oculocerebrorenal syndrome of Lowe	AL022162	2.0
634	splicing factor 3a, subunit 2, 66kD	L21990	2.0
635	tyrosine kinase 2	X54637	2.0
636	stromal cell-derived factor 2	D50645	2.0
637	chromogranin B (secretogranin 1)	Y00064	2.0
638	Ras-like without CAAX 1	Y07566	2.0
639	gem (nuclear organelle) associated protein 4	AL080150	2.0
640	ADP-ribosyltransferase (NAD+; poly(ADP-ribose) polymerase)-like 2	AJ236876	2.0
641	leukocyte-associated Ig-like receptor 1	AF013249	1.9
642	laminin, beta 2 (laminin S)	X79683	1.9
643	zinc finger protein 103 homolog (mouse)	D76444	1.9
644	cadherin 18, type 2	U59325	1.9
645	retinoblastoma binding protein 6	AI538172	1.9
646	homeo box A5	M26679	1.9
647	Homo sapiens, clone IMAGE:5301034, mRNA	AL036744	1.9
648	Human AMP deaminase (AMPD3) gene	U29926	1.9
649	kinesin family member C1	D14678	1.9
650	PCTAIRE protein kinase 1	X66363	1.9
651	cyclin-dependent kinase inhibitor 2C (p18, inhibits CDK4)	AF041248	1.9
652	cleavage stimulation factor, 3' pre-RNA, subunit 2, 64kDa	M85085	1.9
653	7-dehydrocholesterol reductase	AF034544	1.9
654	myotubularin related protein 9	AL080178	1.9
655	DiGeorge syndrome critical region gene 6	X96484	1.9
656	N-myc downstream regulated gene 1	D87953	1.9
657	heat shock 90kDa protein 1, beta	M16660	1.9
658	eukaryotic translation initiation factor 4A, isoform 2	D30655	1.9
659	TGFb inducible early protein and early growth response protein	AF050110	1.9
660	promyelocytic leukemia	M79463	1.9

661	suppression of tumorigenicity 5	U15131	1.9
662	CDC42 effector protein (Rho GTPase binding) 4	W27541	1.9
663	granulin	AF055008	1.9
664	hypermethylated in cancer 2	AB028943	1.9
665	growth arrest-specific 1	L13698	1.9
666	zinc finger protein 216	AF062346	1.9
667	Human nonmuscle	M22919	1.9
668	ubiquitin carrier protein	M91670	1.9
669	mitogen-activated protein kinase 7	U29725	1.9
670	phosphoinositide-3-kinase, regulatory subunit, polypeptide 3 (p55, gamma)	D88532	1.9
671	transcription factor A, mitochondrial	M62810	1.9
672	coatomer protein complex, subunit epsilon	AJ131182	1.9
673	inhibitor of growth family, member 1	AB024401	1.9
674	phosducin-like	AF031463	1.9
675	zinc finger protein 253	AF038951	1.9
676	desmocollin 3	D17427	1.9
677	Human cytosolic adenylate kinase (AK1) gene	J04809	1.9
678	actin, alpha 2, smooth muscle, aorta	X13839	1.9
679	chemokine (C-X3-C motif) receptor 1	U20350	1.9
680	E coli bioB gene biotin synthetase	J04423	1.9
681	pim-1 oncogene	M54915	1.9
682	WD-repeat protein	U94747	1.9
683	UDP-N-acetylglucosamine-2-epimerase	AJ238764	1.9
684	LIM domain binding 1	AF064491	1.9
685	cell division cycle 2, G1 to S and G2 to M	D88357	1.9
686	angio-associated, migratory cell protein	M95627	1.9
687	hypothetical protein MGC5576	AI525633	1.9
688	ATP-binding cassette, sub-family G (WHITE), member 2	AF093771	1.9
689	ubiquitin-activating enzyme E1	M58028	1.9

690	nuclear factor related to kappa B binding protein	X80878	1.9
691	protein phosphatase 2, regulatory subunit B (B56), delta isoform	L76702	1.9
692	zinc finger protein 3 (A8-51)	X07290	1.9
693	poly(rC) binding protein 3	AL046394	1.9
694	putative mitochondrial space protein 32.1	AF050198	1.9
695	CDC-like kinase 2	L29218	1.9
696	KIAA0543 protein	AB011115	1.9
697	protein kinase C, delta	D10495	1.9
698	zinc finger protein	AF060503	1.9
699	KIAA0346 protein	AB002344	1.9
700	phosphatidylserine receptor	AI950382	1.9
701	Williams Beuren syndrome chromosome region 20C	N29665	1.9
702	lymphocyte antigen 9	L42621	1.9
703	G protein-coupled receptor 116	AB018301	1.9
704	MYST histone acetyltransferase 1	AI417075	1.9
705	F-box and leucine-rich repeat protein 11	AB023221	1.9
706	acetyl-Coenzyme A acyltransferase 1	X14813	1.9
707	tripartite motif-containing 29	L24203	1.9
708	KIAA0459 protein	AB007928	1.9
709	lung cancer candidate	AF055479	1.8
710	SRY (sex determining region Y)-box 4	X70683	1.8
711	cAMP responsive element modulator	S68271	1.8
712	transforming growth factor, beta receptor I	L11695	1.8
713	arachidonate 12-lipoxygenase	M62982	1.8
714	peroxisome receptor 1	Z48054	1.8
715	KIAA1118 protein	AB029041	1.8
716	tumor necrosis factor (ligand) superfamily, member 9	U03398	1.8
717	cortistatin	AF013252	1.8
718	tetranectin (plasminogen binding protein)	X64559	1.8

719	protocadherin gamma subfamily B, 7	D88799	1.8
720	ornithine decarboxylase antizyme 2	AF057297	1.8
721	HMBA-inducible	AI796944	1.8
722	BRCA1 associated protein-1	AF045581	1.8
723	lectin, galactoside-binding, soluble, 3 (galectin 3)	AB006780	1.8
724	histamine receptor H1	Z34897	1.8
725	protocadherin gamma subfamily B, 7	D88799	1.8
726	excision repair cross-complementing rodent repair deficiency	L04791	1.8
727	hypothetical protein MGC14480	U95006	1.8
728	growth arrest-specific 2 like 1	Y07846	1.8
729	DKFZP566C243 protein	AL050274	1.8
730	tropomyosin 2 (beta)	M12125	1.8
731	signal transducer and activator of transcription 4	L78440	1.8
732	desmuslin	AB002351	1.8
733	similar to gamma-glutamyltransferase 1	D87002	1.8
734	serine/threonine kinase 19	L26260	1.8
735	fibroblast growth factor receptor 1	M34641	1.8
736	splicing factor 3b, subunit 2, 145kDa	U41371	1.8
737	glutamate receptor, metabotropic 4	X80818	1.8
738	H.sapiens hsr1 mRNA (partial)	X66436	1.8
739	von Hippel-Lindau syndrome	L15409	1.8
740	vesicle-associated membrane protein 1	AF060538	1.8
741	Weakly similar to DBSHUMAN Guanine nucleotide exchange factor	AA916905	1.8
742	spermidine/spermine N1-acetyltransferase	AL050290	1.8
743	protocadherin gamma subfamily B, 7	D88799	1.8
744	cysteine and histidine rich 1	AB007965	1.8
745	aldehyde dehydrogenase 1 family, member A3	U07919	1.8
746	Cytochrome c-like polypeptide	S80864	1.8
747	transgelin 2	D21261	1.8

748	integrin beta 4 binding protein	AF022229	1.8
749	eukaryotic translation initiation factor 5	AL080102	1.8
750	phosphatidylserine receptor	AI950382	1.8
751	ubiquitin carrier protein	M91670	1.8
752	Fc fragment of IgG binding protein	D84239	1.8
753	promyelocytic leukemia	M82827	1.8
754	Human sequence clone 8B22 on chromosome 1p35.1-36.21	AL031737	1.8
755	Homo sapiens Chromosome 16 BAC clone CIT987SK-A-152E5	AC004382	1.8
756	KIAA0431 protein	AB007891	1.8
757	spondyloepiphyseal dysplasia, late, pseudogene	AF058918	1.8
758	acetyl-Coenzyme A acyltransferase 1	AF035295	1.8
759	zinc finger protein 263	D88827	1.8
760	KIAA0595 protein	AB011167	1.8
761	adaptor-related protein complex 2	D63475	1.8
762	ribosomal protein S6 kinase, 70kDa, polypeptide 2	AB016869	1.8
763	KIAA0247 gene product	D87434	1.8
764	H.sapiens lactate dehydrogenase B gene exon 1 and 2	X13794	1.8
765	zinc finger protein ZFP100	AL080143	1.8
766	SGC32445 protein	AF070551	1.8
767	serine/threonine kinase 18	Y13115	1.8
768	muscle, skeletal, receptor tyrosine kinase	AF006464	1.8
769	KIAA1536 protein	W72733	1.8
770	tubulin, beta, 2	X02344	1.8
771	BTG family, member 3	D64110	1.8
772	Human gene for ornithine decarboxylase ODC (EC 4.1.1.17)	X16277	1.8
773	Human Chromosome 16 BAC clone CIT987SK-A-735G6	AC002400	1.8
774	uroplakin 1A	AC002115	1.8
775	KIAA0354 gene product	AB002352	1.8
776	integrin-linked kinase	U40282	1.8

777	arsenate resistance protein ARS2	AI972631	1.8
778	mitochondrial ribosomal protein S11	AI432190	1.8
779	Homo sapiens mRNA; cDNA DKFZp586I0523	H98552	1.8
780	ribosomal protein L37	D23661	1.8
781	GM2 ganglioside activator protein	AA224768	1.8
782	leukocyte receptor cluster (LRC) member 4	S82470	1.8
783	sulfotransferase family 4A, member 1	N63574	1.8
784	tyrosine kinase, non-receptor, 1	U43408	1.8
785	ATPase, H+ transporting, lysosomal 21kDa,	D89052	1.8
786	solute carrier family 3	J02939	1.8
787	pleiomorphic adenoma gene 1	U65002	1.8
788	small nuclear RNA activating complex,	AF032387	1.8
789	methyl-CpG binding domain protein 4	AF072250	1.8
790	KIAA0605 gene product	AB011177	1.8
791	LIV-1 protein, estrogen regulated	U41060	1.8
792	zinc finger protein with interaction domain	X82018	1.8
793	uracil-DNA glycosylase	Y09008	1.8
794	zinc finger protein 23 (KOX 16)	AL080123	1.8
795	Human pigment epithelium-derived factor gene, complete cds	U29953	1.8
796	hypothetical protein DKFZp667O2416	H18080	1.8
797	uroporphyrinogen decarboxylase	AF104421	1.8
798	urocortin	AI857458	1.8
799	Human DNA sequence from clone 37E16 on chromosome 22 Contains a novel gene, a	Z83844	1.8
800	keratin 19	Y00503	1.8
801	hypothetical protein MGC5576	W27939	1.8
802	retinoblastoma binding protein 6	W25798	1.8
803	progesterone receptor membrane component 1	Y12711	1.8
804	tumor necrosis factor, alpha-induced protein 3	M59465	1.7
805	phytanoyl-CoA hydroxylase interacting protein	D87463	1.7

806	hypothetical protein MGC5560	L13720	1.7
807	immunoglobulin mu binding protein 2	L14754	1.7
808	Homo sapiens cDNA FLJ38383 fis, clone FEBRA2003726.	AI827895	1.7
809	nl75c09.s1 Homo sapiens cDNA, 3 end	AA557228	1.7
810	CDC28 protein kinase regulatory subunit 2	X54942	1.7
811	sin3-associated polypeptide, 18kDa	W27641	1.7
812	GM2 ganglioside activator protein	X62078	1.7
813	KIAA0352 gene product	AB002350	1.7
814	cell division cycle 25A	M81933	1.7
815	inositol polyphosphate phosphatase-like 1	L36818	1.7
816	Homo sapiens mRNA; cDNA DKFZp586F1322 (from clone DKFZp586F1322)	AL050172	1.7
817	proteasome (prosome, macropain) activator subunit 2 (PA28 beta)	D45248	1.7
818	mutated in colorectal cancers	M62397	1.7
819	rhomboid, veinlet-like 1 (Drosophila)	Y17108	1.7
820	Human Alu-Sq subfamily consensus sequence.	U14573	1.7
821	ring finger protein 40	AB014561	1.7
822	leukocyte receptor cluster (LRC) member 4	S82470	1.7
823	kinesin family member C1	D14678	1.7
824	nuclear DNA-binding protein	X95592	1.7
825	period homolog 1 (Drosophila)	AF022991	1.7
826	2'-5'-oligoadenylate synthetase 2, 69/71kDa	M87434	1.7
827	palmitoyl-protein thioesterase 2	AF020543	1.7
828	hepsin (transmembrane protease, serine 1)	X07732	1.7
829	BCE-1 protein	AF068197	1.7
830	KIAA0446 gene product	AB007915	1.7
831	small nuclear RNA activating complex, polypeptide 2, 45kDa	U44755	1.7
832	zinc finger protein 42 (myeloid-specific retinoic acid- responsive)	M58297	1.7
833	arrestin, beta 2	AF106941	1.7
834	KIAA1076 protein	AB028999	1.7

835	tubulin, gamma complex associated protein 2	AI961040	1.7
836	ceroid-lipofuscinosis, neuronal 5	AF068227	1.7
837	guanylate binding protein 2, interferon-inducible	M55543	1.7
838	coproporphyrinogen oxidase (coproporphyria, harderoporphyria)	D16611	1.7
839	ribosomal protein L28	U14969	1.7
840	cisplatin resistance associated	U78556	1.7
841	ubiquitin carrier protein	M91670	1.7
842	JM4 protein	AJ005896	1.7
843	guanine nucleotide binding protein (G protein), alpha inhibiting activity polype	X04828	1.7
844	upstream binding transcription factor, RNA polymerase I	X56687	1.7
845	Human prolyl 4-hydroxylase beta-subunit and disulfide isomerase (P4HB) gene	M22806	1.7
846	polymerase (RNA) II (DNA directed) polypeptide L, 7.6kDa	U37690	1.7
847	collagen, type XVI, alpha 1	AI982638	1.7
848	KIAA0152 gene product	D63486	1.7
849	X-ray repair complementing defective repair in Chinese hamster cells 3	AF035586	1.7
850	tumor necrosis factor, alpha-induced protein 2	M92357	1.7
851	eukaryotic translation initiation factor 4 gamma, 2	U73824	1.7
852	Human hsc70 gene for 71 kd heat shock cognate protein	Y00371	1.7
853	Finkel-Biskis-Reilly murine sarcoma virus (FBR-MuSV)	X65923	1.7
854	prostaglandin D2 synthase 21kDa (brain)	AI207842	1.7
855	major histocompatibility complex, class II, DR beta 4	M16941	1.7
856	synaptic vesicle glycoprotein 2A	AB018279	1.7
857	solute carrier family 9 (sodium/hydrogen exchanger), isoform 1	S68616	1.7
858	signal recognition particle receptor	X06272	1.7
859	MAD2 mitotic arrest deficient-like 1 (yeast)	AJ000186	1.7
860	3-hydroxy-3-methylglutaryl-Coenzyme A reductase	M11058	1.7
861	Friedreich ataxia region gene X123	L27479	1.7
862	eukaryotic translation elongation factor 1 alpha 1	W28170	1.7
863	putatative 28 kDa protein	L48692	1.7

864	HTGN29 protein	AF035313	1.7
865	KIAA0226 gene product	D86979	1.7
866	histone 1, H2al	AI200373	1.7
867	KIAA1030 protein	AB028953	1.7
868	v-akt murine thymoma viral oncogene homolog 1	M63167	1.7
869	H.sapiens gene encoding mitochondrial citrate transport protein	X96924	1.7
870	Homo sapiens, clone IMAGE:3659798, mRNA	W26851	1.7
871	phosphatidylinositol transfer protein, membrane-associated	X98654	1.7
872	peroxisome biogenesis factor 10	AA194159	1.7
873	phosphoglucomutase 3	AF102265	1.7
874	ELL-RELATED RNA POLYMERASE II, ELONGATION FACTOR	U88629	1.7
875	DKFZP434M154 protein	AL080159	1.7
876	tripartite motif-containing 9	D87458	1.7
877	nucleolar cysteine-rich protein	AJ006591	1.7
878	SEC24 related gene family, member C (S. cerevisiae)	D38555	1.7
879	prostaglandin E receptor 4 (subtype EP4)	L28175	1.7
880	molybdenum cofactor synthesis 3	AF102544	1.7
881	solute carrier family 22	AB009698	1.7
882	Bernardinelli-Seip congenital lipodystrophy 2 (seipin)	AF052149	1.7
883	ret finger protein 2	AJ224819	1.7
884	Era G-protein-like 1 (E. coli)	AF082657	1.7
885	E2F transcription factor 6	AF041381	1.7
886	Homo sapiens (clone f17252) Rieske Fe-S protein	L32977	1.7
887	synovial sarcoma, X breakpoint 4	U90841	1.7
888	amplified in osteosarcoma	U41635	1.7
889	PCTAIRE protein kinase 1	X66363	1.7
890	pituitary tumor-transforming 2	AF095288	1.7
891	copper chaperone for superoxide dismutase	AF002210	1.7
892	transcription termination factor, RNA polymerase I	X83973	1.7

893	cofilin 1 (non-muscle)	X95404	1.6
894	kinase insert domain receptor	L04947	1.6
895	centrin, EF-hand protein, 2	X72964	1.6
896	cytochrome c, somatic	D00265	1.6
897	ribonuclease P (14kD)	AF001175	1.6
898	Nuclear factor of κ light polypeptide gene enhancer in B-cells 2	X61498	1.6
899	KIAA0138 gene product	D50928	1.6
900	basic leucine zipper and W2 domains 1	D13630	1.6
901	Homo sapiens trinucleotide repeat DNA binding protein p20-CGGBP	AF094481	1.6
902	ATPase, H+ transporting, lysosomal 14kDa, V1 subunit F	D49400	1.6
903	similar to S. cerevisiae RER1	AF091071	1.6
904	zinc finger protein 124 (HZF-16)	S54641	1.6
905	TAF11 RNA polymerase II	X83928	1.6
906	chromobox homolog 3 (HP1 gamma homolog, Drosophila)	AI740522	1.6
907	clone 886K2 on chromosome 1p35.1-36.12	AL031295	1.6
908	erythropoietin receptor	X97671	1.6
909	homeodomain interacting protein kinase 1-like protein	AB014530	1.6
910	TAF5-like RNA polymerase II, p300/CBP-associated factor (PCAF)-associated factor	AJ009770	1.6
911	prohibitin	S85655	1.6
912	transient receptor potential cation channel, subfamily C, member 1	X89066	1.6
913	GM2 ganglioside activator protein	X61094	1.6
914	PAS domain containing serine/threonine kinase	D50925	1.6
915	origin recognition complex, subunit 1-like (yeast)	U40152	1.6
916	tubulin, alpha, ubiquitous	K00558	1.6
917	5-hydroxytryptamine (serotonin) receptor 6	L41147	1.6
918	PCTAIRE protein kinase 1	X66363	1.6
919	interferon induced transmembrane protein 3 (1-8U)	X57352	1.6
920	protocadherin gamma subfamily B, 7	D88799	1.6
921	zinc finger protein 354A	D89928	1.6

922	nudix (nucleoside diphosphate linked moiety X)-type motif 1	D16581	1.6
923	zinc finger protein 91 (HPF7, HTF10)	L11672	1.6
924	G antigen 3	U19144	1.6
925	calreticulin	AD000092	1.6
926	tubby like protein 3	AF045583	1.6
927	KIAA0561 protein	AB011133	1.6
928	KIAA0211 gene product	D86966	1.6
929	KIAA1094 protein	AB029017	1.6
930	acyl-Coenzyme A oxidase 1, palmitoyl	X71440	1.6
931	Ras-related GTP-binding protein	U41654	1.6
932	membrane-associated tyrosine- and threonine-specific cdc2-inhibitory kinase	AF014118	1.6
933	cytochrome P450 isoform 4F12	AC004523	1.6
934	homologous to yeast nitrogen permease	AF040707	1.6
935	TAP binding protein (tapasin)	AF029750	1.6
936	angiopoietin 1	D13628	1.6
937	KIAA0397 gene product	AB007857	1.6
938	kinesin family member 22	AB017430	1.6
939	transgelin	M95787	1.6
940	H2A histone family, member N	Z98744	1.6
941	lysosomal-associated membrane protein 2	X77196	1.6
942	v-ets erythroblastosis virus E26 oncogene homolog 2 (avian)	J04102	1.6
943	MCM2 minichromosome maintenance deficient 2, mitotin	D21063	1.6
944	cysteine-rich protein 1 (intestinal)	AI017574	1.6
945	ras homolog gene family, member C	L25081	1.6
946	zona pellucida glycoprotein 3 (sperm receptor)	X56777	1.6
947	Human RNA polymerase II subunit hsRPB4 gene, complete cds	U89387	1.6
948	parathymosin	M24398	1.6
949	calcium channel, voltage-dependent, beta 3 subunit	U07139	1.6
950	major histocompatibility complex, class II, DM alpha	X62744	1.6

951	angiomotin like 2	AB023206	1.6
952	Homo sapiens hAWMS1 mRNA, complete cds.	AW026656	1.6
953	ATP synthase, H+ transporting, mitochondrial F1 complex, delta subunit	X63422	1.6
954	katanin p80 (WD40-containing) subunit B 1	AF052432	1.6
955	hypothetical protein FLJ22678	AA165701	1.6
956	FK506 binding protein 4, 59kDa	M88279	1.6
957	ATX1 antioxidant protein 1 homolog (yeast)	U70660	1.6
958	H.sapiens SCAD gene, 5 UTR exon 1 and 2 (and joined CDS)	Z80345	1.6
959	fibroblast growth factor receptor 1	X66945	1.6
960	DKFZP586D2223 protein	AL050196	1.6
961	Homo sapiens chromosome 21 derived BAC	AF017257	1.6
962	CD81 antigen (target of antiproliferative antibody 1)	M33680	1.6
963	G antigen 1	U19142	1.6
964	fibroblast growth factor receptor 3	M64347	1.6
965	SEC13-like 1 (S. cerevisiae)	AF052155	1.6
966	methionine adenosyltransferase II, alpha	X68836	1.6
967	baculoviral IAP repeat-containing 2	U37547	1.6
968	abhydrolase domain containing 3	AF007152	1.6
969	ribonuclease H2, large subunit	Z97029	1.6
970	eukaryotic translation elongation factor 1 delta	Z21507	1.6
971	colony stimulating factor 1 (macrophage)	M37435	1.6
972	mitogen-activated protein kinase kinase kinase 11	L32976	1.6
973	glyceraldehyde-3-phosphate dehydrogenase	M33197	1.6
974	APG12 autophagy 12-like (S. cerevisiae)	AA151922	1.6
975	nicastrin	D87442	1.6
976	glyceraldehyde-3-phosphate dehydrogenase	U34995	1.6
977	lectin, galactoside-binding, soluble, 3 binding protein	L13210	1.6
978	glycoprotein (transmembrane) nmb	X76534	1.6
979	forkhead box G1B	X74142	1.6

980	phospholipase D3	U60644	1.6
981	acrosin	Y00970	1.6
982	ribosomal protein, large, P1	M17886	1.6
983	polymerase (RNA) II (DNA directed) polypeptide L,	N24355	1.6
984	dermatopontin	Z22865	1.6
985	Homo sapiens mRNA; cDNA DKFZp586H201	AL049430	1.6
986	sulfotransferase family, cytosolic, 2B, member 1	U92315	1.6
987	KIAA0652 gene product	AB014552	1.6
988	Homo sapiens clone 23700 mRNA sequence	AF038185	1.6
989	GTP cyclohydrolase 1 (dopa-responsive dystonia)	U19523	1.6
990	adenylate cyclase 6	AB007882	1.6
991	synaptopodin	AB028952	1.6
992	KIAA1115 protein	AB029038	1.6
993	ubiquitin C	AB009010	1.6
994	cytochrome c oxidase subunit VIa polypeptide 1	AI540925	1.6
995	Homo sapiens, clone IMAGE:5123182, mRNA,	C18655	1.6
996	corticotropin releasing hormone receptor 2	AF011406	1.6
997	stress-induced-phosphoprotein 1	M86752	1.6
998	chondroitin sulfate proteoglycan 5 (neuroglycan C)	AF059274	1.6
999	ras homolog gene family, member G (rho G)	X61587	1.6
1000	disrupter of silencing 10	W25932	1.6
1001	protein kinase, cAMP-dependent, regulatory, type I, alpha	M33336	1.6
1002	DNA replication factor	AF070552	1.6
1003	FAST kinase	X86779	1.6
1004	ribosomal protein S20	L06498	1.6
1005	holocytochrome c synthase (cytochrome c heme-lyase)	U36787	1.6
1006	pleckstrin homology, Sec7 and coiled/coil domains 2	U70728	1.6
1007	BCL2-associated athanogene	Z35491	1.6
1008	polymerase (RNA) II (DNA directed) polypeptide A	X63564	1.6

1009	BCL2-antagonist/killer 1	X84213	1.6
1010	hypothetical protein LOC91966	U66042	1.6
1011	phospholipase C-like 1	D42108	1.6
1012	RCD1 required for cell differentiation1 homolog	D87957	1.6
1013	cAMP responsive element modulator	S68134	1.6
1014	Homo sapiens full length insert cDNA YU79F10	AF009267	1.6
1015	ribosomal protein S15	J02984	1.6
1016	Human DNA sequence from clone 425C14	Z99129	1.6
1017	signal recognition particle 14kDa	AI525652	1.6
1018	Homo sapiens Chromosome 16 BAC clone CIT987SK-A-152E5	AC004382	1.6
1019	POM121 membrane glycoprotein (rat)	AL080109	1.6
1020	cleft lip and palate associated transmembrane protein 1	AF037339	1.6
1021	follistatin-like 1	U06863	1.5
1022	T-box 19	AJ010277	1.5
1023	KIAA0107 gene product	D14663	1.5
1024	aminolevulinate, delta-, dehydratase	M13928	1.5
1025	hypothetical protein MGC2650	AI885381	1.5
1026	tumor rejection antigen (gp96) 1	X15187	1.5
1027	ribosomal protein L36a-like	AI708983	1.5
1028	colony stimulating factor 2 receptor, beta	H04668	1.5
1029	phospholipase C, gamma 1 (formerly subtype 148)	M34667	1.5
1030	metallothionein 2A	AI547258	1.5
1031	ubiquitin C	M26880	1.5
1032	ribosomal protein, large, P1	M17886	1.5
1033	actin related protein 2/3 complex, subunit 5, 16kDa	AF006088	1.5
1034	ubiquitin specific protease 20	AB023220	1.5
1035	SNARE protein Ykt6	AI925356	1.5
1036	jerky homolog (mouse)	AF072468	1.5
1037	hypothetical protein FLJ22709	W26021	1.5

1038	NF-kappa homolog 2 (p49/p100)	S76638	1.5
1039	histone 1, H3e	AA904505	1.5
1040	chromosome 14 open reading frame 79	AF038188	1.5
1041	phosphatidylinositol 4-kinase, catalytic, beta polypeptide	U81802	1.5
1042	crystallin, beta A4	U59057	1.5
1043	calreticulin	AD000092	1.5
1044	amine oxidase pseudogene	AF047485	1.5
1045	hypothetical protein LOC90410	AI651368	1.5
1046	Ras-induced senescence 1	AL080235	1.5
1047	GNAS complex locus	X56009	1.5
1048	T-box 5	Y09445	1.5
1049	Human ENO2 gene for neuron specific (gamma) enolase	X51956	1.5
1050	Human DNA sequence from clone 508I15 on chromosome 22q12-13	AL021707	1.5
1051	phosphoglycerate mutase 1 (brain)	J04173	1.5
1052	START domain containing 3	D38255	1.5
1053	Homo sapiens mRNA; cDNA DKFZp586D0918	AL049370	1.5
1054	ligase IV, DNA, ATP-dependent	X83441	1.5
1055	ubiquitin-conjugating enzyme E2M (UBC12 homolog, yeast)	AA587372	1.5
1056	CD83 antigen	Z11697	1.5
1057	jerky homolog (mouse)	AF072468	1.5
1058	zinc finger protein 200	AJ003147	1.5
1059	isocitrate dehydrogenase 3 (NAD+) beta	U49283	1.5
1060	proteasome (prosome, macropain) 26S subunit,	D31889	1.5
1061	epithelial membrane protein 3	U87947	1.5
1062	retinoblastoma binding protein 6	X85133	1.5
1063	testis enhanced gene transcript (BAX inhibitor 1)	X75861	1.5
1064	skeletal muscle and kidney enriched inositol phosphatase	U45973	1.5
1065	fibroblast growth factor receptor 1	M34641	1.5
1066	endosulfine alpha	AI658639	1.5

1067	tumor protein p53-binding protein	U82939	1.5
1068	histidyl-tRNA synthetase-like	U18937	1.5
1069	FAT tumor suppressor homolog 2 (Drosophila)	AB011535	1.5
1070	D4, zinc and double PHD fingers family 1	U43843	1.5
1071	fuse-binding protein-interacting repressor	U51586	1.5
1072	dystonia 1, torsion (autosomal dominant; torsin A)	AF007871	1.5
1073	CDP-diacylglycerol--inositol 3-phosphatidyltransferase	AL050383	1.5
1074	pinin, desmosome associated protein	U77718	1.5
1075	ORF	M68864	1.5
1076	hypothetical protein DT1P1A10	U92980	1.5
1077	TAF6 RNA polymerase II	L25444	1.5
1078	CDC37 cell division cycle 37 homolog (S. cerevisiae)	U43077	1.5
1079	laminin, alpha 2	Z26653	1.5
1080	hypothetical protein MGC27165	J04164	1.5
1081	Human natural killer cell enhancing factor (NKEFB)	L19185	1.5
1082	ribosomal protein S9	U14971	1.5
1083	KIAA0628 gene product	AB014528	1.5
1084	Vacuolar H(+)-ATPase subunit [Homo sapiens], mRNA sequence	AF038954	1.5
1085	cold inducible RNA binding protein	D78134	1.5
1086	serine/threonine kinase 17b (apoptosis-inducing)	AB011421	1.5
1087	zinc finger protein 267	X78925	1.5
1088	eukaryotic translation initiation factor 2B, subunit 2 beta, 39kDa	AF035280	1.5